

OPTIMUM DESIGN OF PIN-JOINTED 3-D DOME STRUCTURES
USING GLOBAL OPTIMIZATION TECHNIQUES

A THESIS SUBMITTED TO
THE GRADUATE SCHOOL OF NATURAL AND APPLIED SCIENCES
OF
MIDDLE EAST TECHNICAL UNIVERSITY

BY

YAVUZ SARAÇ

IN PARTIAL FULFILLMENT OF THE REQUIREMENTS
FOR
THE DEGREE OF MASTER OF SCIENCE
IN
CIVIL ENGINEERING

NOVEMBER 2005

Approval of the Graduate School of Natural and Applied Sciences

Prof. Dr. Canan Özgen
Director

I certify that this thesis satisfies all the requirements as a thesis for the degree of Master of Science

Prof. Dr. Erdal Çokca
Head of Department

This is to certify that we have read this thesis and that in our opinion it is fully adequate, in scope and quality, as a thesis for the degree of Master of Science.

Asst. Prof. Dr. Oğuzhan Hasańebi
Supervisor

Examining Committee Members

Prof. Dr. Engin Keyder (CE, METU) _____

Asst. Prof. Dr. Oğuzhan Hasańebi (CE, METU) _____

Assoc. Prof. Dr. Uğurhan Akyüz (CE, METU) _____

Assoc. Prof. Dr. Can Balkaya (CE, METU) _____

Asst. Prof. Dr. Alp Caner (CE, METU) _____

I hereby declare that all information in this document has been obtained and presented in accordance with academic rules and ethical conduct. I also declare that, as required by these rules and conduct, I have fully cited and referenced all material and results that are not original to this work.

Name, Last name : Yavuz SARAÇ

Signature :

ABSTRACT

OPTIMUM DESIGN OF PIN-JOINTED 3D DOME STRUCTURES USING GLOBAL OPTIMIZATION TECHNIQUES

Saraç, Yavuz

M.Sc., Department of Civil Engineering

Supervisor: Asst. Prof. Dr. Oğuzhan Hasançebi

November 2005, 204 pages

Difficult gradient calculations, converging to a local optimum without exploring the design space adequately, too much dependency on the starting solution, lacking capabilities to treat discrete and mixed design variables are the main drawbacks of conventional optimization techniques. So evolutionary optimization methods received significant interest amongst researchers in the optimization area. Genetic algorithms (GAs) and simulated annealing (SA) are the main representatives of evolutionary optimization methods. These techniques emerged as powerful and modern strategies to efficiently deal with the difficulties encountered in conventional techniques, and therefore rightly attracted a substantial interest and

popularity. The underlying concepts of these techniques and thus their algorithmic models have been devised by establishing between the optimization task and events occurring in nature. While, Darwin's survival of the fittest theory is mimicked by GAs, annealing process of physical systems are employed to SA.

On the other hand, dome structures are among the most preferred types of structures for large unobstructed areas. Domes have been of a special interest in the sense that they enclose a maximum amount of space with a minimum surface. This feature provides economy in terms of consumption of constructional materials. So merging these two concepts make it possible to obtain optimum designs of dome structures.

This thesis is concerned with the use of GAs and SA in optimum structural design of dome structures, which range from some relatively simple problems to the problems of increased complexity. In this thesis, firstly both techniques are investigated in terms of their practicality and applicability to the problems of interest. Then numerous test problems taken from real life conditions are studied for comparing the success of the proposed GA and SA techniques with other discrete and continuous optimization methods. The results are discussed in detail to reach certain recommendations contributing to a more efficient use of the techniques in optimum structural design of pin-jointed 3-D dome structures.

Keywords: Optimization, Structural Optimization, Evolutionary Algorithms, Genetic Algorithms, Simulated Annealing, Dome Structures, Pin-Jointed Structures, Span Length

ÖZ

GLOBAL OPTİMİZASYON TEKNİKLERİ KULLANILARAK ÜÇ BOYUTLU MAFSALLI KUBBE YAPILARIN OPTİMUM TASARIMI

Saraç, Yavuz

Yüksek Lisans, İnşaat Mühendisliği Bölümü

Tez Yöneticisi: Yard. Doç. Dr. Oğuzhan Hasançebi

Kasım 2005, 204 sayfa

Zor türev hesaplamaları, tasarım kümesini yeterli derecede araştırmaksızın lokal bir optimuma yakınsama, başlangıç çözümüne fazlasıyla bağımlılık ve ayrık ve karma tasarım değişkenlerini ele alabilme yeteneğinden yoksunluk klasik (konvansiyonel) optimizasyon tekniklerinin başlıca yetersizlikleridir. Bu nedenle evrimsel optimizasyon metotları, optimizasyon alanındaki araştırmacılar arasında kayda değer bir ilgi çekmiştir. Genetik algoritmalar ve tavlama simülasyonu evrimsel optimizasyon metotlarının başlıca temsilcilerindedir. Bu teknikler klasik optimizasyon tekniklerinde karşılaşılan zorlukların üstesinden gelebilecek güçlü ve modern stratejiler olarak ortaya çıkmış ve önemli ilgi görmüş ve popülerite

kazanmıştır. Bu tekniklerin temelinde yatan kavramlar ve dolayısıyla onların algoritmik modelleri, optimizasyon ile doğada yer alan olaylar arasındaki benzerliklerin saptanmasıyla kurulmuştur. Genetik algoritmalar Darwin'in en güçlü olanın yaşaması prensibini kopyalarken, fiziksel sistemlerin tavlama işlemi tavlama simülasyonunca uyarlanmıştır.

Öte yandan, kubbe yapıları engelsiz geniş açıklıklı alanlar için yapılan yapı sistemleri içinde en çok tercih edilenlerdendir. Kubbelere, minimum yüzey alanı ile maksimum hacmi kaplamaları nedeniyle özel bir ilgi duyulmuştur. Bu özellik kullanılan malzeme yönünden ekonomi sağlamaktadır. Böylece bu iki konuyu birleştirilmesi kubbe sistemlerin optimum çözümlerinin üretilmesini olanaklı kılmaktadır.

Bu tez, genetik algoritmalar ve tavlama simülasyonu tekniklerinin, optimum yapı tasarımının nispeten basit problemlerden çok daha kompleks nitelikli problemlerine uzanan uygulamalarında kullanımını araştırmaktadır. Bu tezde, öncelikle her iki teknik ilgili problemlere elverişliliği ve uygulanabilirliği açısından incelenmektedir. Daha sonra gerçek yaşam koşullarından alınmış pek çok deneme problemi, genetik algoritmalarının ve tavlama simülasyonu tekniklerinin diğer ayrık ve sürekli metotlarla kıyaslanması için ele alınmaktadır. Elde edilen sonuçlar, bu tekniklerle üç boyutlu mafsallı kubbe yapıların optimum tasarımının daha etkin bir şekilde kullanılması açısından, bazı öneriler ışığında geniş olarak tartışılmaktadır.

Anahtar Kelimeler: Optimizasyon, Yapı Optimizasyonu, Evrimsel Algoritmalar, Genetik Algoritmalar, Tavlama Simülasyonu, Kubbe Yapılar, Mafsallı Yapılar, Açıklık

To my family

ACKNOWLEDGMENTS

I would like to offer my sincere thanks and appreciation to Asst. Prof. Dr. Oğuzhan Hasaebi for his commendable endeavour, supervision and encouraging approach that kept my motivation alive. I also have to thank him once more time for letting me use two softwares (SSTOGA and SSTOSA) in the design of test problems.

I am also grateful to Prof. Dr. Fuat Erbatur for making me known about structural optimization. I first took his lecture on structural optimization in 2003 and made my mind to prepare a thesis on this subject.

Finally, I would like to offer my special thanks to my wife and son for their encouragement, patience and endless support.

TABLE OF CONTENTS

ABSTRACT	iv
ÖZ	vi
ACKNOWLEDGMENTS	ix
TABLE OF CONTENTS	x
LIST OF TABLES	xv
LIST OF FIGURES	xvi
CHAPTER	
1. INTRODUCTION	1
1.1 Dome Structures	1
1.2 Structural Optimization	2
1.3 Evolutionary Algorithms	2
1.4 Genetic Algorithms	3
1.5 Simulated Annealing	3
1.6 Aim and Scope of the Thesis	5
2. DOME STRUCTURES	8
2.1 Space Structures	8
2.1.1 Barrel Vaults	11
2.1.2 Domes	13
2.2 Types of Braced Domes	17
2.2.1 Ribbed Domes	19
2.2.2 Schwedler Dome	19
2.2.3 Lamella Domes	20
2.2.4 Two- and Three-Way Grid Domes	20
2.2.5 Geodesic Domes	20

2.3 Load-Carrying Characteristics of Braced Domes	21
2.3.1 Double-Layer Domes	22
2.3.2 Stressed-Skin Geodesic Domes	23
2.4 Components of the Braced Domes	24
3. ANALYSIS AND DESIGN OF BRACED DOMES	28
3.1 Types of Analysis	28
3.1.1 Braced Dome Behaviour	29
3.1.2 The Instability Phenomenon	30
3.2 Analysis	33
3.2.1 Linear Elastic Analysis	37
3.2.2 Non-Linear Analysis	45
3.3 Design Loads	46
3.3.1 Wind Loads	47
3.3.2 Snow Loads	51
3.3.3 Live Load, Dead Load	51
3.3.4 Earthquake Loads	52
3.3.5 Temperature Changes	52
4. LOADS ACTING ON DOME STRUCTURES	53
4.1 Introduction	53
4.2 ASCE 7-98	53
4.2.1 Load Combinations	53
4.2.2 Wind Loads	54
4.2.2.1 Method-1, Simplified Procedure	55
4.2.2.2 Method-2, Analytical Procedure	58
4.2.2.3 Method-3, Wind Tunnel Procedure	62
4.2.3 Snow Loads	65
5. OPTIMIZATION TECHNIQUES	68
5.1 Structural Optimization	68
5.2 Stochastic Search Techniques	71
5.2.1 Evolutionary Algorithms	71
5.2.1.1 Evolutionary Strategies	74

5.2.1.2 Evolutionary Programming	74
5.2.1.3 Genetic Algorithms	74
5.2.2 Simulated Annealing	74
6. GENETIC ALGORITHMS	76
6.1 Introduction	76
6.2 Fundamentals of GAs	77
6.3 GA Terminology	79
6.4 Flowchart of GAs	79
6.5 Coding	82
6.6 Decoding	85
6.7 Fitness Evaluation	86
6.8 Population Size	87
6.9 Objective Function	87
6.10 Fitness Function	89
6.11 Fitness Scaling Function	90
6.12 Selection	92
6.13 Crossover	94
6.14 Mutation	96
6.15 Elitist Strategy	97
6.16 Constraint Handling in GAs	97
6.17 Penalty Function Approach	98
6.17.1 Homaifar, Qi and Lai's Method	99
6.17.2 Joines and Houck's Method	100
6.17.3 Hasaņebi Method	100
6.18 Formulation of Size Optimum Design Problem of Truss Structures.	101
7. SIMULATED ANNEALING	104
7.1 Introduction	104
7.2 Simulated Annealing Process	106
7.3 The Algorithm	107
7.4 Advantages of SA Over a Local Search Algorithm	108
7.5 Stages of the Procedure	110

7.5.1 Cooling Procedure	110
7.5.2 Starting Temperature	110
7.5.3 Final Temperature	111
7.5.4 Temperature Decrement	112
7.6 Candidate Design	113
7.7 Iteration of Inner Loop	115
7.8 Constraint Handling	117
8. NUMERICAL EXAMPLES	118
8.1 354-Bar Dome (Height of 4.34 m)	119
8.1.1 Wind Load (Analytical Procedure)	121
8.1.2 Snow Loads	124
8.1.3 Dead Loads	126
8.1.4 Roof Live Load	126
8.1.5 Combined Loaded Case	126
8.1.6 Load Combinations	129
8.1.7 Loads Acting on Joints	132
8.1.8 Results	135
8.2 354-Bar Dome (Height of 8.28 m)	137
8.2.1 Wind Load (Analytical Procedure)	138
8.2.2 Snow Loads	140
8.2.3 Dead Loads	142
8.2.4 Roof Live Load	143
8.2.5 Combined Loaded Case	143
8.2.6 Load Combinations	147
8.2.7 Loads Acting on Joints	150
8.2.8 Results	152
8.3 756-Bar Dome	155
8.3.1 Wind Load (Analytical Procedure)	157
8.3.2 Snow Loads	158
8.3.3 Dead Load	158
8.3.4 Roof Live Load	158

8.3.5 Combined Loaded Case	158
8.3.6 Load Combinations	160
8.3.7 Loads Acting on Joints	163
8.3.8 Results	165
8.4 444-Bar Dome	167
8.4.1 Results	170
8.5 208-Bar Dome	171
8.5.1 Results	173
8.6 354-Bar Dome	175
8.6.1 Results	175
8.7 560-Bar Dome	176
8.7.1 Results	178
8.8 Discussion of Results	182
9. SUMMARY AND CONCLUSIONS	184
9.1 Overview of the Thesis	184
9.2 Summary of the Thesis	185
9.3 Conclusion	188
9.3 Recommendations for Future Works	189
REFERENCES	191

LIST OF TABLES

TABLE

4.1	The Importance Factors	56
4.2	Design Wind Pressure	58
4.3	Wind Directionality Factor	59
4.4	Design Wind Load Formulation	61
4.5	Exposure Factor	66
4.6	Thermal Factor	67
8.1	Result of 354-Bar Dome (Height of 4.34 m)	135
8.2	Result of 354-Bar Dome (Height of 8.28 m)	153
8.3	Result of 756-Bar Dome	166
8.4	Result of 444-Bar Dome	170
8.5	Comparison of the Results	170
8.6	Results of 208-Bar Dome For Different Rise-to-Span Ratios	174
8.7	Results of 354-Bar Dome For Different Rise-to-Span Ratios	175
8.8	Result of 208-Bar Dome	179
8.9	Result of 560-Bar Dome	179
8.10	Comparison of the Results of Problems 8.1, 8.2, 8.3	182

LIST OF FIGURES

FIGURES

2.1	A Space Structure (Double-Layer Grid)	10
2.2	Barrel Vault Structure	11
2.3	Examples of Barrel Vault Configurations	12
2.4	Dimensions of Barrel Vault	13
2.5	Nagoya Dome, Japan	14
2.6	The Blouedel Conservatory, Queen Elizabeth Park, Vancouver/Canada	15
2.7	Astrodome (Steel Lamella Dome), Houston/USA	15
2.8	Tokyo Dome “Big Egg”, Japan	15
2.9	Ontario Place, Toronto/Canada	16
2.10	Roller Skating Track, Ankara	16
2.11	Café Building, Istanbul	16
2.12	Terzi Baba Mosque, Erzincan	17
2.13	Bird Cage, Gaziantep	17
2.14	Water Fowl Cage, Bursa	17
2.15	Examples of Single Layer Domes	18
2.16	US Pavilion Building for Expo 67 (Double-Layer Grid Dome)	23
2.17	The Inside View and Support Detail of Stressed-Skin Geodesic Dome	24
2.18	Node Detail	25
2.19	Member End Details	25
2.20	Support Details of Dome Structures	26
2.21	Support Details of Dome Structures	26
2.22	Connection Details of Dome Structures	27

3.1	Arrangements of Bracing	30
3.2	Non-Linear vs. Eigenvalue Buckling Behaviour	31
3.3	“Snap-Through” Buckling	33
3.4	“Snap-Through” Buckling	33
3.5	Load-Displacement Relationship	36
3.6	Local and Global Coordinate Axes of a 2-D Element	39
3.7	Transformation of Forces From Local to Global Coordinates	40
3.8	Combining Element Stiffness to Form the Global Stiffness Matrix ..	42
3.9	Flowchart of Stiffness Method	44
3.10	Newton-Raphson Method	46
3.11	Arc-Length Method	46
3.12	Pressure Distribution on Circular Domes Rising Directly from the Ground: Plan Views	49
3.12	Pressure Distribution on Circular Domes Mounted on Cylindrical Bases: Plan Views	50
4.1	Wind Tunnel test (The 1:500 Model of the Four Times Square Tower In the center of New York)	65
5.1	Search Techniques	69
6.1	The Flowchart of Genetic Algorithms	80
8.1	Top View (354-Bar)	119
8.2	Side View (354-Bar)	119
8.3	Top View of 354-Bar Dome	120
8.4	Side View of 354-Bar Dome	120
8.5	3-D View of 354-Bar Dome	121
8.6	Side View of the Dome (354-Bar)	125
8.7	Unbalanced Snow Load (354-Bar)	126
8.8	Load Case 1 of 354-Bar Dome (h=4.34 m)	127
8.9	Load Case 2 of 354-Bar Dome (h=4.34 m)	127
8.10	Load Case 3-4 of 354-Bar Dome (h=4.34 m)	127
8.11	Load Case 5-6 of 354-Bar Dome (h=4.34 m)	128
8.12	Pieces of 354-Bar Dome (h=4.34 m)	128

8.13	Graph of Number of Structural Analysis vs Feasible Best Design of 354-Bar Dome (h=4.34 m) Using SSTOGA and SSTOSA	136
8.14	Top View (354-Bar)	137
8.15	Side View (354-Bar)	137
8.16	Side View of 354-Bar Dome	137
8.17	Side View of the Dome (354-Bar)	141
8.18	Unbalanced Snow Load (354-Bar)	142
8.19	Load Case 1 of 354-Bar Dome (h=8.28 m)	144
8.20	Load Case 2 of 354-Bar Dome (h=8.28 m)	144
8.21	Load Case 3 of 354-Bar Dome (h=8.28 m)	144
8.22	Load Case 4 of 354-Bar Dome (h=8.28 m)	145
8.23	Load Case 5 of 354-Bar Dome (h=8.28 m)	145
8.24	Load Case 6 of 354-Bar Dome (h=8.28 m)	145
8.25	Pieces of 354-Bar Dome (h=8.28 m)	146
8.26	Graph of Number of Structural Analysis Versus Feasible Best Design of 354-Bar Dome (h=8.28 m) Using SSTOGA and SSTOSA	154
8.27	Top View (756-Bar)	155
8.28	Side View (756-Bar)	155
8.29	Top View of 756-Bar Dome	156
8.30	Side View of 756-Bar Dome	156
8.31	3-D View of 756-Bar Dome	157
8.32	Pieces of 756-Bar Dome	159
8.33	Graph of Number of Structural Analysis Versus Feasible Best Design of 756-Bar Dome Using SSTOGA and SSTOSA	167
8.34	Top View of 444-Bar Dome	168
8.35	Side View of 444-Bar Dome	168
8.36	3-D View of 444-Bar Dome	169
8.37	Top View of 208-Bar Dome	171
8.38	Side View of 208-Bar Dome	172
8.39	3-D View of 208-Bar Dome	172
8.40	Half View of 208-Bar Dome	173

8.41 Rise-to-Span Ratio vs. Weight Graph (208-Bar)	174
8.42. Rise-to-Span Ratio vs. Weight Graph (354-Bar)	176
8.43 Top View of 560-Bar Dome	177
8.44 Side View of 560-Bar Dome	177
8.45 3-D View of 560-Bar Dome	178
8.46 Comparison of Member Forces of Single and Double-Layer Domes	181

CHAPTER 1

INTRODUCTION

1.1 Dome Structures

Structural systems, which enable the designers to cover large spans, have always been popular during the history. Beginning with the worship places in the early times, sports stadia, assembly halls, exhibition centres, swimming pools, shopping centers and industrial buildings have been the typical examples of structures with large unobstructed areas nowadays. Dome structures are the most preferred type of large spanned structures. Domes have been of a special interest in the sense that they enclose a maximum amount of space with a minimum surface. This feature provides economy in terms of consumption of constructional materials.

The development of domes has been closely associated with the development of available materials. Although, stone was the only structural material to use in the ancient times, brickwork gradually replaced the stone masonry. Later, timber was used in the Middle Ages for the same purpose. But the great improvements in dome structures commenced with the development of the steel industry beginning in the 19th century. This enabled the engineers to design large spanned and multi-storey structures using steel. Nowadays it is very common to use steel in order to enclose large spans such as 200 m length.

1. 2 Structural Optimization

Traditionally, the design process has been achieved through intuition, experience and repeated trials. The advances in computer methods and computer technology led to development of new techniques aiming to find better solutions. Then finding the best systems has become the designer's main goal in addition to fulfilling the design criteria. These all made improvements on optimization techniques.

In classical approach of structural optimization, the derivations of objective functions and constraints with respect to design variables are calculated. This approach is referred to as gradient-based search. Because of the facts that it is very hard to calculate the derivative of objective functions explicitly, and that some functions may not be continuous, some new techniques that do not depend on the derivatives are developed.

The most popular global optimization techniques, which have emerged in the second half of twentieth century, are evolutionary algorithms, tabu search, neural networks and simulated annealing. Genetic Algorithms represent one of the mainstays of evolutionary algorithms, and are well-known optimization techniques. In this thesis, two powerful optimization techniques, Genetic Algorithms and Simulated Annealing, will be presented as modern optimization tools.

1. 3 Evolutionary Algorithms

Evolutionary Algorithms (EAs) are computer-based problem solving systems. They use computational models of evolution mechanisms in their design and implementation. The idea behind evolutionary algorithms is to imitate the natural evolution to solve optimization problems. A relationship between evolution of the nature and optimization of design is established in order to find the optimum. The

main representatives of evolutionary algorithms are genetic algorithms (GAs), evolution strategies (ESs) and evolutionary programming (EP).

The main concept of natural evolution is the theory of Darwin's survival of the fittest. This theory implies that the members that are strong and capable of adapting themselves to natural habitat survive, while the weaker ones die out. So the better individuals are evolved throughout generations. This leads to a more superior generation with respect to the former one.

Evolutionary Algorithms simulate the evolution of individual structures via processes of selection, mutation and recombination. EAs maintain a population of structures that evolve according to genetic operators. The capabilities of EAs for exploitation of the design space are due to these genetic operators. In this regard, selection operator focuses to exploit the available information, whereas recombination and mutation provide general heuristics for exploration.

1. 4 Genetic Algorithms

Genetic Algorithms are the most well-known representatives of evolutionary algorithms. they were first introduced by Holland in 1975. In GAs, a population with a fixed number of individuals is created. After evaluating the fitness scores of individuals, highly fit members are allowed to survive and poor individuals with low fitness scores are discarded. Good individuals go through some genetic operators such as selection, crossover and mutation to produce next generation. Aforementioned process is repeated in the same way for a fixed number of generations or until a predefined convergence criterion is achieved.

1. 5 Simulated Annealing

Another powerful optimization technique, which has emerged in the second half of twentieth century, is simulated annealing. In this method, fitness scores in GAs are

replaced by energy levels. An energy is defined such that it represents how good the solution is. The goal is to find the best solution by minimizing the energy. This method makes use of the annealing process of a thermodynamical system. In annealing process, the temperature of a thermodynamical system initially at a high energy level is dropped to a level at which the system reaches its minimum energy. In this technique, unlike genetic algorithms, only two states (current and candidate state) are evaluated instead of a fixed number population. If the candidate state gives a lower energy level, then it is accepted as current state. But if the candidate state gives a higher energy level, it is not thrown away at once. A test called Metropolis test is performed whether the candidate state is accepted or not. This test depends on the temperature and difference between the energy levels of the two states. The procedure outlined above is repeated a certain number of times at this temperature. Then the temperature is cooled down and the whole procedure is repeated again. When the temperature is dropped to a value around zero, it is hoped that the system has its minimum energy level.

This method has a certain advantage over classical hill-climbing techniques. The main advantage is due to the Metropolis test which accepts the poorer designs with a certain probability. This test gives the technique an exploration capability. The main concepts of Metropolis test are outlined below:

- (i) At early stages of the procedure, a more explorative search is used. Poorer designs are accepted in the beginning. As the temperature drops, the technique becomes greedy and only downhill moves are accepted.
- (ii) The difference between energy levels of current and candidate states affects the acceptance probability. If the difference is low, a higher acceptance probability assigned to the candidate design, even though it is not promising. Occasional acceptance of uphill moves avoids getting stuck in local optima. This property makes the simulated annealing technique more powerful over other classical optimization techniques.

1. 6 Aim and Scope of the Thesis

This thesis intends to give a general knowledge about modern optimization techniques, such as Genetic Algorithms and Simulated Annealing, and to implement these techniques in optimum design of steel braced domes. A step-by-step presentation is followed in the thesis. First general information about GAs, SA and braced dome structures are given. The design of such systems is then implemented by using these modern optimization techniques.

The main topics covered in the thesis are explained briefly in the following:

Chapter 2 gives comprehensive information about dome structures. First a brief history of these structures is overviewed, in which space structures are given a special emphasis since braced dome structures are the sub-groups of space structures. The examples of braced dome structures in Turkey and in the world are shown, and the general types of these structures are explained in this chapter. The main components of the braced dome structures are introduced.

Chapter 3 is devoted to analysis and design of braced domes. The general linear and non-linear analysis is discussed and the instability phenomenon of these structures are explained. The loads which act these structures are introduced briefly.

Chapter 4 presents loads acting on dome structures. The design code ASCE 7-98 Minimum Design Loads for Buildings and Other Structures is presented. Since, the most critical loads are snow and wind loads for dome structures, a special emphasis is given to these types of loads.

Chapter 5 gives a general description of optimization techniques and their advantages over classical design methods. Modern stochastic optimization techniques are given special emphasis. General frameworks of these techniques are introduced and a comparison between modern and classical optimization techniques

is conducted. Since the following chapters make detailed explanations about GAs and SA, this chapter is intended to play an introductory role to these optimization techniques.

Chapter 6 gives a detailed overview of GAs as an optimization technique. After the brief history of GAs, the basic principles of this technique are explained. The main terminology of GAs is presented. The genetic operators used in GAs such as selection, crossover and mutation are made clear. Penalty function approach which is used in constrained optimization problems is introduced. At the end of the chapter, the formulation of size optimum design problem of space structures is given.

Chapter 7 focuses on SA, another powerful optimization technique. First the physical meaning of annealing in thermodynamics is represented. Then the adaptation of this process to optimization problems is introduced. The general terminology of SA is defined while the algorithm is explained step by step. The mathematical test problem, which is solved in Chapter 6 is solved again by using SA technique. Each step of the procedure is explained as performed with GAs technique. The results obtained from both methods are compared, in order to emphasize the merits of the techniques.

Chapter 8 is devoted to test problems in structural steel design of dome structures. These test problems are also important to show the efficiency of the techniques. Seven test problems of different dome structures are solved by using two optimization techniques (GAs and SA). The first three problems are of one-layer domes which have the same span length. Real load conditions are implemented to these problems according to ASCE 7-98. Two domes with same geometry but different configuration (second and third test problems) are used in order to make a comparison of the results. Following problem is taken from the literature. The result found in this work is compared to the one found in the related article. The last three

problems are used in order to investigate the effects of rise-to-span ratio and double layer.

Chapter 9 makes a conclusion of the thesis by emphasizing the results and drawing attention to some critical points in optimum structural design. Some recommendations for the further work are underlined in this chapter.

CHAPTER 2

DOME STRUCTURES

2.1 Space Structures

Large spans have always fascinated people since unobstructed closed places have been demanded for many purposes. In the early periods of the history, stone was the only material to use. Then brickwork gradually replaced the stone masonry. Primitive type of concrete was also used extensively by the Romans. Timber was another principal roofing material used in the Middle Ages. At last, the introduction of iron in the 19th century opened up an exciting new era for structural engineers and architects. They were quick to realize the potential and advantages of relatively high strength and comparatively light weight (Makowski, 1984).

Several types of buildings have been used to enclose large spans, such as barrel vaults, domes, arches, etc. But apparently the dome providing an easy and economic method of roofing large areas and impressive beauty is the most fascinating one for the designers since the earliest times.

Before introducing domes, it will be more convenient to define the term “**space structure**”. It is important to note that pin-connected braced domes which will be investigated in this thesis are all space structures.

The term “**space structure**” refers to a structural system that involves three dimensions. In practice, the term “**space structure**” is simply used to refer to a number of families of structures that include grids, barrel vaults, domes, towers, cable nets, membrane systems, foldable assemblies and tensegrity forms. Space structures cover an enormous range of shapes and are constructed using different materials such as steel, aluminium, timber, concrete, fibre reinforced composites, glass, or a combination of these. Space structures may be divided into three categories, namely;

“**Lattice space structures**” that consist of discrete, normally elongated elements,
“**Continuous space structures**” that consist of components such as slabs, shells, membranes,
“**Biform space structures**” that consist of a combination of discrete and continuous parts.

In this thesis, the term “**space structure**” will be used to refer to “**lattice space structure**” only.

There are numerous examples of space structures around. These structures are built for sports stadia, gymnasiums, cultural centres, auditoriums, shopping malls, railway stations, aircraft hangars, leisure centres, transmission towers, radio telescopes, supernal structures (that is, structures for outer space) and many other purposes. An example of space structure (double-layer grid) is shown in Figure 2.1.



Fig. 2.1. A Space Structure (Double-Layer Grid)

The term “**spatial structure**” is also used instead of “**space structure**”. The two terms are considered to be synonymous.

The advantages of space structures are listed below:

- (i) They are three dimensional structures which can withstand loads from any direction.
- (ii) They are hyperstatic, and buckling of some compression members does not cause the whole system to collapse as has been demonstrated by mathematical models and experiments.
- (iii) Their rigidity minimizes deflections.
- (iv) Their composition allows factory pre-fabrication in modular elements, which are easily transported. Fabrication precision ensures ease of assembly and erection.
- (v) They allow a wide choice of support positions owing to modular construction.
- (vi) For double layer space structures, the space between the two layers may be used to install electricity, electrical and thermal piping, etc.

- (vii) Installation is carried out by bolting and can be done regardless of the atmospheric conditions.
- (viii) They provide aesthetic qualities.

Aforementioned structures such as grids (double layer grids, biform grids), towers, cable nets, membrane systems, foldable assemblies and tensegrity forms which are the general kinds of space structures will not be discussed here in order not to digress. However barrel vaults will shortly be introduced, due to their strong analogies with domes.

2.1.1 Barrel Vaults

A “**barrel vault**” is obtained by “arching” a grid along one direction. The result is a cylindrical form that may involve one, two or more layers of elements. Barrel vaults are also called “**cylindrical vaults**”. In history of construction, cylindrical vault appears as an evolution of arch. The use of metal has enabled its construction to be carried out with factory-prefabricated elements which may be assembled on site. A typical example of barrel vault is shown in Figure 2.2.



Fig. 2.2. Barrel Vault Structure

Some examples of barrel vault configurations are shown in Figure 2.3. A barrel vault with a diagonal pattern referred to as a “lamella barrel vault”, the barrel vault which has a three-way pattern, double layer barrel vaults, hyperboloidal lamella barrel vault, ellipsoidal lamella barrel vault, compound barrel vault consists of two or more barrel vaults that are connected together along their sides are shown in Figure 2.3, respectively.

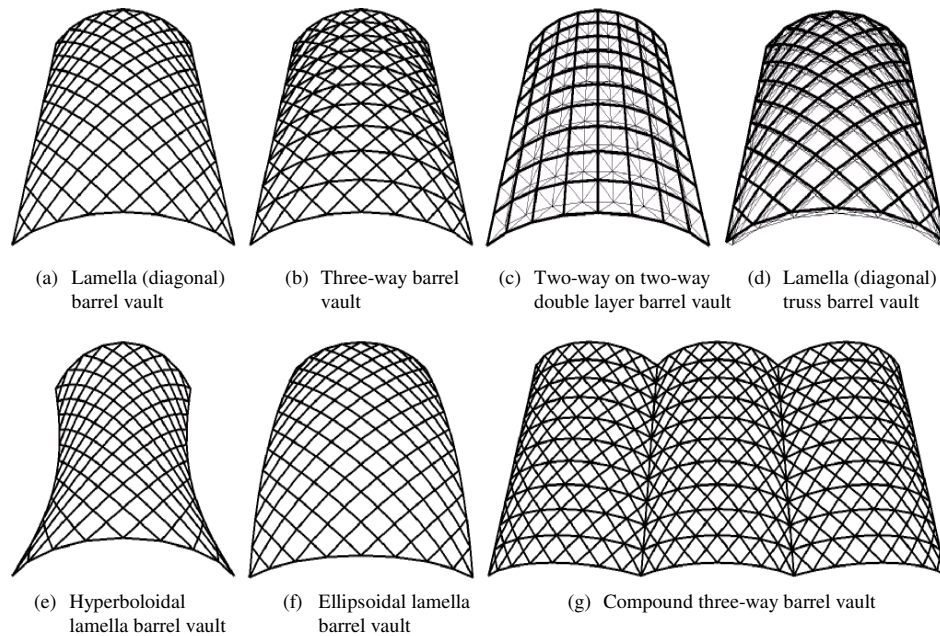


Fig. 2.3. Examples of Barrel Vault Configurations

Barrel vaults have been proved to be suitable for roofs of halls, railway stations and sports facilities (e.g. in-door tennis courts).

As seen from Figure 2.4, a regular barrel vault has three dimensions which are width (span), length and rise. So the ratios of length-to-width and rise-to-span are important for defining a barrel vault.

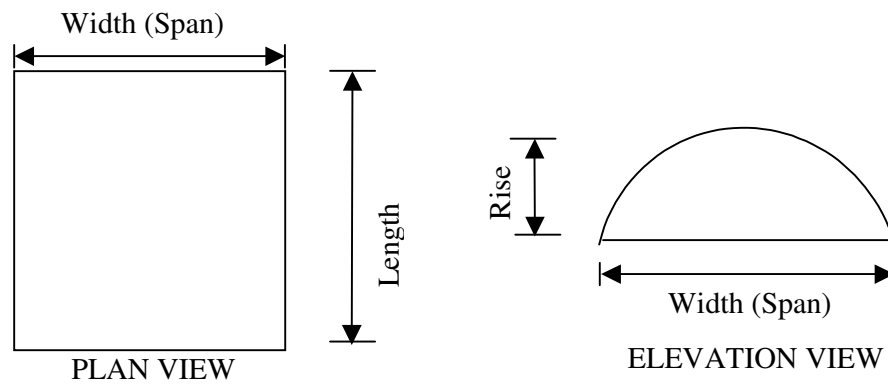


Fig. 2.4. Dimensions of Barrel Vault

Maximum efficiency may be attained for shapes with rectangular surfaces and a length-to-width ratio between 1 and 2. The rise-to-span ratio is more important for barrel vault and dome structures. A further description of rise-to-span ratio for domes will be given in the following chapters. For barrel vaults, the optimum shape (rise-to-span ratio) is in the region of 0,15 to 0,20.

Economical spans for single layer vaults are about 20 m. Spans may be increased by inserting diagonal elements. They reach 60 m for double layer systems, in some cases even more. Appropriate weights for double layer systems vary between 0,13 and 0,25 kN/m² depending on the intended shape, support conditions and the geometry of the sheets (for a uniform load of between 0,75 and 1,50 kN/m²).

2.1.2 Domes

A “**dome**” is a structural system that consists of one or more layers of elements that are arched in all directions. The surface of a dome may be a part of a single surface such as a sphere or a paraboloid, or it may consist of a patchwork of different surfaces.

Domes are of special interest to engineers and architects as **they enclose a maximum amount of space with a minimum surface** and have proved to be very economic in the consumption of constructional materials. Domes are also exceptionally suitable for covering sports stadia, assembly halls, exhibition centres, swimming pools and industrial buildings in which large unobstructed areas are essential and where minimum interference from internal supports is required. The provision of unobstructed sight-lines for large numbers of people is the primary requirement in sports halls and can easily be satisfied through the adoption of a domical shape. In the last 25 years construction with steel sections has largely replaced reinforced concrete. This fact has encouraged record spans of more than 200 m.

Braced steel dome structures have been widely used all over the world during last three decades. Some examples of braced steel domes in the world are shown in Figure 2.5 through 2.9.



Fig.2.5. Nagoya Dome, Japan



Fig.2.6. The Bloudel Conservatory, Queen Elizabeth Park, Vancouver/Canada



Fig.2.7. Astrodome (Steel Lamella Dome), Houston/USA

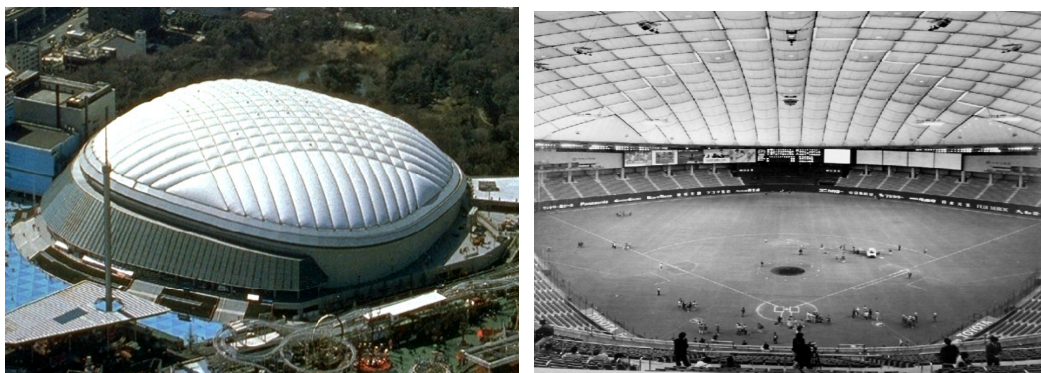


Fig.2.8. Tokyo Dome "Big Egg", Japan



Fig.2.9. Ontario Place, Toronto/Canada

In Turkey, these types of structures are not used as commonly as in the world. Besides, steel structures with space grid systems are preferred mostly. The photographs of some sample works built in Turkey are presented in Figure 2.10 through 2.14. These are smaller structures as compared to those in the world. Dome structures in Turkey have span lengths generally shorter than 40-50 m.

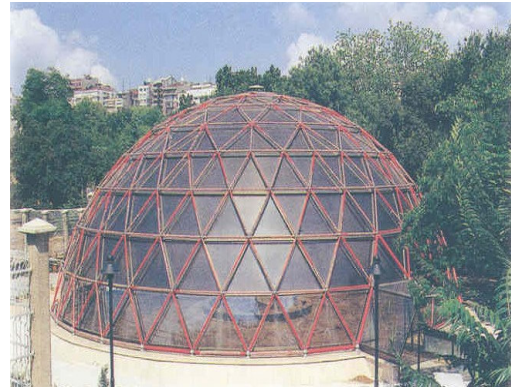


Fig.2.10. Roller Skating Track, Ankara Fig. 2.11. Cafe Building, Istanbul

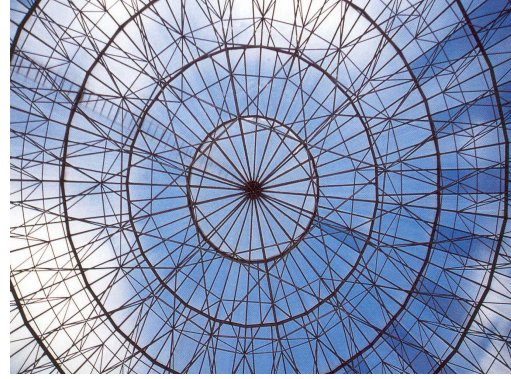
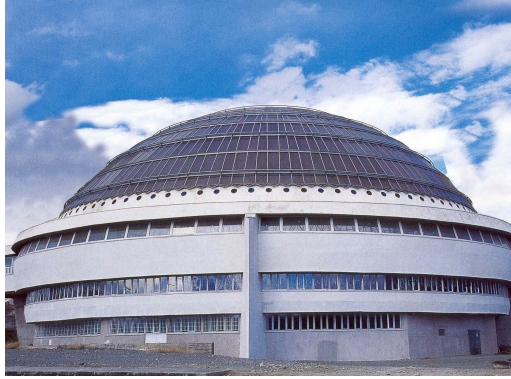


Fig.2.12. Terzi Baba Mosque, Erzincan



Fig.2.13. Bird Cage, Gaziantep

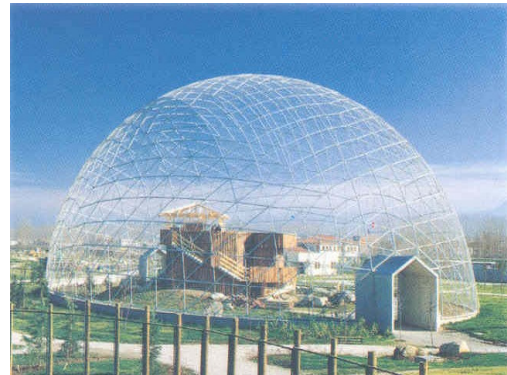


Fig.2.14. Water Fowl Cage, Bursa

2.2 Types of Braced Domes

Braced domes which have been built within the last years can be mainly classified in five groups:

- (i) Ribbed domes,
- (ii) Schwedler domes,
- (iii) Lamella domes,
- (iv) Two- and three-way (also four-way) grid domes,
- (v) Geodesic domes.

The commonly used basic single layer dome configurations are shown in Figure 2.15. There are also other types of domes which resemble the former ones with slight differences. These are network domes, plate-type domes, Zimmermann domes, Kiewitt domes and diamatic domes.

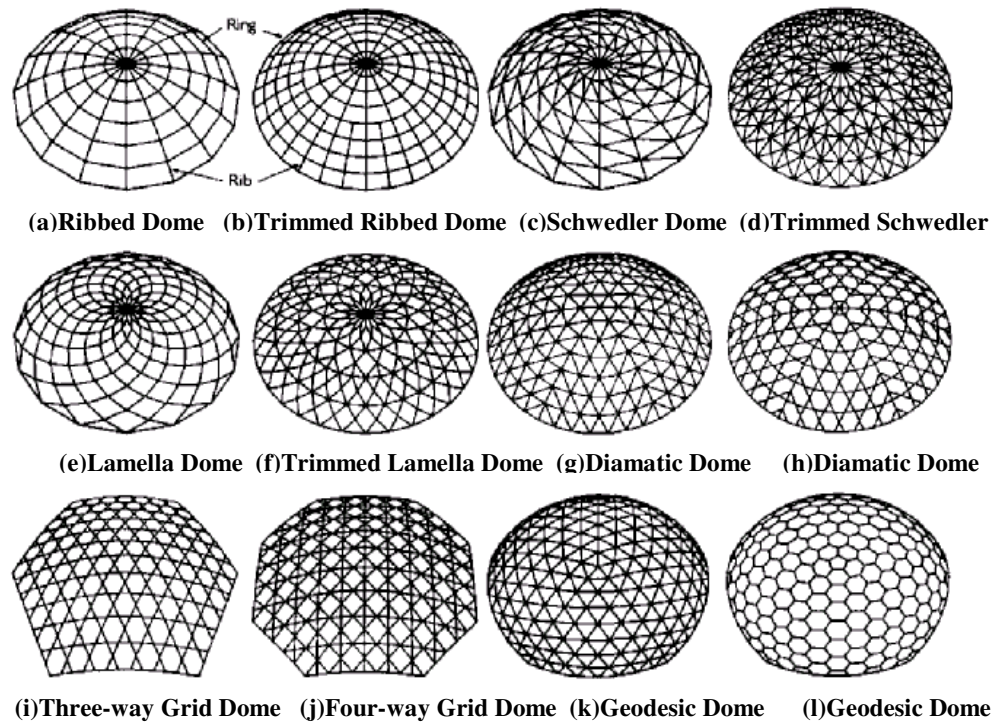


Fig. 2.15. Examples of Single Layer Domes

Braced domes are generally made up of steel, but sometimes aluminium and glass-fibre reinforced plastics can be used. Especially, aluminium is preferred due to the light weight, high corrosion resistance and ease of fabrication.

Domes are constructed as single layer or double layer. Single layer systems permit smaller spans of about 40 m while double layer systems can enclose more than 200 m span lengths. Double layer domes are exceptionally rigid and are used for very large spans.

These systems can be designed as rigidly-jointed system or pin-connected system. Since perfect pin connection is not possible, semi-rigid connected systems are also used nowadays. The analysis and connection details of these systems will be introduced in detail in the following chapters. Now we further look into the types of the braced domes and their structural behaviours.

2.2.1 Ribbed Domes

Ribbed dome consists of a number of intersecting “**ribs**” and “**rings**”. A “**rib**” is a group of elements that lie along a meridional line and a “**ring**” is a group of elements that constitute a horizontal polygon. Ribs can be radial trussed or solid. They generally interconnect at the crown and a tension ring at the foundation stiffen the ribs. A ribbed dome will not be structurally stable unless it is designed as rigidly-jointed system, since it does not have diagonal elements.

2.2.2 Schwedler Domes

J.W.Schwedler, a German engineer, who introduced this type of dome in 1863, built numerous braced domes during his lifetime. A Schwedler dome, one of the most popular types of braced dome, consists of meridional ribs connected together to a number of horizontal polygonal rings. To stiffen the resulting structure so that it will be able to resist unsymmetric loads, each trapezium formed by intersecting meridional ribs with horizontal rings is subdivided into two triangles by introducing a diagonal member.

Many attempts have been made in the past to simplify the analysis of Schwedler domes, but it is only during the last decade that precise methods of analysis using computers have finally been applied to find the actual stress distribution in these structures.

2.2.3 Lamella Domes

The lamella system was invented in Europe in 1906 by Mr.Zollinger, a German city architect. The lamella dome consists of a large number of similar units, called lamellas, arranged in a diamond or rhombus pattern. Each lamella unit has a length which is twice the length of the side of a diamond. Roof covering or purlins used to triangulate the diamond complete the stability requirement of the surface of the dome. A lamella dome has a diagonal pattern and may involve one or more rings.

The great popularity of lamella domes is due to their exceptionally good behaviour under excessive wind loadings, as well as in fire and seismic disturbances.

2.2.4 Two- and- Three-Way Grid Domes

A grid dome is obtained by projecting a plane grid pattern onto a curved surface. Grid domes are normally rather shallow with their rise to span ratios being smaller than the other types of domes.

The intersection of three-way grid dome members form a triangular space lattice. A modified type of three-way grid is four-way grid dome which has denser pattern.

2.2.5 Geodesic Domes

Richard Buckminster Fuller, the inventor of geodesic domes, has made a phenomenal impact on architects since 1954. Nature – said Buckminster Fuller- always builds the most economic structures. He claimed that geodesic domes based on mathematical principles embodying force distributions similar to those found in atoms, molecules and crystals will be the lightest, strongest and cheapest constructions ever made.

A geodesic dome configuration is obtained by mapping patterns on the faces of a polyhedron and projecting the resulting configuration onto a curved surface. In Figure 2.15.(k), geodesic dome is obtained by mapping a triangulated pattern on five neighbouring faces of an icosahedron (20-faced regular polyhedron) and projecting the result onto a sphere which is concentric with the icosahedron. The geodesic dome of Figure 2.15.(l) is obtained in a similar manner with the initial pattern chosen such that the resulting dome has a honeycomb appearance.

The truth of the matter is that geodesic domes are simply another type of triangulated dome in which the elements forming the skeleton of the structure are curved and lying on the great circles of a true sphere.

Five regular polyhedra (tetrahedron, cube, octahedron, dodecahedron, icosahedron) and fifteen semi-regular polyhedra (i.e. truncated tetrahedron, truncated cube, truncated octahedron, truncated dodecahedron, truncated icosahedron, semi-regular prism, rhombicuboctahedron, semi-regular prismoid, cuboctahedron, icosidodecahedron, snub-cube, snub-dodecahedron, rhombicosidodecahedron, truncated cuboctahedron, truncated icosidodecahedron) can be used in the design form of geodesic domes.

2.3 Load-Carrying Characteristics of Braced Domes

A different classification of dome structures can be made according to the types of load-carrying styles. These are;

- (i) Frame or skeleton-type single-layer domes,
- (ii) Truss-type domes and double-layer domes (used for covering large spans),
- (iii) Stressed skin type domes,
- (iv) Formed surface type domes (in which thin steel, aluminium or other sheets are bent and interconnected along their edges to form the main skeleton system of the dome, resembles the shell structures)

Since single-layer domes are introduced previously, the other types will be discussed in the following.

2.3.1 Double-Layer Domes

For domes built from light material (such as aluminium) and having clear spans over 60 m., the arrangement of the bars of the framework in a single layer no longer provides the necessary rigidity. Experiences show that, in such a case, especially when the structure is under the action of unsymmetrical loading, such as snow loads, the dome may fail, not on account of high stresses exceeding the maximum strength of the material, but instead due to insufficient elastic stability of the compression bars. Introducing light materials to the dome design, such as aluminium, results in a great reduction in the dead weight of the structure, on the other hand this can lead to slender members susceptible to elastic instability.

Experiences show that this difficulty can be overcome by the use of double-layer braced domes. Outer and inner surfaces of double-layer domes are interconnected with bracing elements. Two surfaces (outer and inner) can be identical or different depending on the design. The famous structure of US Pavilion for Expo 67, Montreal, Canada was three-quarter sphere designed as a double-layer grid. The dome was 61 m high and has a diameter of 76 m. The photographs of this structure are presented in Figure 2.16.

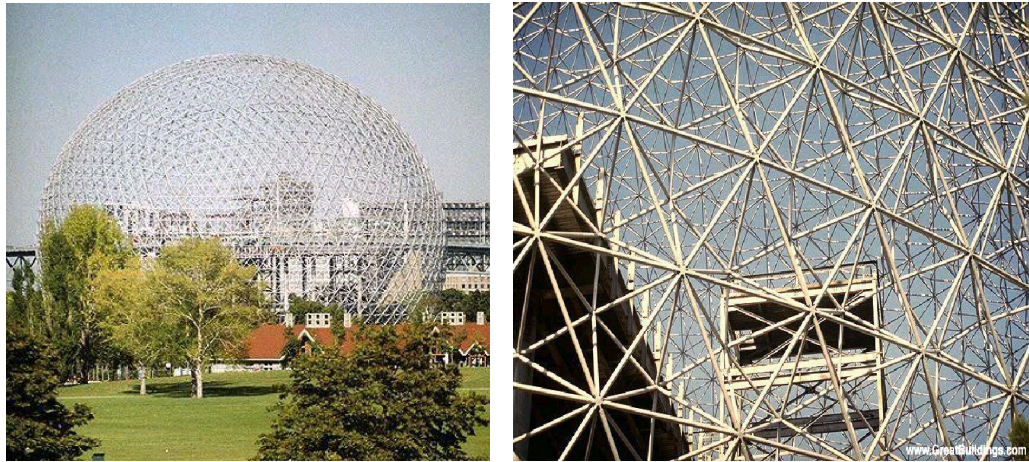


Fig.2.16. US Pavilion Building for Expo 67 (Double-Layer Grid Dome)

2.3.2 Stressed-Skin Geodesic Domes

In the design of domes, it is usually assumed that the covering does not contribute to the overall stiffness of the structure. But one kind of dome is produced by combining both frame and skin into a single structural element. This type is called stressed-skin geodesic dome. Basic unit is a panel (for example diamond shape) of aluminium sheet, with an aluminium strut stretching across its surface. In this way, skin's structural strength is taken advantage. Such a structure was produced first by Kaiser Aluminium firm, in 1957. The advantages claimed by Kaiser Aluminium for their first aluminium dome over the conventionally designed buildings included lower cost, remarkable speed of erection and remarkable structural strength. However, the practical experience showed that the sealing of the joints can become an extremely difficult problem. Pictures of stressed-skin geodesic domes are shown in Figure 2.17.

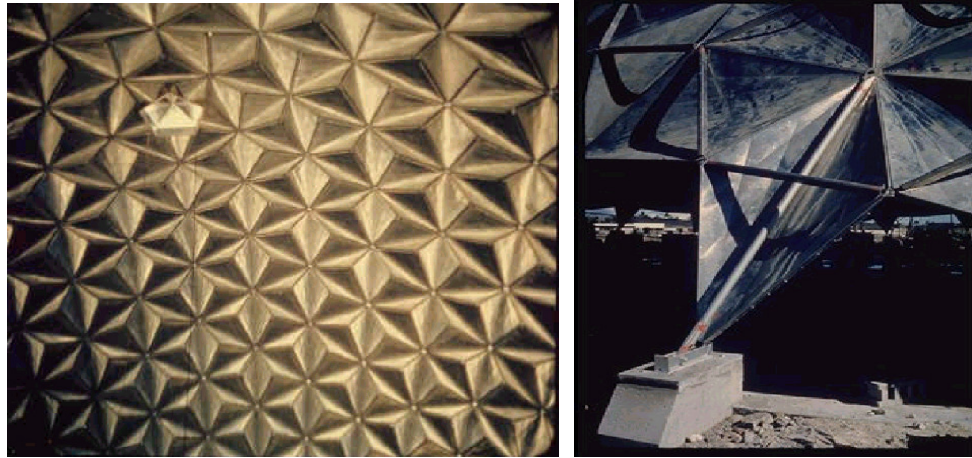


Fig.2.17. The Inside View and Support Detail of Stressed-Skin Geodesic Dome

2.4 Components of the Braced Domes

This thesis is concentrated on investigating the design and optimization of pin-connected truss type dome structures. These structures are modeled as 3-D truss which consists of 1-D steel bars. Generally, steel bars having circular cross-sectional area (tubular sections) are used as truss elements, because of their large and uniform radius of gyration. The details of analysis and design of these systems will be given more thoroughly in the following chapters.

The pin-connected dome structures mainly consist of three structural parts; bars, truss joints (nodes) and bolts.

Bars consist of circular pipes with conical tips welded at both ends. These conical tips can transmit both tensile and compressive forces. The bars and cones are manufactured of St-37 and St-52 quality steel.

Truss joints (nodes) are manufactured in the form of spheres or half-spheres by hot-forcing technique. Spheres have bolt holes all threaded. The bar elements can be screwed into these holes at the site. These elements are produced from St-52 or St-60 quality steel.

Bolts with their heads inside the conical tips are free to rotate. A hexagonal member very similar to a nut is placed between the conical tip and the sphere node. These nut-like members which contain pin holes are doweled to the bolts and help to fix the bolts to the spheres. The connection, node, member end and support details are presented in Figure 2.18 through 2.22.

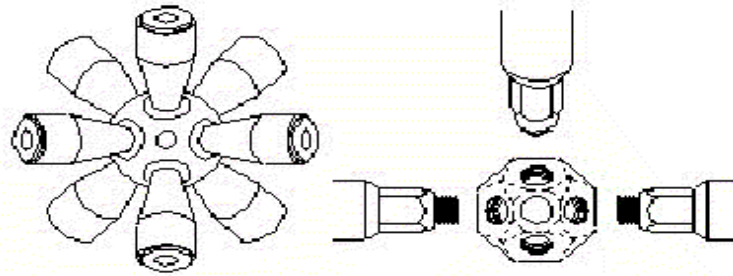


Fig.2.18. Node Detail

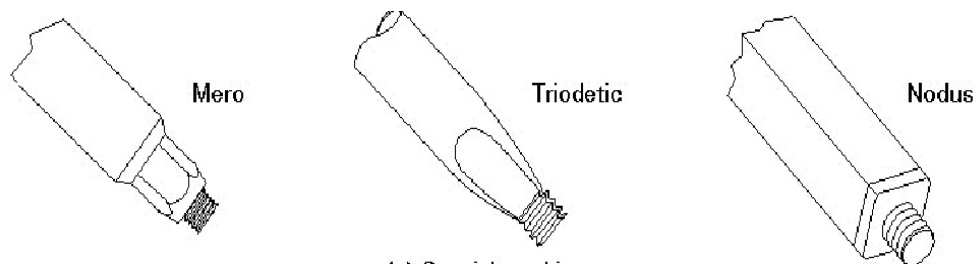


Fig.2.19. Member End Details

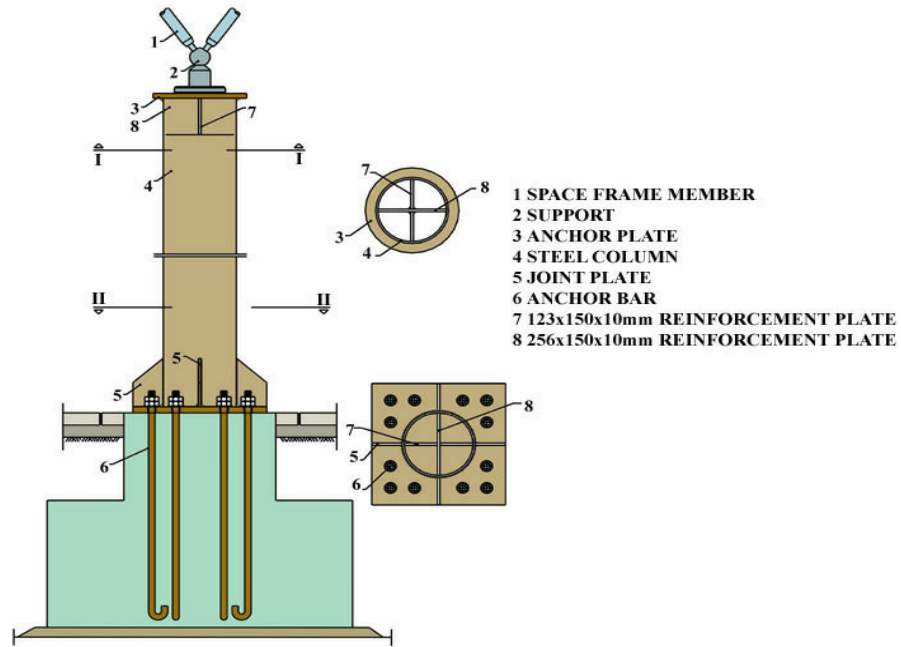


Fig.2.20. Support Details of Dome Structures (taken from Technical Specification of USKON)

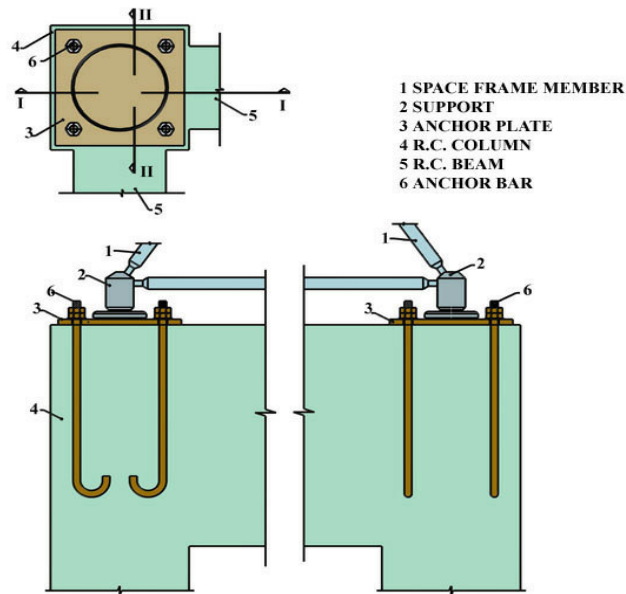


Fig.2.21. Support Details of Dome Structures (taken from Technical Specification of USKON)

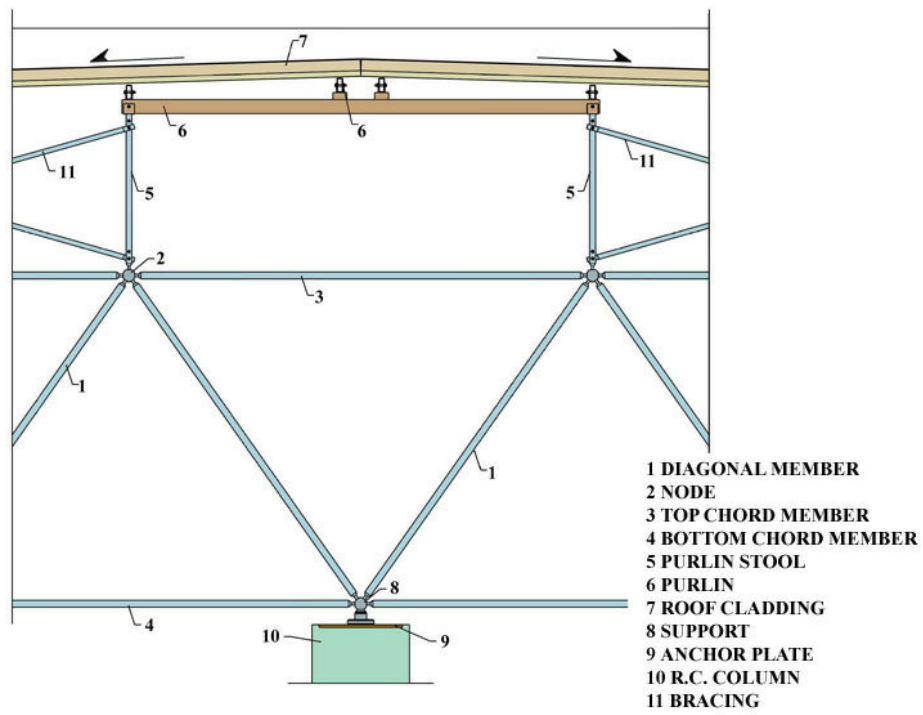


Fig.2.22. Connection Details of Dome Structures (taken from Technical Specification of USKON)

CHAPTER 3

ANALYSIS AND DESIGN OF BRACED DOMES

3.1 Types of Analysis

Before engineering structure is analysed, it is represented by an idealized mathematical model whose behaviour is sufficiently close to that of the original engineering structure. The idealizations available for braced dome structures fall into two distinct groups: the equivalent shell methods and the discrete structure methods.

The equivalent shell methods make use of orthotropic shell theory. The orthotropic shell stiffnesses which occur in the theory are replaced by equivalent shell stiffnesses. So this method is a coarse approximation, which was used widely before the availability of powerful computers. The equivalent shell methods are best used in the early design stages and for structures which are too large to be analyzed as discrete structures.

In the second group of methods, the analyst tackles the discrete structure directly. Within this group it is still necessary to select one of the several possible idealizations. The principal choice is between a space truss analysis (joints assumed pinned) and a space frame analysis (joints assumed continuous). There are also various non-linear effects which can and sometimes must be considered. The

discrete structure methods lead to a large set of simultaneous equations which can only be solved with the help of a computer.

3.1.1 Braced Dome Behaviour

Before an engineer design or analyze a structure, he should have a sound qualitative understanding of how the structure will behave. A shell dome resists loads with a force system acting in the surface of the shell. Typically, there will be a principal compressive force acting vertically in the surface of the dome and a lesser horizontal force (usually tensile) acting around the dome.

The way a braced dome works depends on the configuration of the members. Braced domes which are fully triangulated will have a high stiffness in all directions in the surface of the dome. These configurations are also kinematically stable (no mechanism) when idealized as a space truss. Accordingly, the forces in a fully triangulated dome will be principally axial and will have direction and magnitude similar to those in a shell dome. As recall from the figures of domes built in Turkey, they are all single-layer triangulated truss type (assumed as pin-connected joints) structures due to the instability (mechanism) concern.

Dome with a single layer must be triangulated as shown in Fig.3.1.(a) in order to be stable. A dome which is not fully triangulated is kinematically unstable when idealized as a truss and may also have widely different stiffnesses in different directions in the surface of the dome. The dome shown in Figure 3.1.(b) can only support loads by developing bending moments in the members and joints. The dome shown in Figure 3.1.(c) will require continuous joints or structural cladding to give the dome stability and to resist non-axisymmetric loading.

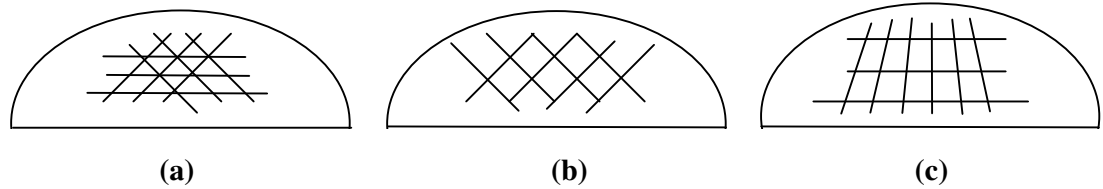


Fig.3.1. Arrangements of Bracing

3.2.2 The Instability Phenomenon

General buckling, local buckling (involving the snap-through buckling which will be discussed later) and individual member buckling are the types of instability that must be checked in the design. An important point that should be kept in mind is that one should be careful in using single layer domes unless the jointing system provides sufficient rigidity for the connections and that the elements are designed for resisting bending and shear in addition to the axial forces. Otherwise, the structures will be susceptible to snap-through buckling. This comment also applies to the case of single layer barrel vaults.

Critical buckling load is the maximum load which a member can support before it becomes unstable. Buckling is a form of failure which is often thought to be anathema within the plastic theorems and plastic design.

Buckling and its analysis can be divided into two parts as linear (eigenvalue) buckling analysis and non-linear buckling analysis.

Linear (eigenvalue) buckling analysis predicts the theoretical buckling strength (bifurcation point) of an ideal linear elastic structure. An eigenvalue buckling analysis of a column will match the classical Euler solution.

Non-linear buckling analysis is usually the more accurate approach and is recommended for design or evaluation of actual structure. This technique employs a non-linear static analysis with gradually increasing loads to seek the load level at which your structure becomes unstable. To summarize, one major characteristic of non-linear buckling, as opposed to eigenvalue buckling, is that non-linear buckling phenomenon includes a region of instability in the post-buckling region, whereas eigenvalue buckling only involves linear, pre-buckling behaviour up to the bifurcation (critical loading) point. This behaviour is shown graphically in Figure 3.2.

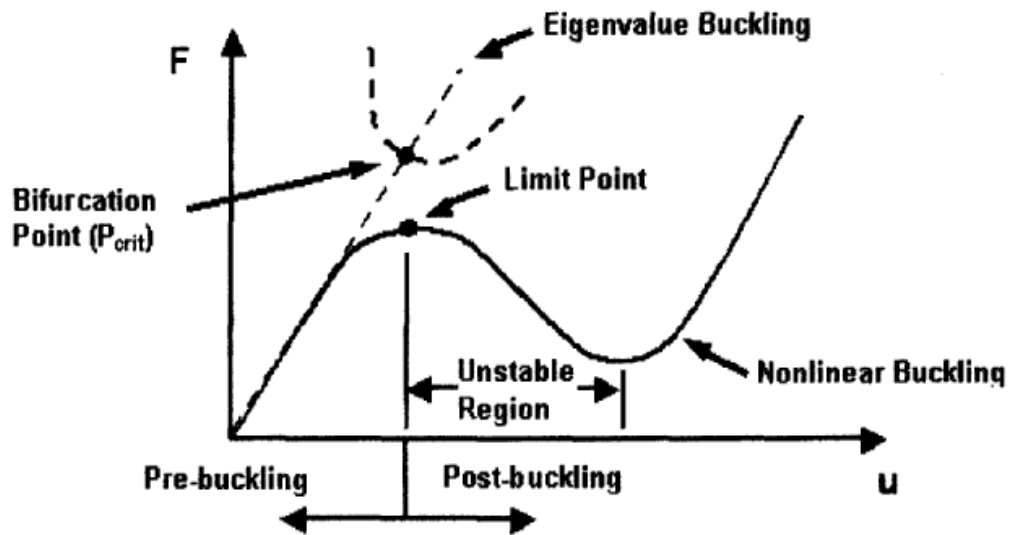


Fig.3.2. Non-linear vs. Eigenvalue Buckling Behaviour

An elastic structure with non-linear unstiffening characteristics may lose its stability in one of two ways. First, the unstiffening associated with the initial mode of deformation may, by gradual reduction, reach the stage where the stiffness is lost completely. It is then said that the load-deflection equilibrium path of the structure has reached a "limit point" and a dynamic jump occurs to a highly deformed configuration. This process is referred to as snap through or snap buckling and is typical of the symmetric deformation of shallow arches and domes (Fig.3.3. and

3.4). Snap through buckling of steel arches (or domes) occurs when the combination of axial load and moment at a point causes the arch (or dome) to reverse curvature locally. Eventually, the curvature may mean that the thrust generates enough moment to remove the stiffness of the section all together, at this point, the arch (or dome) sags through and comes to rest as a tension structure, if its supports can sustain it (Fig.3.3). Snap through results in total failure. Moment redistribution cannot then occur. It is vitally important that snap through is not allowed to develop. The severity of the snap through under controlled or dead loading depends upon the degree of non-linearity or contortion of the equilibrium path in the load-deflection space. This is governed by the rise-to-span ratio of arches or domes and is well understood. A very shallow dome (arch) may show no snap through characteristic at all; the load-deflection equilibrium path would be non-linear but stable throughout. This, however, is not a practical dome (arch) geometry. As the rise-to-span ratio is increased, the non-linearity of the response increases and the equilibrium path is characterized by a limit point. The severity of the instability increases as the rise-to-span ratio increases.

The second way in which a non-linear unstiffening structure such as a dome may lose its stability is by a sudden buckling into a mode of deformation which is quite distinct from the initial unstiffening mode. For uniformly loaded domes, this means the abrupt adoption of a rotationally unsymmetric mode with associated loss of stability before the limit point on the equilibrium path of the symmetric mode is reached. For a geometrically symmetric structure under symmetric loading, this event occurs at a distinct critical point or “bifurcation point” on the non-linear initial load path (Fig.3.2). A second equilibrium path, which is unstable and represents the unsymmetric buckling mode, intersects the initial load path at this point and the initial load path itself becomes unstable. In the terminology of the general theory of elastic stability, the post-buckling characteristic of the unsymmetric buckling mode is “unstable symmetric”.

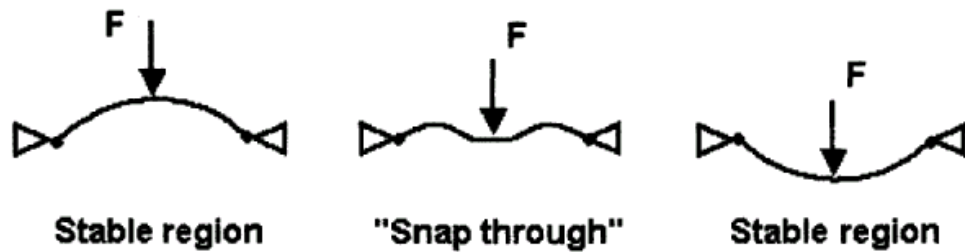


Fig.3.3. "Snap-Through" Buckling

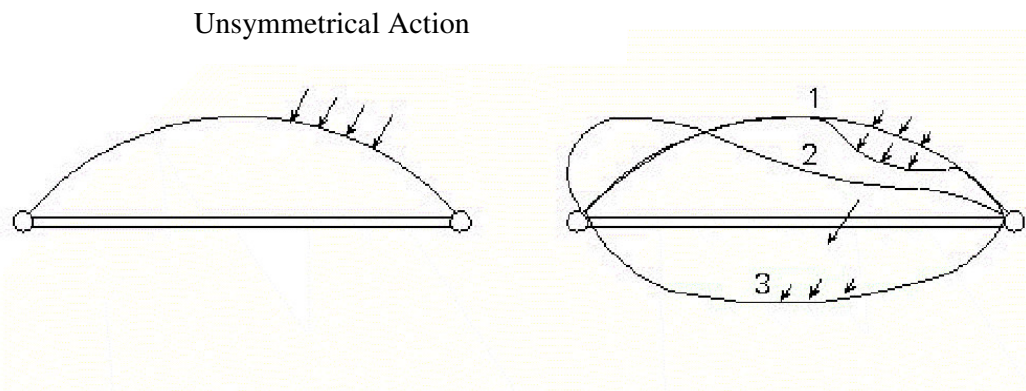


Fig.3.4. "Snap-Through" Buckling

3.2 Analysis

The analysis of a structure is an integral part of the design process applied to that structure. Analysis can be divided into linear and non-linear analysis. A simple linear elastic analysis in association with suitable permissible stresses can check for all types of local member (or joint) failure. These include yield, member buckling, fracture, fatigue and sliding at joints. The first yield load is also a lower bound on the shakedown load. However, to check for instability effects involving more than one member or geometry change and also to exploit any post first yield strength that might be available in the structure, the designer must include non-linear effects in

the analysis. Non-linear effects can be divided into member effects such as plastic yielding and geometric effects.

Methods of non-linear analysis can be divided into three approaches. The first is the plastic mechanism approach, which is not really applicable to braced domes. The second is the stability approach, which involves the location of bifurcation points in a perfect structure. This approach can accommodate geometric but not member non-linearities. The third is the incremental approach. In this approach, the load is applied in small increments. At each increment, the stiffness of the structure is recalculated to accommodate changes in member stiffness, structure geometry, indeed all relevant non-linear phenomena. The structure is normally given assumed initial deformations and locked-in stresses to give a more representative analysis.

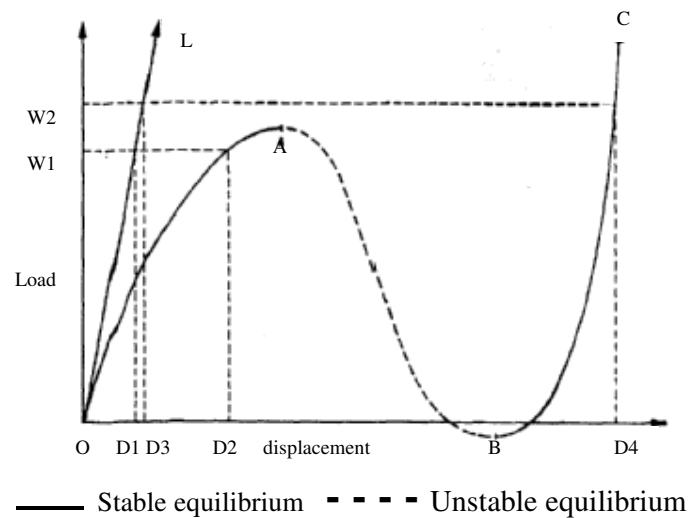
Member non-linearities are accommodated by assuming a stress-dependent member stiffness. The easiest to program is the elastic-perfectly plastic case, where the member stiffness simply changes to zero. An improvement is the non-linear elastic case, which can model the falling force in a buckled member. Further sophistication can be obtained by modeling elasto-plastic flow using a yield criteria and flow rule containing the member stress resultants. Finally, the member can be subdivided into layers.

Geometric non-linearities can be critical in braced domes; in particular, with shallow or unevenly loaded domes, it may be essential to check for snap-through buckling.

For many braced domes a space truss idealization will be sufficient. A space truss analysis can incorporate both member and geometric non-linearity. A full space-frame analysis is only required for structures which have a significant bending action, such as non-triangulated domes, domes with continuous curved members and possibly some very shallow single-layer domes.

Linear structural analysis, as the name implies, deals with the analysis of structures which behave linearly. Virtually no structural systems behave in a truly linear fashion, but most practical systems behave almost linearly within the range of loadings for which they are designed. In the analysis of a linear system, the equations of equilibrium are set up in terms of the undisplaced shape of the structure and solved to evaluate the displacements. Most techniques for non-linear analysis consist of a series of linear analyses, each iteration resulting in successively closer approximations to the solution of the system. The first iteration is generally the same as the basic linear analysis with subsequent iterations taking into account non-linearities such as geometric effects and the effect of axial forces on bending moments. After the first iteration, the equilibrium equations are generally set up in terms of the displaced shape of the structure calculated by the previous iteration. From this it can be seen that linear analysis is simpler than non-linear analysis and that a knowledge of linear analysis is an essential prerequisite for an understanding of non-linear analysis.

Although, discussed formerly, it is worth emphasizing the differences between linear and non-linear analyses of domes once again. The load-displacement relationships for a typical simple shallow single-layer braced dome are shown in Figure 3.5. This shows that a linear analysis will not predict such phenomena as local or global snap through of the structure, suggesting that a linear analysis is unsuitable for such structures as the results are a first approximation of indeterminate accuracy. This is true to a large extent, but a linear analysis is still useful as a guide for sizing members.



- OL - load-displacement relationship for linear analysis
- OASC - load-displacement relationship for structure
- A - snap-through occurs and stability is lost
- B - dome is now inverted and regains stability
- D1 - displacement due to load W1 as predicted by linear analysis
- D2 - actual displacement occurring due to W1
(non-linear analysis would predict this value)
- D3 - displacement due to load W2 as predicted by linear analysis
- D4 - actual displacement occurring due to W
(non-linear analysis would either predict this value or indicate instability at point A)

Fig. 3.5. Load-Displacement Relationship

Linear structural analysis may be safely used in the majority of structural analysis problems to predict structural behaviour. However, there are certain classes of problems which are inherently non-linear and for which linear analyses should be used with caution if at all. The displacements of structural systems which display *non-linear stiffening* behaviour, such as some cable structures, will be overestimated by linear analyses, whereas the displacements of structural systems displaying *non-linear unstiffening* behaviour will be underestimated by linear analysis. The latter cases are potentially more dangerous, since safe-load values predicted by linear analysis may in reality lead to excessive displacements and instability. However, for structures which behave in a non-linear manner, there is

generally a range of load and displacement values for which a linear analysis will approximate the behaviour sufficiently accurately. The problem facing the designer is the determination of this range, having already decided that the structure is potentially non-linear. If this range is found to be too restrictive, a nonlinear analysis will be required. By its very nature, a non-linear analysis will be more expensive than a linear one and so the decision to opt for the former will be an important one for the designer. The problem seems to be, therefore, whether a non-linear analysis is required and, if so, whether analytical techniques are available and suitable for the structure under consideration.

3.2.1 Linear Elastic Analysis

Stiffness method is used commonly as linear elastic analysis. The stiffness method allows us to analyze a structure which is an arbitrary assembly of simple structural members. This method is sometimes referred to as the displacement method or stiffness matrix method. In this method of analysis, equations of equilibrium are set up in terms of the nodal displacements as unknowns. These equations are solved to evaluate the nodal displacements and from the displacements, member forces are calculated using the force-displacement relationships for each element.

The analysis requires a large amount of linear algebraic manipulation and the most suitable branch of mathematics for representing such manipulations is matrix algebra. In addition to being ideally suited to computer implementation, matrix algebra allows the basic concepts to stand out, allowing the fundamental principles to be easily and readily appreciated.

Undeformed geometry can be used in a structure undergoing small displacements. The behaviour of such a structural system is described by Hooke's law, which has the general form

$$P=kx \qquad (3.1)$$

The fundamental equation used in matrix structural analysis, which is analogous to the basic expression of Hooke's law, is;

$$\bar{P} = \bar{K}.x \quad (3.2)$$

where

\bar{K} : Stiffness matrix of the structure,

x : Displacement vector of the structure,

\bar{P} : Appended force vector of the structure.

The basic difference is that simultaneous linear equations are dealt in the structural analysis. The force vector \bar{P} contains all of the forces that act at the structural coordinates. Displacement vector, x , contains the displacements at each of the structural coordinates.

The stiffness matrix, \bar{K} is analogous to the spring constant, k in Hooke's law. Stiffness can be defined as the force required to cause a unit deformation in an elastic material. The stiffness matrix can be divided into element stiffness matrix and structural stiffness matrix. So two different coordinate systems are defined for these stiffness matrices. These are local (element) coordinate system and global (structure) coordinate system. The local coordinate system is a relative coordinate system which differs for each member. The direction of the longitudinal element is chosen as x-axis. The global coordinate system is associated with the entire structure. The local and global coordinate axes for a 2-D structural element are shown in Fig.3.6

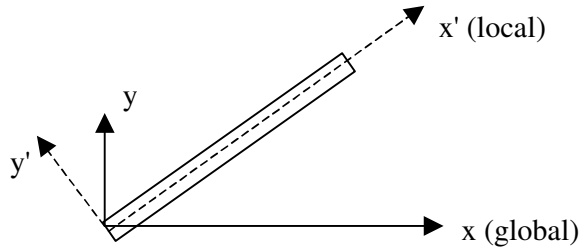


Fig.3.6. Local and Global Coordinate Axes of A 2-D Element

So the stiffness matrix which is formed by using the local coordinate system is called local (member or element) stiffness matrix or stiffness matrix in local coordinates. The stiffness matrix which is formed by assembling the local stiffness matrices in global coordinates is called global stiffness matrix or stiffness matrix in global coordinates. The global structural coordinates are used to define the displacements and forces acting on the entire structure. The local coordinate systems do not have to be oriented in the same direction as global coordinates.

The equation (3.2) can be written for a 3-D truss member in local coordinates;

$$\bar{p} = \bar{k}.x \quad (3.3)$$

$$\begin{bmatrix} F_{x1} \\ F_{y1} \\ F_{z1} \\ F_{x2} \\ F_{y2} \\ F_{z2} \end{bmatrix} = \bar{k} \begin{bmatrix} u_i \\ v_i \\ \omega_i \\ u_j \\ v_j \\ \omega_j \end{bmatrix} \quad (3.4)$$

where

u_i, v_i, w_i : displacements at node i for an element in the x, y, and z directions, respectively.

u_j, v_j, w_j : displacements at node j for an element in the x, y, and z directions, respectively.

Now, the stiffness matrix with respect to local coordinates (\bar{k}) must be converted to stiffness matrix with respect to global coordinates (\bar{K}). The transformation equation of stiffness matrix from local to global coordinates is given below:

$$\bar{K} = T^T \bar{k} T \quad (3.5)$$

where

\bar{K} : Global stiffness matrix,

\bar{k} : Local stiffness matrix,

T : Transformation matrix (from local to global coordinates) between the two-axis system (shown below for axial truss members).

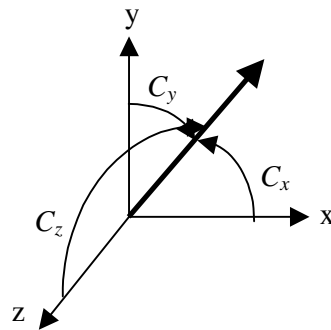


Fig.3.7. Transformation of Forces From Local to Global Coordinates

The global stiffness matrix for a 3-D truss member with respect to global coordinates is found as:

$$\bar{K} = \frac{E.A_x}{L} \begin{bmatrix} C_x^2 & C_y C_x & C_z C_x & -C_x^2 & -C_y C_x & -C_z C_x \\ C_x C_y & C_y^2 & C_z C_y & -C_x C_y & -C_y^2 & -C_z C_y \\ C_x C_z & C_y C_z & C_z^2 & -C_x C_z & -C_y C_z & -C_z^2 \\ -C_x^2 & -C_y C_x & -C_z C_x & C_x^2 & C_y C_x & C_z C_x \\ -C_x C_y & -C_y^2 & -C_z C_y & C_x C_y & C_y^2 & C_z C_y \\ -C_x C_z & -C_y C_z & -C_z^2 & C_x C_z & C_y C_z & C_z^2 \end{bmatrix} \quad (3.6)$$

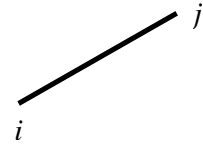
where C_x , C_y , C_z are direction cosines with respect to axes x, y and z respectively.

$$C_x = \frac{x_j - x_i}{L} \quad (3.7)$$

$$C_y = \frac{y_j - y_i}{L} \quad (3.8)$$

$$C_z = \frac{z_j - z_i}{L} \quad (3.9)$$

$$L = \sqrt{(x_j - x_i)^2 + (y_j - y_i)^2 + (z_j - z_i)^2} \quad (3.10)$$



After developing the stiffness matrices for each member of the entire structure in terms of global coordinates, these matrices can be assembled to form the global stiffness matrix for the entire structure. Total stiffness at a coordinate is the sum of the stiffness contributed to that coordinate by each element attached to that coordinate. A scheme shown as in Fig.3.8 is employed in order to develop the global stiffness matrix from the local (element) stiffness matrices.

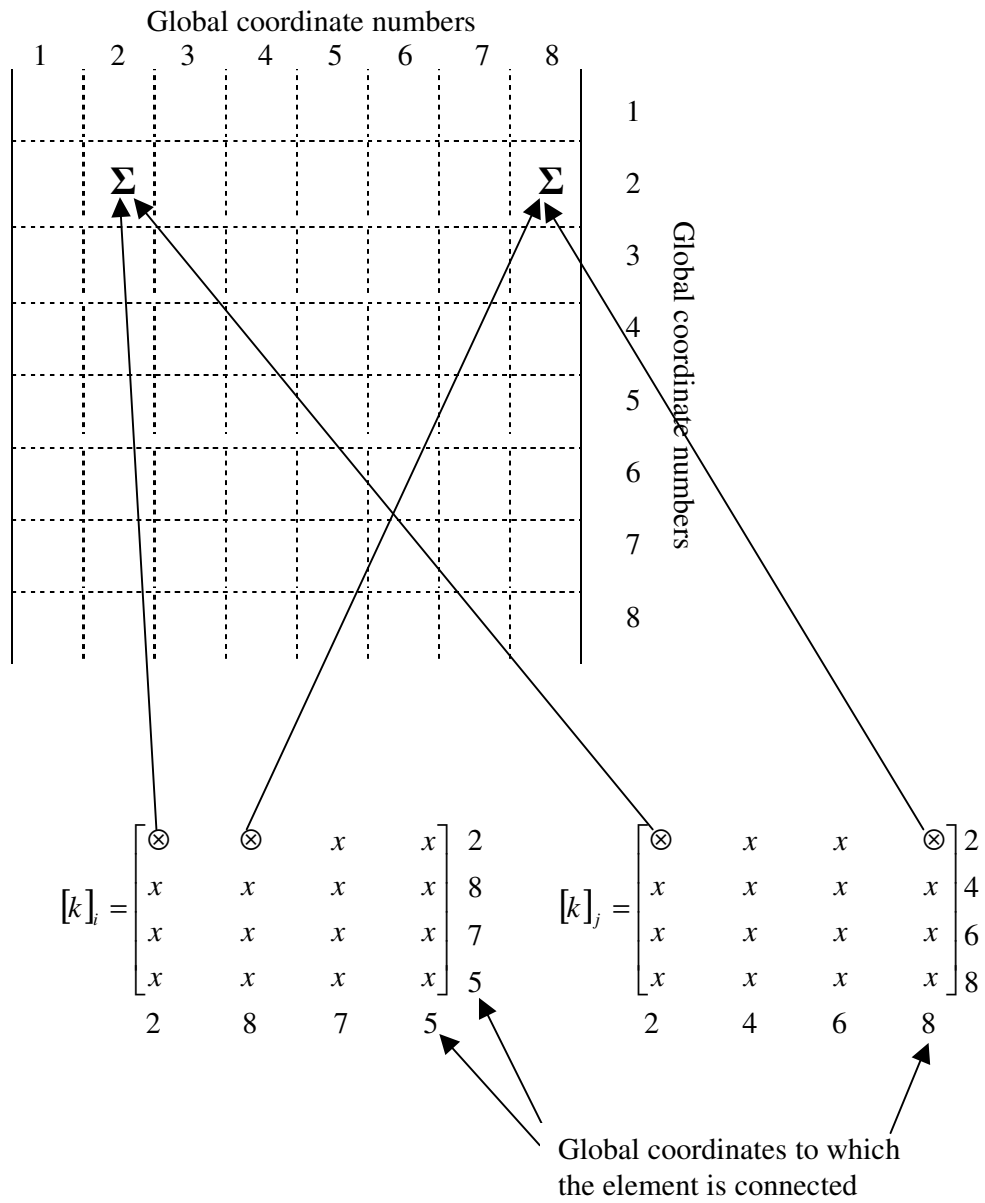


Fig.3.8. Combining Element Stiffness to Form the Global Stiffness Matrix

The solution of linear structure problems involves finding the solution to a set of simultaneous linear equations of the form shown above.

General procedure of solution consists of the following steps:

- (i) Forming local and global stiffness matrices,
- (ii) Decomposing stiffness matrices (by Choleski method or Gauss-Jordan elimination),
- (iii) Forming load vector,
- (iv) Solving system and evaluating displacements,
- (v) Evaluating member forces and reaction with the help of detected displacements,

Of course the preceding steps can be performed by a computer software in a short time. The general flowchart of stiffness method is presented in Fig.3.9.

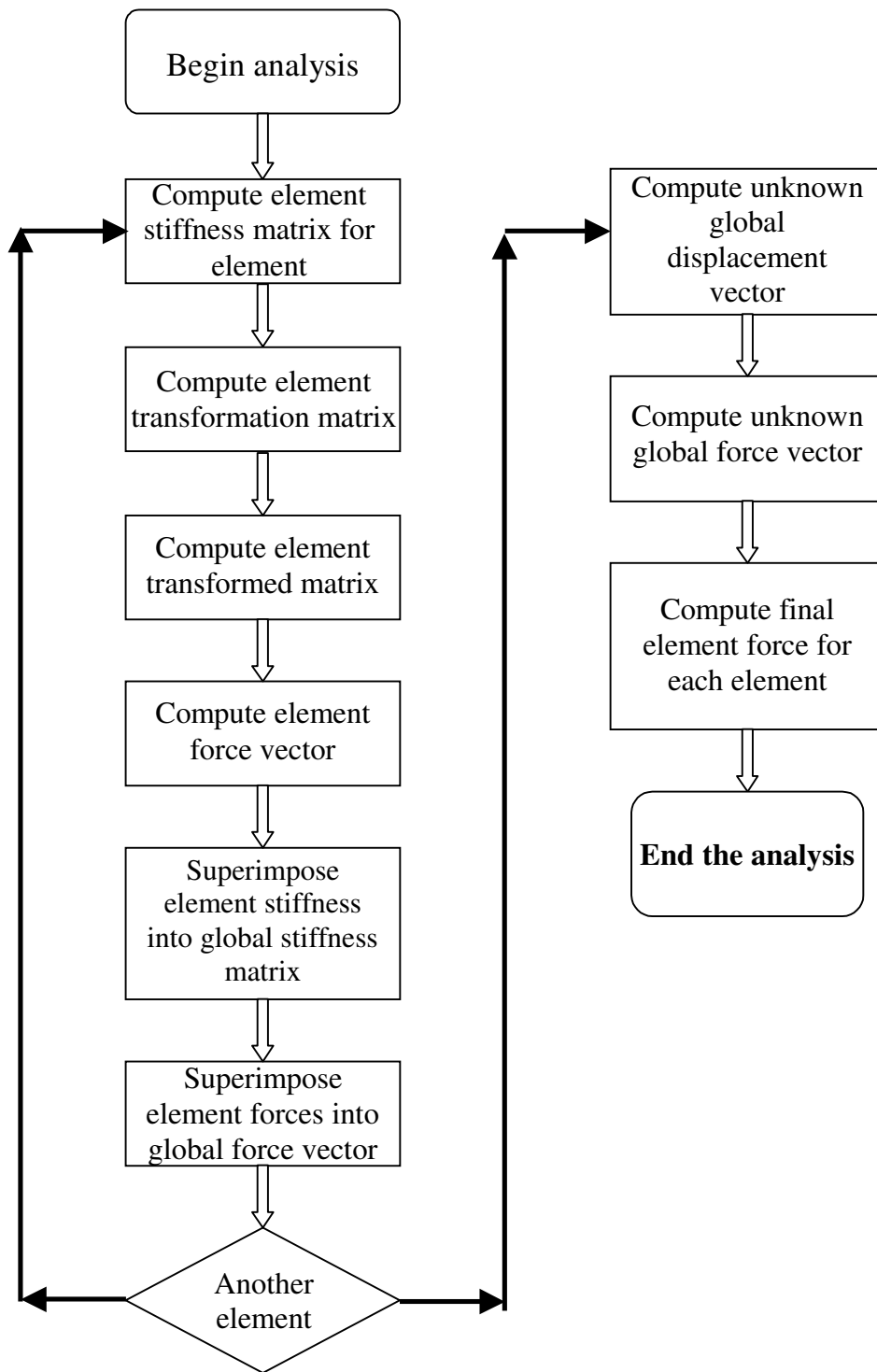


Fig.3.9. Flowchart of Stiffness Method

3.2.2 Non-linear Analysis

Non-linear structural analysis comprises a series of linear analyses and involves iteration.

The non-linear problem may be expressed as

$$K.x = P \quad (3.11)$$

where the matrix K has elements which are functions of x . The non-constant term of K are due to a change in geometry of the structure, and/or the non-linearity of the stress-strain curve for the structure material.

The classical method of solution is the Newton-Raphson iterative method, which attempts to converge the solution at each time step along the force deflection curve and can be expressed in the form

$$x_{(n+1)} = x_n + (K_n)^{-1}.e_n \quad (3.12)$$

where the residual e_n is given by

$$e_n = p - K_n x_n \quad (3.13)$$

and in which K_n represents K evaluated at $x = x_n$.

The inverse of K_n is not usually determined in practice but equation (3.11) is arranged in the form;

$$K_n (x_{(n+1)} - x_n) = e_n \quad (3.14)$$

and this linear system is solved for a particular x_n to determine the next iteration $x_{(n+1)}$. The process is repeated until the residual e_n is sufficiently small.

The Newton-Raphson method increments the load a finite amount at each substep and keeps that load fixed throughout the equilibrium iterations. Because of this, it cannot converge if the tangent stiffness (the slope of the force-deflection curve at

any point) is zero. See Figure 3.10. To avoid this problem, one should use the arc-length method for solving nonlinear post-buckling. To handle zero and negative tangent stiffnesses, the arc-length multiplies the incremental load by a load factor, λ , where λ is between -1 and 1. This addition introduces an extra unknown, altering the equilibrium equation slightly. To deal with this, the arc-length method imposes another constraint, stating that

$$l = \sqrt{\Delta \cdot x_n^2 + \lambda^2} \quad (3.15)$$

throughout a given time step, where is l the arc-length radius. The arc-length method therefore allows the load and displacement to vary throughout the time step as shown in Figure 3.11.

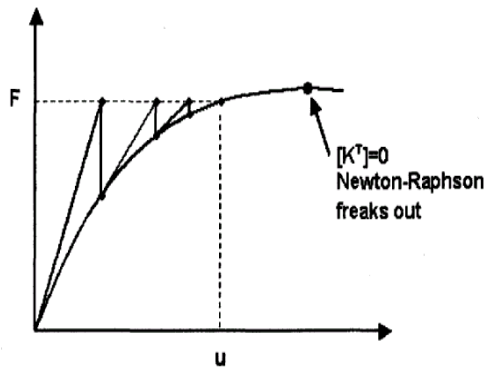


Fig.3.10. Newton-Raphson Method

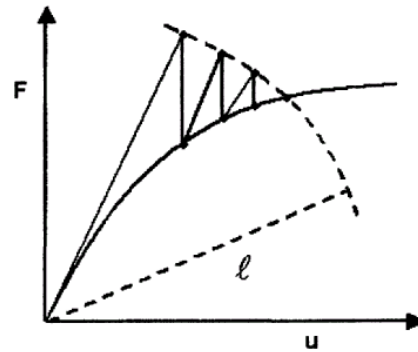


Fig.3.11. Arc-Length Method

3.3 Design Loads

The practical design of any large dome requires that at least three different loading systems should be fully analysed:

- (i) Dead load and snow over the whole dome.
- (ii) Dead load and unsymmetric snow load. It is usual to allow for the possibility of a build up of snow on one side of the dome.
- (iii) Dead load and wind.

3.3.1 Wind Loads

The determination of wind distribution on domic surfaces is still based on some very approximate assumptions. Experimental work, based on wind-tunnel tests, usually provides more reliable information. The researches show that the intensity of wind distribution varies greatly, depending mainly on rise-to-span ratios, and that the adjacent buildings have an important influence upon the distribution. Entrances, surface conditions, vents, etc., all have an effect on the flow conditions and pressure distribution. Designers of large-span domes should consider that the use of the usual wind-distribution formulas can be applied only to preliminary analysis; the final design should be based on wind-tunnel tests. Although it is thought that applying an equivalent vertical load to replace the wind load is a conservative procedure, the more detailed analysis based on the wind-tunnel tests shows that the pressure on the windward side combined with suction on the leeward side can frequently lead to much more unfavourable load conditions. Several researchers show that the approximate methods of analysis applied to unsymmetrical loading acting on a dome could produce a completely erroneous stress pattern.

Some tests carried out on large models and also, in one or two cases, on actual structures, show that the rigidity of the joints is a major influence upon the stress distribution and should be considered in the analysis.

The research results indicate that it is very difficult to obtain a reliable relationship between wind-tunnel tests and actual pressure distributions on real structures as the turbulence level, velocity profile in the wind tunnel and dimensional compatibility between model and prototype govern the model results. Also Reynolds number and its relation to boundary layer thickness are important. The tests reveal that an increase in turbulence leads to greater values of C_p (pressure coefficient). This influence grows as the span-to-rise ratio increases. The suction diminishes with increasing Reynolds number.

In short, it can be concluded that surface pressures depend on mainly Reynolds number, turbulence intensity and length scale, boundary layer immersion and surface roughness.

Dragone (1979) confirms that the wind pressure distribution on hemispherical domes has been found to have a small amount of positive pressure at the front of the dome and a large region of negative pressure at the back of the structure. As a consequence of that, the lift force in a particular region could be more critical than the total drag force of the structure.

For a dome immersed in a smooth and rough thick boundary layer of tunnel-test, where the height of the dome is less than half that of the boundary layer, different pressure distributions are obtained. With increasing boundary layer thickness the following observations can be made:

- (i) The base pressure (between approximately 120° and 180°) remain fairly constant at approximately - 0.15.
- (ii) The maximum suction force is markedly reduced.
- (iii) The maximum positive pressure is markedly reduced.
- (iv) A greater portion of the front part of the dome is affected by the boundary layer.

Despite the fact that the wind distribution coefficients are greatly varying in different codes and wind-tunnel tests depending on the factors mentioned above, two pressure distribution charts are given in Figure 3.12 and 3.13 in order to show a wind distribution profile on domic structures.

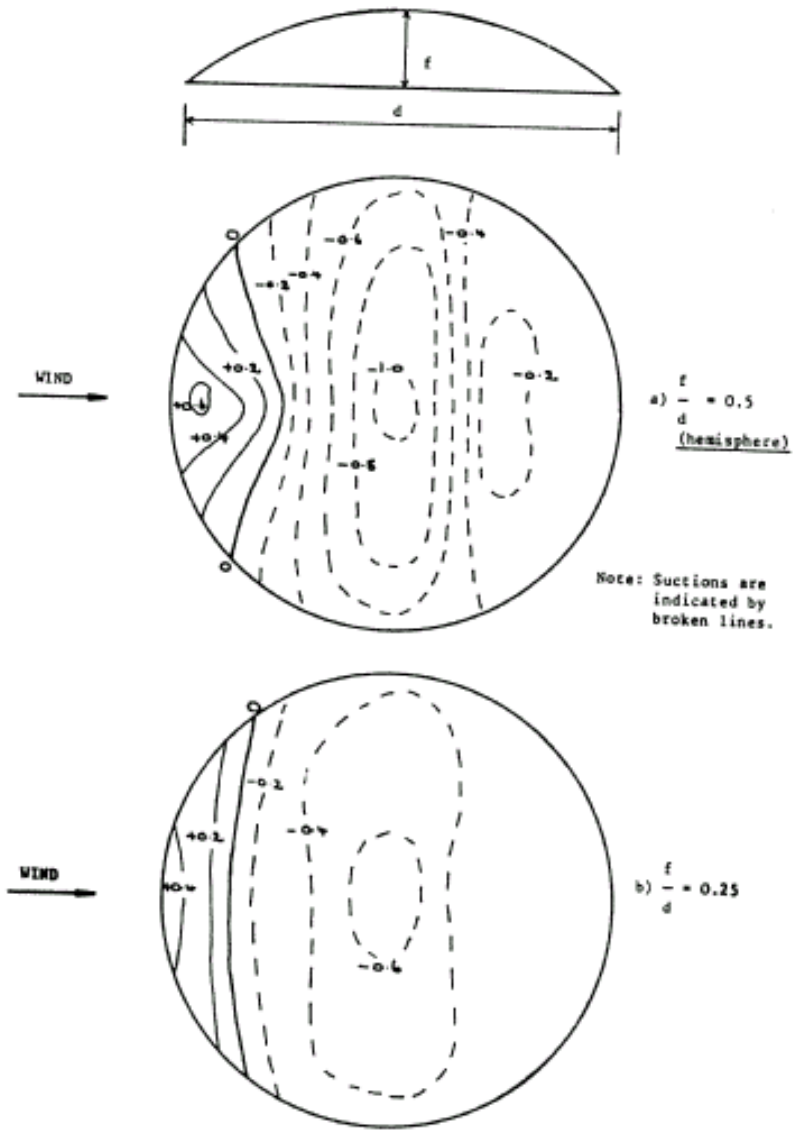


Fig.3.12. Pressure Distribution on Circular Domes Rising Directly from the Ground: Plan Views (quoted from *Wind Loading Handbook* (Newberry and Eaton, 1974))

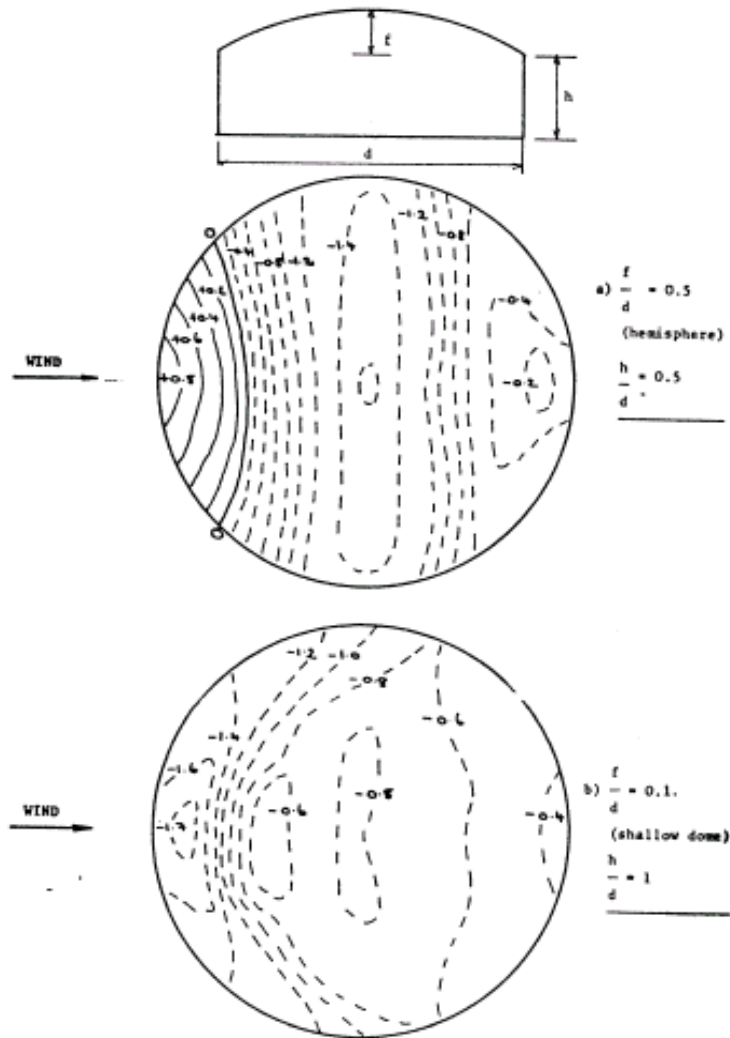


Fig.3.13. Pressure Distribution on Circular Domes Mounted on Cylindrical Bases: Plan Views (quoted from *Wind Loading Handbook* (Newberry and Eaton,1974))

In wind-tunnel tests, it is essential to simulate the velocity profile and turbulence of the natural wind and the Reynolds number effects associated with curved structures.

3.3.2 Snow Loads

The present state of analysis has reached a point where, with the use of computers, the linear elastic behaviour of these structures can be predicted with a very high degree of accuracy. However, single-layer domes of large span, especially under unsymmetric loads, do not behave linearly or fully elastically.

The collapse of some dome structures in the past (especially the collapse of the exhibition centre hall in Bucharest, Romania, in 1963, due to excessive snow load) have initiated new researches and studies and have led to further progress made in the design of domes. One of the most important factors which must be bear in mind is the influence of climatic loads.

Excessive snow accumulation on some part of a dome can cause the failure of the structure. In order to prevent this negativity, a uniform distribution of snow load must be applied not only over the entire dome surface (balanced case), but also over one half of the surface (unbalanced case).

3.3.3 Live Load, Dead Load

For dome structures, live load corresponds to the weight of the men climbing on the roof for various purposes, such as cleaning the roof, periodical care, etc. In load combinations, the effect of live load is not considered together with snow and wind loads due to fact that a structure is very less likely to be exposed to all these loads simultaneously.

Dead loads are the weight of the members, joints, cladding, purlins and other permanent elements (including service loads such as lighting equipment, ventilation system elements, catwalk, suspended ceiling, etc.). Dead load is taken as a uniformly distributed load acting on the surface.

3.3.4 Earthquake Loads

Since the braced domes are very light structures as compared to the reinforced concrete structures, in many cases earthquake loads will not be critical as compared to wind and snow loads. Despite this fact, they are taken into account with respect to earthquake zone specified in the codes.

3.3.5 Temperature Changes

Since the elements of braced domes are made of metal, the temperature changes may create additional loads on the members and joints. Therefore, it is recommended that the effect due to temperature change be included in the analysis of domes.

As stated before, the most important loads for domic structures are wind and snow loads. These loads will be examined more thoroughly in Chapter 4.

CHAPTER 4

LOADS ACTING ON DOME STRUCTURES

4.1 Introduction

Loads are forces or other actions that result from the weight of construction materials, occupants, environmental effects, differential movement and dimensional deficits. The most well-known loads can be classified as: dead load, earthquake load, load due to fluids, flood load, load due to lateral earth pressure, load due to ground water pressure, live load, rain load, snow load and wind load. Among these loads, wind and snow loads are more critical for dome structures. In this chapter, wind and snow loads according to ASCE 7-98 Minimum Design Loads for Buildings and Other Structures are to be examined.

4.2 ASCE 7-98

4.2.1 Load Combinations

According ASCE 7-98, combining nominal loads using allowable stress design are listed below:

- (i) D
- (ii) $D + L + F + H + T + (L_r \text{ or } S \text{ or } R)$
- (iii) $D + (W \text{ or } 0.7 E) + L + (L_r \text{ or } S \text{ or } R)$
- (iv) $0.6 D + W + H$
- (v) $0.6 D + 0.7 E + H$

where

D : dead load,

E : earthquake load,

F : load due to fluids with well-defined pressures and maximum heights,

H : load due to lateral earth pressure, ground water pressure, or pressure of bulk materials,

L : live load,

L_r : roof live load,

R : rain load,

S : snow load,

T : self-restraining force,

W : wind load.

4.2.2. Wind Loads

In ASCE 7-98, for application of wind load, the load-carrying systems of buildings and other structures are grouped into two parts. These are as follows;

- (i) Main wind force resisting system,
- (ii) Components and cladding.

Main wind-force resisting system is an assemblage of structural elements assigned to provide support and stability for the overall structure. The system generally receives wind loading from more than one surface.

Components and cladding are elements of the building envelope that do not qualify as part of the main-force resisting system.

In addition, buildings are divided into two groups as rigid buildings and flexible buildings. Buildings and other structures which have fundamental natural frequency greater than or equal to 1 Hz. are called rigid and those with a fundamental natural frequency less than 1 Hz. are called flexible.

For application of wind loads, three different methods are recommended in ASCE 7-98. These are listed below:

- (i) Method-1, simplified procedure,
- (ii) Method-2, analytical procedure,
- (iii) Method-3, wind tunnel procedure,

4.2.2.1. Method-1, Simplified Procedure

This method is used for buildings that satisfy all the following conditions;

- (i) The building is a simple diaphragm building which is defined as a fully or partially enclosed building in which wind loads are transmitted through floor and roof diaphragms to the vertical main wind force resisting system,
- (ii) The building has roof slopes less than 10° ,
- (iii) The mean roof height of the building is less than or equal to 30 ft. (9 m.),
- (iv) The building is a regular shaped building or structure, which has no unusual geometrical irregularity in spatial form,
- (v) The building is not classified as a flexible building which has a fundamental natural frequency less than 1 Hz,
- (vi) The building structure has no expansion joints or separations,
- (vii) The building is not subject to the topographic effects such as wind speed-up over hills, ridges and escarpments, constituting abrupt changes in the general topography,

As seen from the conditions listed above, this method is applied to simple, low-rise and regular buildings, which have two stories at most. The design procedure is outlined below:

- (i) **The basic wind speed, V** is determined according to the regions specified in Fig.6.1 of ASCE 7-98. The basic wind speed varies from 85 mph (38 m/s) to 150 mph (67 m/s) for the USA in the given map of the code.
- (ii) **The importance factor, I** is determined according to Table 6.1 of ASCE 7-98. The buildings are divided into four categories. While category I includes the buildings or other structures that represent a low hazard to human life in the event of failure, such as agricultural facilities, storage facilities, etc., category IV contains essential facilities including hospitals, communication centers, power generating stations, water storage facilities, etc. The chart of importance factors is reproduced below:

Table 4.1. The Importance Factors (Quoted from Table 6.1 of ASCE 7-98)

Category	Non-hurricane prone regions and hurricane prone regions with $V= 85-100$ mph.	Hurricane prone regions with $V > 100$ mph.
I	0.87	0.77
II	1.00	1.00
III	1.15	1.15
IV	1.15	1.15

- (iii) An exposure category is determined according to the definitions given below.

Exposure A. Large city centers with at least 50% of the buildings having a height in excess of 70 ft (21.3 m). Use of this exposure category shall be limited to those

areas for which terrain representative of Exposure A prevails in the upwind direction for a distance of at least 1/2 mi (0.8 km) or 10 times the height of the building or other structure, whichever is greater. Possible channeling effects or increased velocity pressures due to the building or structure being located in the wake of adjacent buildings shall be taken into account.

Exposure B. Urban and suburban areas, wooded areas, or other terrain with numerous closely spaced obstructions having the size of single-family dwellings or larger. Use of this exposure category shall be limited to those areas for which terrain representative of Exposure B prevails in the upwind direction for a distance of at least 1,500 ft (460 m) or 10 times the height of the building or other structure, whichever is greater.

Exposure C. Open terrain with scattered obstructions having heights generally less than 30 ft (9.1 m). This category includes flat open country, grasslands and shorelines in hurricane prone regions.

Exposure D. Flat, unobstructed areas exposed to wind flowing over open water (excluding shorelines in hurricane prone regions) for a distance of at least 1 mi (1.61 km). Exposure D extends inland from the shoreline a distance of 1,500 ft (460 m) or 10 times the height of the building or structure, whichever greater.

- (iv) An enclosure classification is determined such as enclosed, partially enclosed or open.
- (v) The design wind loads for the main wind force resisting system is determined from the Table 4.2.

Table 4.2. Design Wind Pressure (Quoted from Table 6.2 of ASCE 7-98)

Location	Building	Basic Wind Speed V (MPH)									
	Classification	85	90	100	110	120	130	140	150	160	170
Roof	Enclosed	-14	-16	-20	-24	-29	-33	-39	-45	-51	-57
	Partially Enclosed	-19	-21	-26	-31	-37	-44	-51	-58	-66	-74
Wall	Enclosed or Partially Enclosed	12	14	17	20	24	29	33	38	43	49

(vi) The design wind load for component and cladding elements is determined from Table 6.3 of ASCE 7-98.

4.2.2.2 Method-2, Analytical Procedure

This method is used for buildings or other structures, that satisfy all of the following conditions:

- (i) The building is a regular shaped building or structure.
- (ii) The building or other structure does not have response characteristics making it subject to across wind loading, vortex shedding, instability due to galloping or flutter; or does not have a site location for which channeling effects or buffeting in the wake of upwind obstructions warrant special consideration.

The design procedure is summarized below:

- (i) **The basic wind speed, V and wind directionality factor, K_d** are determined. The basic wind speed, V is determined according to the map given (Table 6.1

of ASCE 7-98) in ASCE 7-98. Wind directionality factor, K_d is taken from the Table 4.3

Table 4.3. Wind Directionality Factor (Quoted from Table 6.6 of ASCE 7-98)

Structure Type	Directionality Factor K_d
Buildings	
Main Wind Force Resisting System	0.85
Components and Cladding	0.85
Arched Roofs	0.85
Chimneys, Tanks and Similar Structures	
Square	0.90
Hexagonal	0.95
Round	0.95
Solid Signs	0.85
Open Signs and Lattice Framework	0.85
Trussed Towers	
Triangular, square, rectangular	0.85
All other cross sections	0.95

- (ii) **Importance factor, I** is determined as explained in Method-1.
- (iii) **Exposure category** is determined as explained in Method-1. **Velocity pressure exposure coefficient K_z or K_h** is determined according to Table 6.5 given in ASCE 7-98. These coefficients vary with respect to height above ground level and exposure category.
- (iv) A **topographic factor K_{zt}** , is determined as;

$$K_{zt} = (1 + K_1 K_2 K_3)^2 \quad (4.1)$$

where K_1 , K_2 and K_3 are given in Fig.6.2 presented in ASCE 7-98.

- (v) **A gust effect factor G** (for rigid structures) or G_f (for flexible or dynamically sensitive structures) is determined in two different ways for rigid and flexible structures. But it is stated to take gust effect factor as 0.85 for rigid structures in ASCE 7-98.
- (vi) Enclosure classification is determined such as enclosed, partially enclosed or open.
- (vii) **Internal pressure coefficient, GC_{pi}** and **external pressure coefficients, C_p** (for main wind force resisting systems) or GC_{pf} (for components and cladding) are determined according to Fig.6.3 through Fig.6.8 presented in ASCE 7-98.

(viii) **Velocity pressure, q_z** is found using the formula

$$q_z = 0.00256K_zK_{zt}K_dV^2I \quad (\text{lb/ft}^2) \quad (4.2)$$

[in SI $q_z = 0.613K_zK_{zt}K_dV^2I \quad (\text{N/m}^2)] \quad (4.3)$

where

q_z : velocity pressure, evaluated at height z ,

K_z : velocity pressure exposure coefficient,

K_{zt} : topographic factor,

K_d : wind directionality factor,

V : basic wind speed,

I : importance factor,

q_h is the velocity pressure calculated using equation above at mean roof height h .

- (ix) Design wind load P or F is calculated. P is the design wind pressure for enclosed and partially enclosed buildings. The formulation used for various cases are listed in Table 4.4.

Table 4.4. Design Wind Load Formulation

Formula	Case
$p = qGC_p - q_i(GC_{pi})$ (lb/ft ²)(N/m ²)	Design wind pressures for main force resisting system for rigid buildings of all heights
$p = qh[(GC_{pf}) - (GC_{pi})]$ (lb/ft ²)(N/m ²)	Design wind pressures for main force resisting system for low-rise buildings.
$p = qG_f C_p - q_i(GC_{pi})$ (lb/ft ²)(N/m ²)	Design wind pressures for main force resisting system for flexible buildings.
$p = qh[(GC_p) - (GC_{pi})]$ (lb/ft ²)(N/m ²)	Design wind pressures on components and cladding for low-rise buildings (with h ≤ 60 ft (18.3 m.)
$p = q(GC_p) - q_i(GC_{pi})]$ (lb/ft ²)(N/m ²)	Design wind pressures on components and cladding for buildings with h > 60 ft. (18.3 m.)

where

$q = q_z$ for windward walls evaluated at height z above the ground,

$q = q_h$ for leeward walls, side walls, and roofs, evaluated at height h ,

$q_i = q_h$ for windward walls, side walls, leeward walls, and roofs of enclosed buildings and for negative internal pressure evaluation in partially enclosed buildings;

$q_i = q_z$ for positive internal pressure evaluation in partially enclosed buildings where height z is defined as the level of the highest opening in the building that could affect the positive internal pressure. For buildings sited in wind borne debris regions, glazing in the lower 60 ft (18.3 m) that is not impact resistant or protected with an impact resistant covering, the glazing shall be treated as an opening. For positive internal pressure evaluation, q_i may conservatively be evaluated at height h ($q_i = q_h$);

G : gust effect factor,

C_p : external pressure coefficient,

(GC_{pi}) : internal pressure coefficient,

q_h : velocity pressure evaluated at mean roof height h using exposure,

(GC_{pf}) : external pressure coefficient,

Design wind loads on open buildings are determined from the equation below :

$$F = q_z GC_f A_f \quad (\text{lb}) \text{ (N)} \quad (4.4)$$

where

q_z : velocity pressure evaluated at height z of the centroid of area A_f using exposure,

G : gust effect factor,

C_f : net force coefficients,

A_f : projected area normal to the wind except where C_f is specified for the actual surface area.

4.2.2.3 Method-3, Wind Tunnel Procedure

Wind tunnels date back to the 1870's. Scientists realized it didn't matter if an object was stationary (not moving) and air was blown over the object or if the object was moving through the air. The resultant forces over the object would be the same. The idea of blowing air over an object and determining the forces led to the invention of the wind tunnel.

A wind tunnel is generally sort of a duct or pipe shape and air is either blown or pulled out of the tunnel. Typically in about the middle of the tunnel is what is called the "test section". This is where the model object to be tested is placed.

According to ASCE 7-98, wind tunnel testing is performed in lieu of methods 1 and 2 for any building or structure. Wind-tunnel tests are recommended when the building or other structure satisfies one or more of the following conditions:

- (i) Building has a shape which differs from a uniform rectangular prism or "box-like" shape,

- (ii) Building is flexible with fundamental natural frequencies normally below 1 Hz.,
- (iii) Building is subject to buffeting by the wake of upwind buildings or other structures,
- (iv) Building is subject to accelerated flow caused by channeling or local topographic features.

Tests for determination of mean and fluctuating forces and pressures are required to meet the following conditions:

- (i) The natural atmospheric boundary layer is modeled to account for the variation of wind speed with height,
- (ii) The relevant macro length and micro length scales of longitudinal component of atmospheric turbulence are modeled to approximately the same scale as that used to model the building or structure.
- (iii) The modeled building or other structure and surrounding structures and topography are geometrically similar to their full-scale counterparts, except low-rise buildings.
- (iv) The projected area of the modeled building or other structure and surroundings is less than 8 % of the test section cross-sectional area unless correction is made for blockage.
- (v) The longitudinal pressure gradient in the wind tunnel test section is accounted for.
- (vi) Reynolds number effects on pressures and forces are minimized.
- (vii) Response characteristics of the wind tunnel instrumentation are consistent with the required measurements.

Boundary-layer wind tunnels capable of developing flows typically have test-section dimensions in the following ranges; width of 6-12 ft (2-4 m), height of 6-10 ft. (2-3 m) and length of 50-100 ft. (15-30 m). Maximum wind speeds can be either obtained from an open-circuit or closed-circuit type.

Three basic types of wind-tunnel test models are commonly used. These are designated as follows:

- (i) Rigid pressure model (PM),
- (ii) Rigid high-frequency base balance model (H-FBBM),
- (iii) Aeroelastic model (AM).

PM provides local peak pressures for design of elements such as cladding and mean pressures for the determination of overall mean loads. The H-FBBM measures overall fluctuating loads for the determination of dynamic responses. When motion of a building or structure influences the wind loading, the AM is employed for direct measurement of overall loads, deflections and accelerations.

Wind tunnel tests frequently measure wind loads which are significantly lower than required by analytical method due to the shape of the building, shielding in excess of that implied by exposure categories and necessary conservatism in enveloping load coefficients. Additional wind tunnel testing without specific nearby building (or with additional buildings if they might cause measured loads through channeling or buffeting) is an effective method for determining the influence of adjacent buildings.

Forces and pressures determined by wind tunnel testing shall be limited to not less than 80 % of the design forces and pressures which would be obtained from analytical method for the structure unless specific testing is performed to show that it is the aerodynamic coefficient of the building itself, rather than shielding from nearby structures, that is responsible for the lower values.

The design pressures for components and cladding on walls or roofs shall be selected as the greater of the wind tunnel test results or 80 % of the pressure obtained for zone 4 for walls and zone 1 for roofs as determined from analytical

method, unless the criterion specified above. An example of wind tunnel test is shown in Figure 4.1.



Fig.4.1. Wind Tunnel Test (The 1:500 Model of the Four Times Square Tower in the Center of New York)

4.2.3 Snow Loads

In ASCE 7-98, snow loads are divided into three groups as ground snow loads, flat-roof snow loads and sloped-roof snow loads.

Ground snow load determination is based on an extreme value statistical analysis of data available in the vicinity of the site using a value with a 2 % annual probability of being exceeded (50 year mean recurrence interval). Ground snow loads are taken from Fig.7.1 presented in ASCE 7-98. The loads vary from zero for Hawaii to 100 psf (4.79 kN/m²) for northern regions of the USA.

Snow is a variable load. It may cover an entire roof or only some parts of it. On the other hand, it may slide off one roof onto a lower one. While snow may blow off one side of a sloped roof, it may also crust over and remain in position even during

very heavy winds. Therefore, snow loads depend on many factors such as geographic location, the pitch of the roof, sheltering and the shape of the roof.

For roofs with slope equal to or less than 5° the snow load is determined using the following equation:

$$P_f = 0.7C_e C_t I P_g \quad (4.5)$$

where

P_f : snow load in pounds per square foot,

C_e : exposure factor (the values are found from table 4.5 according to exposure category)

C_t : thermal factor (taken from table 4.6)

I : importance factor,

P_g : ground snow loads,

Table 4.5. Exposure Factor (Quoted from Table 7.2 of ASCE 7-98)

Terrain Category	Exposure of Roof		
	Fully Exposed	Partially Exposed	Sheltered
A	N/A	1.1	1.3
B	0.9	1.0	1.2
C	0.9	1.0	1.1
D	0.8	0.9	1.0
Above the treeline in windswept mountainous areas	0.7	0.8	N/A
In Alaska, in areas where trees don not exist within a 2-mile (3-km) radius of the site.	0.7	0.8	N/A

Table 4.6. Thermal Factor (Quoted from Table 7.3 of ASCE 7-98)

Thermal Condition	C_t
All structures except as indicated below	1.0
Structures kept just above freezing and others with cold, ventilated roofs in which the thermal resistance between the ventilated space and the heated space exceeds 25 °F.h.ft ² /Btu (4.4 K.m ² /W)	1.1
Unheated structures and structures intentionally kept below freezing.	1.2
Continuously heated greenhouses with a roof having a thermal resistance (R-value) less than 2.0°F.h.ft ² /Btu (0.4 K.m ² .W)	0.85

Snow loads acting on a sloping surface is assumed to act on the horizontal projections of that surface. The sloped-roof snow load, P_s is obtained by multiplying the flat-roof snow load, p_f by the roof slope factor, C_s :

$$P_s = C_s p_f \quad (4.6)$$

where

C_s : roof slope factor (determined from Fig.7.2 given in ASCE 7-98 for warm and cold roofs),

In ASCE 7-98, the roofs are divided into two groups such as warm and cold roofs. Different thermal factors (C_t) are used for these roof types according to Table 4.6.

In ASCE 7-98, partial loading and unbalanced roof snow loads due to wind are considered for different roof types such as hip and gable roofs, curved roofs, sawtooth roofs, barrel vault roofs. The accumulation of snow on one half of the roof due to the wind pressure is considered by taking account of unbalanced snow load case in ASCE 7-98. Illustrative questions in which this effect is taken account are solved in Chapter 8. A more thoroughly explanation is made in this chapter.

CHAPTER 5

OPTIMIZATION TECHNIQUES

5.1 Structural Optimization

Structural optimization can be defined as designing a structure at the lowest cost, while fulfilling the design requirements at the same time. That is to say, it is to find a reasonable structure with the best objective, while meeting the predefined need (Tang et al. 2005). Usually, the aim is to minimize the weight of the structure (thus the material and cost of the structure) subjected to various loadings under certain design constraints. Design constraints are the limitations which must be obeyed for the safety of the structure such as stresses, displacements, stability, etc.

Abundance of different search and optimization techniques are used in optimum structural design applications. These techniques can be categorized as shown in Fig.5.1 (Langdon and Qureshi).

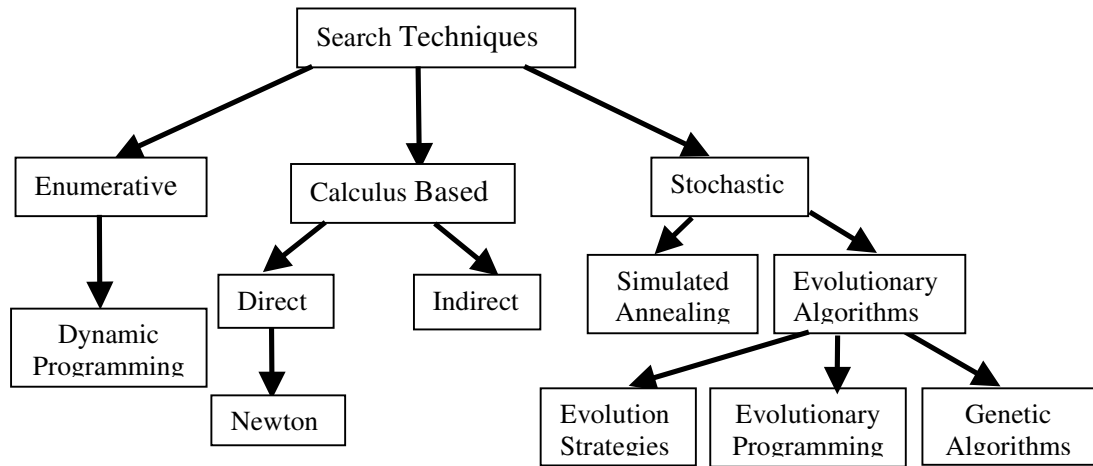


Fig. 5.1. Search Techniques

Enumerative techniques, in principle, search every possible point. They search one point at a time, so the number of possible points may be too large for direct search.

Calculus based techniques look for the maxima or minima using the derivative of continuous multi-dimensional function. These techniques are also called gradient-based search techniques. Calculus based techniques are sub-divided into two groups such as direct and indirect methods. **Indirect methods** use the fact that derivative of the function is zero at the extrema. **Direct calculus based techniques** such as Newton use the gradient/function values to estimate the location of nearby extrema. These techniques are known as hill climbing techniques. They estimate a point around maximum and move to that point, then they make a new estimate and move to it. This process goes on until they reach the top of the hill. The calculus-based techniques have definite disadvantages such as requirement of a continuous design space, danger of entrapment in local optima closest to the starting solution, difficulty to find the derivative of the complex structural optimization problems.

Stochastic search techniques use information from the search so far to guide the probabilistic choice of the next points to try. They are able to solve very complex problems which cannot be solved by enumerative and calculus based techniques (Langdon and Qureshi).

Simulated annealing (SA) which is a well-known member of stochastic search techniques searches for minimum energy states using an analogy based upon the physical annealing process. In this method, the minimum energy level is to be formed by heating the system to a high temperature and then cooling slowly. The objective function is analogous to the energy level of the physical system. In chapter 7, simulated annealing technique will be discussed in detail.

Evolution algorithms are based upon Darwin's Natural Selection (survival of the fittest) theory of evolution, where a population is progressively improved by selectively discarding the worse individuals and breeding new children from the better ones.

In **Evolutionary Strategies** (ES) points in the search space are represented by a vector of real values. Each new point is created by adding random noise to the current one. If the new point is better than the former one search proceeds from this new point, if not the older point is retained. Historically Evolutionary Strategies search only one point at a time but recently they use a population of points like Genetic Algorithms (GAs) (Langdon and Qureshi).

Genetic Algorithms (GAs) represent points in the search space by a vector of discrete bit values. Each new child is produced by combining parts of the bit vector from each parent. Genetic operators such as selection, crossover and mutation are used to produce new individuals. This is analogous to the way which chromosomes of DNA (which contains the inherited genetic material) are passed to children in natural systems. Genetic Algorithms are also to be discussed in detail in Chapter 6 of the thesis.

Some other classifications of optimization techniques are also made in the literature (Camp et al. 1998, Tzan and Pantelides, 1996).

5.2 Stochastic Search Techniques

Since the main subject of this thesis is stochastic search techniques, more information is to be given on these techniques. Stochastic search techniques use probabilistic transition rules to guide their search. But the use of probability does not suggest that these methods are simple random search like tossing a coin. They use random choice as a tool to guide a search toward regions of search space with likely improvements (Goldberg, 1989).

5.2.1 Evolutionary Algorithms

The toughness of solving many design optimization problems by conventional optimization techniques led the researchers to improve new techniques. Evolutionary algorithms, which simulate the natural evolution processes of living organisms are the most promising ones. An evolutionary algorithm (also EA, Evolutionary Computation, Artificial Evolution) is an algorithm using evolutionary techniques inspired by mechanisms from biological evolution such as natural selection, mutation and recombination to find an optimal configuration for a specific system within specific constraints.

Evolutionary Algorithms include:

- (i) Genetic Programming and Genetic Algorithms which use the gene transmission and mutation mechanism as an optimization technique,
- (ii) Evolutionary Programming (EP), which allows one to parameterize computer programs to find optimal solutions according to a goal function,

- (iii) Evolutionary Strategies (ESs), which work with vectors of real numbers as representations of optimization problems; mutation and adaptation of mutation rates are important working mechanisms there.

The source of imitation for these three techniques depend on the evolution process as their names imply (evolutionary algorithms), but there are several major differences between their working mechanism of operators (Back, 1996). These differences will be explained in the forthcoming sub-chapters.

As stated before, Evolutionary algorithms inspire the natural processes of Darwin's theory: survival of the fittest. A global optimum is sought in a population of individuals. The average quality of the population is evolved to higher levels with the help of the operators; recombination, mutation and selection. These operators will be examined in Chapter 6. The quality of the individuals in the population is measured with respect to their fitness values (Ulusoy, 2002).

Darwin's survival of the fittest theory states that the members of species, which are stronger and capable of adapting themselves to the natural habitat survive, while the weaker ones die out. These stronger and more adaptive members of the population propagate to generate the next population so better populations are evolved throughout the successive generations.

In structural optimization problems, evolutionary algorithms have certain advantages over the conventional techniques. These advantages can be listed as follows:

- (i) Evolutionary algorithms need not take derivatives of the objective functions and constraints.
- (ii) A population of candidate solutions is used to explore the design space.
- (iii) Discrete and non-continuous problems can be handled easily.

- (iv) Several near optimum solutions can be obtained yielding alternative designs to the engineer.

Besides the advantages; EAs have some minor drawbacks. The performance of the technique depends mostly on choosing appropriate values of parameters. But it is difficult to choose appropriate values unless the preliminary knowledge is available for the characteristics of the optimization problem. Second drawback is that finding the global optimum cannot be ensured with evolutionary algorithms. Third drawback is the computationally experiences of obtaining a good optimum solution for complex problems (Ulusoy, 2002).

EA techniques require a stochastic and iterative process, which tries to improve a population over a pre-selected number of generations. For this purpose firstly an initial population composed of μ number of parent designs is usually created at random. The population size is kept steady in each generation. Then, the process is continued by assigning a fitness score to each parent in association with the objective function of the problem. These two steps are the same for all EA techniques. Back and Hoeffmeister (1991) and Back et al (1993) gave extensive comparison between these evolutionary algorithms.

A humorous illustration, which is quoted from Sarle (1993), is given below to give a better understanding about the optimization techniques, conventional hill-climbing, simulated annealing and genetic algorithms:

Notice that in all hill-climbing methods, the kangaroo can hope at best to find the top of a mountain close to where he starts. There is no guarantee that this mountain will be Everest, or even a very high mountain. In simulated annealing, the kangaroo is drunk and hops around randomly for a long time. However, he gradually sobers up and tends to hop up hill. In genetic algorithm, there are a lot of kangaroos that are parachuted into Himalayas (if the pilot didn't get lost) at random places. These kangaroos do not know that they are supposed to be looking for the top of Mt.Everest. However, every few years, you shoot the kangaroos at low altitudes and hope the ones that are left will be fruitful and multiply.

5.2.1.1 Evolutionary Strategies

Evolution strategies were developed by Rechenberg (1965, 1973) and Schwefel (1981) in Germany. They are similar to Genetic Algorithms, but originally did not use crossover operator. ES have very complex mutation and replacement functions. Mutation is the main operator while recombination is the secondary in ES. In this technique, selection is a deterministic operator. In ES, real variables are used.

5.2.1.2 Evolutionary Programming

Evolutionary programming (EP) was originally developed by Fogel et al (1966) and refined by Fogel (1991). It is possibly the first genetic approach to artificial intelligence. This technique does not use crossover operator. Mutation is the main operator in EP. Recombination is even omitted in this technique. Probabilistic selection schemes are used in EP. Like ES, real variables are used in EP.

5.2.1.3 Genetic Algorithms

Genetic Algorithms were first introduced by Holland (1975) and further developed by De Jong (1975). Unlike ES and EP, recombination is the main variation in GAs. Probabilistic selection schemes and binary coding in representation are used in GAs. Genetic Algorithms are discussed in detail in Chapter 6.

5.2.2 Simulated Annealing

Simulated annealing is another stochastic optimization technique. In this technique, a natural event, annealing process of a thermodynamical system is used as a source of inspiration. In this process, a solid initially at a high energy level is cooled down gradually to reach its minimum energy and thus to regain proper crystal structure with perfect lattices.

The similarity between annealing and optimization was first introduced by Kirkpatrick et al (1983) and Cerny (1985). These scientists observed the correspondence between minimizing the energy level of a thermodynamical system and lowering the objective function of a optimization problem. As a result of this analogy, simulated annealing is named to this method.

A further investigation of this technique will be given in Chapter 7.

CHAPTER 6

GENETIC ALGORITHMS

6.1 Introduction

Genetic algorithm was first pioneered by Holland in 1975. It has emerged as a robust, practical and reliable search technique (Azid et al, 2002). Genetic algorithm uses a directed random search approach to locate the optimum solution. It is a numerical multipoint search technique that can be used to find progressively better solutions for a problem by an extensive search of the design space.

Genetic algorithms are adaptive heuristic search algorithm based on the evolutionary ideas of natural selection and genetics. As such they represent an intelligent exploitation of a random search used to solve optimization problems. Although randomized, GAs are by no means random, instead they exploit historical information to direct the search into the regions of better performance within the search space. The basic techniques of the GAs are designed to simulate processes in natural systems necessary for evolution, especially those follow the principles first laid down by Charles Darwin of "survival of the fittest".

GA is implemented such that first a population which has a constant number of μ individuals is created randomly. Each individual in the population is called a chromosome, representing a possible solution to an optimization problem at hand.

In GAs, individuals (designs) are represented by finite length strings. Usually, binary strings are used for this purpose. In each iteration, referred to as a generation, a new set of individuals is created using three operators known as selection (reproduction), crossover and mutation. The same process is repeated over a fixed number of generations or until a stopping criteria is satisfied.

As noted, the GA operators are applied to a population of individuals (designs) rather than a single point. This enables GA to explore the search space simultaneously from many different points and find an optimum by a more global search strategy instead of a localized gradient search or hill-climbing approach (Yang and Soh, 1997).

The GA approach has demonstrated certain aspects of intelligence characterized by human beings. That is, it exploits “best” inheritance accumulated during the evolution in a way that efficiently trades off the need to explore new regions of the search space with the need to focus on a high-performance region of that space (Yang and Soh, 1997).

6.2 Fundamentals of GAs

As explained before, the main principle of GAs extend to Darwin’s survival of the fittest theory. The theory emulates the natural process of evolution to find the optimum. It assumes that individuals with certain characteristics are more able to survive and pass their characteristics to their offspring. The mixing of good parental genetic materials causes a better generation which is characterized by term “**evolution**”. The successive generations, which are more adaptive to their environmental conditions tend to evolve of more appropriate individuals. GAs use similar tactic inspired from this law of nature.

Genetic algorithms operate on a population of individuals encoded as strings using the binary alphabet. The term individual and design are used synonymously in GAs.

In each iteration, referred to as a generation, a new set of individuals that represent possible solutions is created through application of genetic operators as to be discussed in the following sections.

Genetic algorithms are different from other search techniques in many aspects, which are listed below:

- (i) They work with encoding of variables,
- (ii) They search via a set of points (population of designs),
- (iii) They only require objective (fitness) function values. They do not need continuity and existence of derivatives,
- (iv) They do not know when they find the optimum. So they must be told when to stop (Sait and Youssef, 1999).

As Goldberg (1989) expresses, while randomized, genetic algorithms are no simple random walk. They efficiently exploit historical information to speculate on new search points with expected improved performance. This is not decision making at the toss of a coin.

In many engineering applications, the variables must be selected from a list of integer or discrete values for practical reasons. For example, structural members must be selected from available section lists, member thicknesses must be selected from the commercially available ones, the number of bolts for a connection must be integer, etc. (Huang and Arora, 1997). GAs are capable of handling discrete variable optimization, which is very suitable for the design selection from an available list. The lack that is caused from rounding up the solution to nearest discrete values in traditional optimization techniques is eliminated in GAs.

6.3 GA Terminology

Basic terminology that is used in GAs is explained below. A further description will be given in the following sections:

Gene : A subsection of a chromosome which usually encodes the value of a single variable.

Chromosome : One encoded string of variables which represents the individual.

Individual : A single member of a population.

Population : A group of individuals which may interact by using genetic operators.

Fitness : A value assigned to an individual which shows how well the individual is.

Generation : An iteration of the algorithm and creation of a new population by means of genetic operators.

Parent : An individual which takes part in recombination (crossover) to generate new individuals.

Offspring : An individual generated by recombination (crossover).

Recombination : The creation of a new individual from two parents.

6.4 Flowchart of GAs

A flowchart representation of this algorithm is given in Fig.6.1.

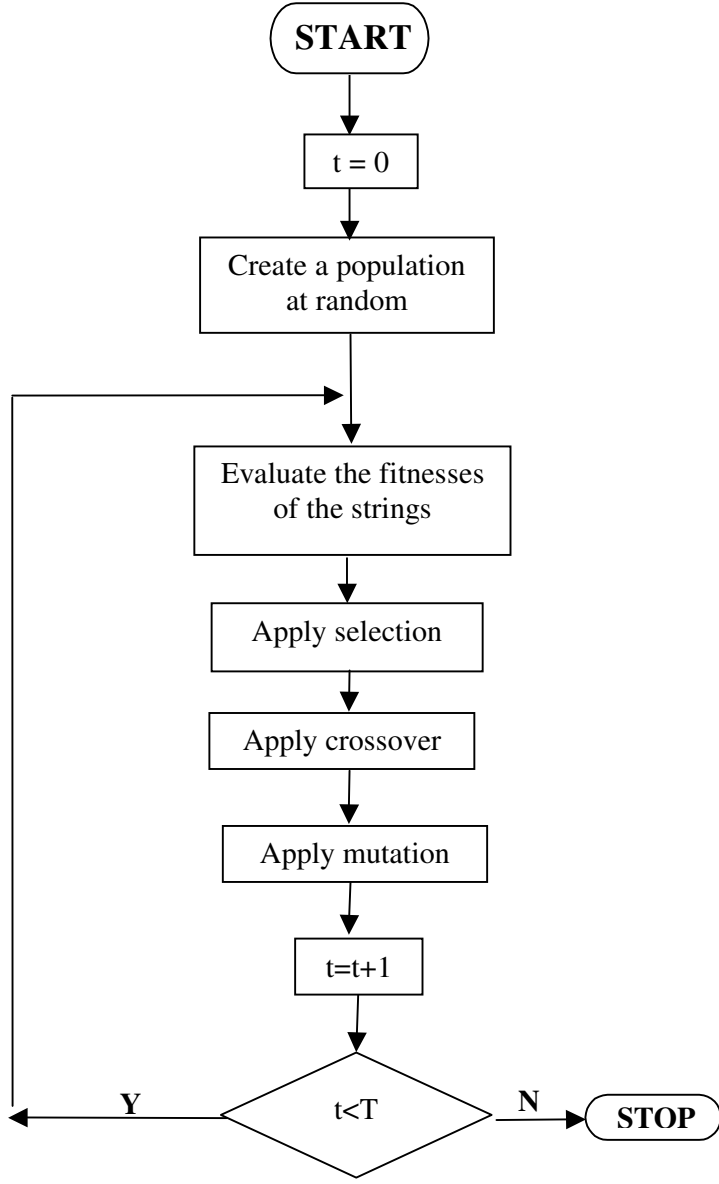


Fig.6.1. The Flowchart of Genetic Algorithm

The first step in GAs is creation of an initial population. This population is used as the starting solutions of the optimization process. The typical formulation of an initial population is done by initializing the binary codings randomly. So it is

obvious that the initial population consists of individuals which are poorly infeasible or feasible but very far from the optimum (Kaveh and Kalatjari, 2004).

Then the initial population is evaluated by calculating the objective functions of all the individuals. If the problem is a constrained one, then a penalty function is defined to account for violation of constraints. The penalty function is combined with the objective function to yield a new (modified) objective function, changing the constrained optimization problem to an unconstrained optimization one (Kaveh and Kalatjari, 2004). Each individual is assigned a single numerical fitness, which indicates the goodness of the individual. The individuals with high fitness scores are preferred more in order to improve the population. But, selection of highly fit individuals to the next generations causes the reduction in the genetic diversity for the child individuals. This can result in a premature convergence of the algorithm due to the lack of exploration. The lack of genetic diversity leads the generations to create the same result. But this result is not the global optimum and named as premature convergence.

In order to prevent the premature convergence, the fitness scaling is carried out to narrow the range of fitness scores of the population to avoid the dominance of highly fit individuals during the selection operator. After scaling the fitness values, a series of genetic operators are used to create the child population. As mentioned above, selection is the first genetic operator. With respect to the scaled fitness values of individuals in the population, individuals with higher fitness values are preferred while the poor ones are eliminated. The selected individuals are then transferred to the intermediate population, where they also produce their other copies to take places of those eliminated ones, in order to keep the population size (μ) constant. The second operator is crossover operator, which creates the child population by an exchange of genetic characteristics between randomly paired individuals of the intermediate population. The third operator is mutation operator. It is occasionally applied on the genes of child individuals after crossover, randomly changing a gene 1 to 0 or 0 to 1. Mutation is a random walk through the string

space. Although mutation operator plays a secondary role in GAs, it is an insurance policy against premature loss of important notion.

After using all three operators, the child individuals are taken to be the parents of the next generation. The process of creating a new population from the previous one is called a single generation in GA terminology. The newly created population has individuals whose average fitness is better than the previous population. The process outlined above is iterated in the same way for a fixed number of generations. After successive generations, it is hoped to find an optimum solution. The implementation of GAs and genetic operators will be discussed in detail in the following sections.

6.5 Coding

In Genetic Algorithms, solutions are represented in binary code as strings of 0 and 1, traditionally. Several other alternative representations are also used in the literature. These representations are real coding (real number representation), integer and Gray coding. The best representation is an ongoing research area. In this thesis, the binary coding representation will be concentrated.

In traditional representation, binary alphabet consisting of ‘1’ or ‘0’ is used. A coded variable is referred to a substring in GA terminology, where each single bit position is called a gene. If there are n_d number of design variables in all, then n_d such strings are added to create a string for representing a potential design. For example, two individuals which consist of four substrings each, where $l_x = 6$ and $l = 24$ are shown below:

	Substring 1	Substring 2	Substring 3	Substring 4
Individual 1	1 0 0 1 0 0	1 1 0 0 0 1	1 0 0 0 1 1	0 0 1 1 0 0
Individual 2	1 1 1 0 0 0	0 0 1 1 1 1	1 1 0 0 0 1	1 0 0 0 0 1

The length (l_x) of a substring used to code a design variable is determined in different ways for discrete and continuous optimization problems. In a discrete design, a set of finite number of design values is used. So it is necessary to designate each design value with a different combination scheme of l_x genes. As a rule, the l_x is chosen such that the number of possible gene combination schemes created with it should exceed the number of design values in the set. To visualize this fact, an example is given below:

If a design set composed of 10 values is used for a discrete design, substring length of l_x will be 4. The following 16 possible gene combination schemes are created:
 (0,0,0,0) , (0,0,0,1) , (0,0,1,0) , (0,1,0,0) , (1,0,0,1) , (1,0,1,0) , (1,0,1,0) , (1,1,0,0) ,
 (0,1,0,1) , (0,0,1,1) , (0,1,1,1) , (0,1,1,0) , (1,1,1,0) , (1,0,1,1) , (1,1,0,1) , (1,1,1,1).

In general, the maximum gene combination capacity of a substring length of l_x is calculated with the formula 2^{l_x} . For example $l_x = 4, 6, 11$, a maximum number of discrete values is 16, 64, 2048 respectively.

For a continuous design variable, the logic given above is the same with a minor difference. This difference is the inclusion of the desired level of precision to the discussion. The distance (Δx_j) between any two neighbour grid points in the continuous design will be as in the equation below:

$$\Delta x_j = \frac{v_j - u_j}{2^{l_x} - 1} \quad (6.1)$$

where

v_j : upper bound for the variable,

u_j : lower bound for the variable,

l_x : substring length,

Encoding decision variables into binary strings is the first step of solution. The length of the string depends on the required precision. Gen and Cheng (1997) proposed:

$$2^{l_x-1} < (v_j - u_j) \times 10^p \leq 2^{l_x} - 1 \quad (6.2)$$

p : required precision (places after the decimal point)

Example:

$$\text{Maximize } f(x_1, x_2) = 21.5 + x_1 \sin(4\pi x_1) + x_2 \sin(20\pi x_2)$$

$$-3.0 \leq x_1 \leq 12.1$$

$$4.1 \leq x_2 \leq 5.8$$

Suppose that the precision is set to 4 places after the decimal point. The required bits for variables x_1 and x_2 is calculated as follows:

$$(12.1 - (-3.0)) \times 10,000 = 151,000$$

$$2^{17} < 151,000 < 2^{18} \quad m_1 = 18$$

$$(5.8 - 4.1) \times 10,000 = 17,000$$

$$2^{14} < 17,000 \leq 2^{15} \quad m_2 = 15$$

$$m = m_1 + m_2 = 18 + 15 = 33$$

The total length of a chromosome is 33 bits.

For example, for a continuous variable $x_{ij}^{(t)}$ such that $u_j = 1.0 \leq x_{ij}^{(t)} \leq v_j = 7.0$, in case $l_x = 6$ is chosen, Δx_j will be approximately 0.10 but the accuracy can be improved by increasing the l_x e.g. for $l_x = 20$, Δx_j will be approximately 0.000006. In short, the l_x can be chosen as any value to provide enough resolution to a continuous design variable depending on the desired level of precision.

Random design generation can be created by using one random number to make decision (between 0 and 1) for each of the m digits in a genetic string. But this is computationally expensive way, so Huang and Arora (1997) propose the following procedure to produce a 30 digit genetic string:

- (i) Generate two double precision numbers,
- (ii) Assuming these two numbers are; 0.876541328301236 and 0.168309254654984, then a string of “876541328301236168309254654984” is created.

- (iii) The first 30 digits of the above string are converted to; “111100001000001011001010110110” in which “0” is converted from any value between 0 and 4, and “1” from any value between 5 and 9.

6.6 Decoding

The binary substrings are transformed to real or integer valued quantities in order to evaluate the quantity of an individual. The decoding process is explained below:

The variation limits of the variable is defined. For a continuous variable, they are lower (u_j) and upper (v_j) bounds. For a discrete variable, a design set is prepared by indexing and sorting the possible values in order of their increasing values. So the variation limits of discrete design will be the index number of the first and last discrete value in the set. These lower and upper bound indexes are indicated by the same symbols (u_j and v_j) for a unified notation.

The binary coding of the variable is assigned to an integer value (V_b) between 0 and $2^{l_x} - 1$, by using the formula below for conversion of base two numbers to base ten numbers. For example, for a substring (1,1,0,0,0,1,0), the V_b will be equal to $1.2^6 + 1.2^5 + 0.2^4 + 0.2^3 + 0.2^2 + 1.2^1 + 0.2^0 = 98$

$$V_b = \sum_{k=0}^{l_x-1} a_{l_x-k} \cdot 2^k \quad (6.3)$$

The decoded value of the variable (V_d) is obtained by associating the substrings $\{0\}^{l_x}$ and $\{1\}^{l_x}$ to the upper and lower bounds u_j and v_j , respectively and mapping the other substrings linearly in between those two values, using the following decoding function, $\Omega : \Omega(x_{ij}^{(t)}) \longrightarrow IN^+ \text{ or } IR$.

$$\Omega(x_{ij}^{(t)}) = V_d = u_j + \frac{v_j - u_j}{2^{l_x} - 1} \cdot V_b \quad (6.4)$$

In the equation above, for the substrings $\{0\}^{l_x}$ and $\{1\}^{l_x}$, the V_b will be equal to 0 and $2^{l_x} - 1$ respectively. Their corresponding decoded values (V_b) will be u_j and v_j . For a discrete variable, if the product of mapping appears to be a real number, it is rounded to a nearest integer.

Example: Assume that the design set includes 75 discrete values. In this case, the lower and upper bound indexes will be $u_j = 1$ and $v_j = 75$. Therefore, a substring length of $l_x = 7$ with $2^7 = 128$ possible gene combinations will be adequate to designate each of them. For a chosen two substrings:

$$x_{i1}^{(t)} = (1,1,1,1,0,0,0) \quad x_{i2}^{(t)} = (0,0,1,1,1,0,0)$$

Using equation (6.4) the V_b values are calculated as

$$V_{b1} = 2^6 + 2^5 + 2^4 + 0.2^3 = 120$$

$$V_{b2} = 2^4 + 2^3 + 2^2 = 28$$

The decoding function (Ω) will then yield rounded values of

$$V_{d1} = u_j + \frac{v_j - u_j}{2^{l_x} - 1} \cdot v_b = 1 + \frac{75 - 1}{2^7 - 1} \cdot 120 = 71 \quad \text{and} \quad V_{d2} = 1 + \frac{75 - 1}{2^7 - 1} \cdot 28 = 17$$

indicating that $x_{i1}^{(t)}$ and $x_{i2}^{(t)}$ represent the 71st and 17th discrete values in the design set respectively.

6.7 Fitness Evaluation

The objective function values of all the individuals in a population are calculated and a single numerical fitness value is given to each individual according to how good a solution in overall population. The terms fitness and objective functions are distinct expressions which should not be confused. Both of them express the quality of an individual, but their utilizations in GAs are different. The objective function measures the performance of an individual in terms of satisfying the chosen goal. The fitness function defines the fitness of an individual as a solution for the required problem. The fitness of an individual is dependent and defined with respect to whole population (Hasançebi, 2001).

6.8 Population Size

The two key parameters are the number of generations and the population size. If the population is too small, there will not be sufficient diversity to find the optimal solution, the genetic algorithm may converge to a local minimum. If the population size is too large, the genetic algorithm may waste computational resource, which means that the waiting time for an improvement is very long (Osyczka, 2002).

The most common sizes of population vary from 50 individuals to 500 individuals but greater populations can also be used seldomly.

6.9 Objective Function

The solutions which satisfy the constraints must be compared with respect to a criterion, in order to find the global optimum. This criterion is called objective function. The most commonly used objective function in engineering is the minimization of volume or mass.

Objective functions can be very different in different disciplines. Some examples of objective functions stated in Nash and Sofer (1996) are running a business to maximize the profit or minimize the loss, designing a bridge to minimize weight or maximize strength, selecting a flight plan to minimize time or fuel use, etc.

For unconstrained optimization problems, the objective function is capable to assess how good a solution of an individual provides. However, in most cases, a practical optimization problem has a number of constraints (Hasançebi, 2001). The inclusion of constraints introduces infeasible regions to the design space. Quite a large number of methods have been developed to handle constraints (Kim&Myung, 1996, Michalewics, 1995, Myung&Kim, 1996, Orvosh&Davis 1995). These methods can be classified as follows:

- (i) Rejecting strategy,
- (ii) Repairing strategy,
- (iii) Modifying genetic operator strategy,
- (iv) Penalty function strategy (Osyczka, 2002).

The last strategy, **Penalty Function Strategy**, has a universal character and thus it is the most often used strategy. This methodology penalizes individuals violating constraints, and thus a lower chance is given to these individuals for surviving. In this way, the search is carried towards feasible regions of the design space. In this strategy, the penalty function is integrated into original objective function to yield a newly defined one. A constrained problem is transferred into an unconstrained problem by associating a penalty with all constant violations;

$$W_c(x_i^{(t)}) = W(x_i^{(t)}) + Penalty(x_i^{(t)}) \quad (6.5)$$

where

$W_c(x_i^{(t)})$: Modified objective function,

$Penalty(x_i^{(t)})$: Penalty function,

For minimization problems, the penalty is equal to zero in case of no violation, otherwise it is a positive value, which is directly proportional to the intensity of violation.

Although constraints handling is not a basic component of a GA, it has a profound effect on its selection operator. An improper penalty can direct the search to infeasible regions of the design space. In the literature, many penalty functions have been proposed.

Constraints can be classified as equality and inequality relations. For minimization of $W(x_i^{(t)})$ subject to constraints $g_k(x_i^{(t)})$, we transform the constrained objective function to the unconstrained form (modified objective function).

$$\text{Minimize } W(x_i^{(t)}) + r_0 \sum_{i=1}^n \text{Penalty}(x_i^{(t)})$$

where

$\text{Penalty}(x_i^{(t)})$: Penalty function,

r_0 : Penalty coefficient

Hasançebi (2001) proposed a new penalty function to enhance the efficiency of GAs in terms of convergence reliability and to reduce considerably the effect of choice of the parameter set for achieving an efficient search.

$$\text{Penalty}(x_i^{(t)}) = (r_0.t)^2 \sum_{k=1}^m [g_k(x_i^{(t)}) . K] \quad (6.6)$$

$$\text{Penalty}(x_i^{(t)}) = c.p. \sum_{k=1}^m [g_k(x_i^{(t)}) . K] \quad (6.7)$$

where

K : Constant multiplier coefficient

c and p : Self-adaptive parameters, which have a capability to adjust themselves automatically during the search to guide the optimization process.

6.10 Fitness Function

The equation

$$W_c(x_i^{(t)}) = W(x_i^{(t)}) + \text{Penalty}(x_i^{(t)}) \quad (6.8)$$

yields the lowest modified objective function value for the best individual and the highest value for the worst individual. In order to arrange the individuals according to their scores (highest score is allocated to the best and the worst is a non-negative lowest value), a fitness function $\Phi: \Phi(W(x_i^{(t)})) \longrightarrow IR^+$ is introduced to appropriately transform them to positive real values in consideration of the above two criteria.

Many fitness functions have been proposed in the literature. A wide range of functions from linear transformations to complicated methods working on the basis of some population measures are proposed. For example, Goldberg (1989) proposed the following one for the minimization problem:

$$\Phi(x_i^{(t)}) = \left[|(W_c)_{\max}| + |(W_c)_{\min}| \right] - W(x_i^{(t)}) \quad (6.9)$$

where

$|(W_c)_{\max}|$: Absolute modified objective function value of best individual at t-th generation,

$|(W_c)_{\min}|$: Absolute modified objective function value of worst individual at t-th generation,

According to the relationship given by (6.9), the individual with the least value of the modified objective function has the highest fitness (Kaveh and Abdi-tehrani, 2004).

It is possible to use inverse transformations if the modified objective function values of all individuals yield positive valued quantities. The one which is proposed by Shestra and Ghaboursi(1998) is shown below:

$$\Phi(x_i^{(t)}) = \frac{(W_c)_{\max}}{W(x_i^{(t)})} \quad (6.10)$$

6.11 Fitness Scaling Function

Since initial population is created randomly, at the early generations a genetic diversity between the individuals of a population is noticed. So an extensive exploration of the design space is achieved. This can be advantageous, but the fact that selection mechanism of GA depends on the proportion of their relative fitnesses, causes the domination of highly fit individuals to the population. By the result of this, the crossover operator produces almost genetically identical child individuals and thus exploration capacity of the algorithm reduces. This results in

the stagnation of the search process in a local optimum, which is referred to a premature convergence in GA terminology. The most used approaches to avoid this problem are fitness ranking, fitness windowing and fitness scaling (Beasley et al 1993)

All these methods try to regulate the distribution of reproductive trials to maintain a sufficient genetic diversity in the population.

Fitness ranking method sorts the individuals in order of their fitness scores and then allocates reproductive trials deterministically according to this rank (Baker,1985, Davis, 1989)

Fitness scaling method performs the same task by narrowing the range of fitness values of individuals to gather around the average population fitness. In this method the individuals whose fitnesses are below and above the average population, fitness are scaled up and scaled down respectively. The fitness scaling function proposed by Goldberg (1989) is shown below:

$$\bar{\Phi}(x_i^{(t)}) = \Phi(x_i^{(t)}) \left[\frac{(C_c - 1)}{(\Phi_{\max} - \Phi_{ave})} \Phi_{ave} \right] + \frac{(\Phi_{\max} - C_c \Phi_{ave})}{(\Phi_{\max} - \Phi_{ave})} \Phi_{ave} \quad (6.11)$$

where

Φ_{\max} : Maximum fitness emerged in the population,

Φ_{ave} : Average fitness emerged in the population,

C_c : Real valued scaling factor (typically 2.0).

This transformation sets the ratio of maximum scaled fitness to average scaled fitness to C_c , and thus to enable the C_c number of reproductive trials of the best individual in the intermediate population during selection. However in case C_c is greater than

$$C_{cr} = \frac{(\Phi_{\max} - \Phi_{\min})}{(\Phi_{\max} - \Phi_{ave})} \quad (6.12)$$

where

Φ_{\min} : Minimum fitness emerged in the population,

Equation (6.12) may lead to negative scaled fitness values for some of the worst individual. In order to prevent this situation, Shestra and Ghaboussi (1998) employed a restriction on the C_c , such that for any generation if $C_c > (C_c - \delta.C_c)$, then the C_c is replaced with $C_c - \delta.C_c$ where $\delta.C_c$ is a small number (e.g. 0.1) which has been introduced to factor in the effect of numerical rounding off.

The fitness scaling function given in Eq.(6.12) results $\overline{\Phi_{\min}} = 30$, $\overline{\Phi_{ave}} = 40$ and $\overline{\Phi_{\max}} = 60$ after scaling with $C_c=1.5$ for the values $\Phi_{\min} = 20$, $\Phi_{ave} = 40$, $\Phi_{\max} = 80$.

6.12 Selection

Selection is an operator where an old string is copied into the new population according to the string's fitness which is defined according to the cost function value. Selection operator is implemented in terms of the magnitude of fitness. In some resources, the term "reproduction" is used in place of selection. These two terms are used synonymously, but in this text "selection" is preferred. Since the number of individuals of the population through all generations is the same, selection mechanism rejects less fitted individuals. Individuals with high fitness have higher probability of surviving and ones with low fitness tend to be extinct (Tang et al. 2005). The major types of selections are tournament selection, ranking selection and proportionate selection (spinning or roulette wheel selection).

In tournament selection, the population is divided into subgroups and the best individual from subgroup is chosen for the next generation. Subgroups may contain 2, 3 or more individuals but the most popular tournament selection is the so called binary tournament in which two individuals chosen at random are compared and better one passes to the next generation (Osyczka, 2002). This process is repeated μ number of times.

Ranking selection proposes to give ranks to the individuals. The population is sorted from the best to the worst chromosomes and the selection probability of each chromosome depends on the given rank but not its fitness. Linear ranking and exponential ranking methods are used in order to achieve this task (Osyczka 2002).

In proportionate selection, also called roulette wheel selection, the number of reproductive trials allocated to individuals is calculated in proportion to their relative scaled fitness scores. The selection probability of an individual, $P_s(x_i^{(t)})$ is defined by

$$P_s(x_i^{(t)}) = \frac{\bar{\Phi}(x_i^{(t)})}{\sum_{k=1}^{\mu} \bar{\Phi}(x_k^{(t)})} = \frac{\bar{\Phi}(x_i^{(t)})}{\mu \cdot \bar{\Phi}_{ave}} \quad (6.13)$$

$$\bar{\Phi}_{ave} = \sum_{k=1}^{\mu} \bar{\Phi}(x_k^{(t)}) / \mu \quad (6.14)$$

where

$$\begin{aligned} \bar{\Phi}_{ave} & : \text{Average scaled fitness of the population} \\ \mu.(x_i^{(t)}) & = \mu.p_s(x_i^{(t)}) = \bar{\Phi}(x_i^{(t)}) / \bar{\Phi}_{ave} \end{aligned} \quad (6.15)$$

which is rounded to a nearest integer.

$\mu.(x_i^{(t)})$: Number of reproductive trials of individual.

If the proportionate selection scheme is used together with the fitness scaling function (6.11), the number of reproductive trials allocated to the fittest individual will exactly be C_c (Hasançebi, 2001).

The most widely used selection type approach is roulette wheel selection. As stated above, the individuals are assumed to distribute on a simulated roulette wheel with respect to their scaled fitness values. The fitter individuals have more chance to be selected. The roulette is spinned μ number of times to select and reproduce the individuals in the intermediate population.

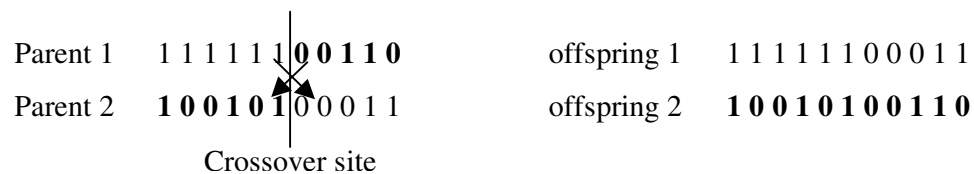
The other selection types which are not commonly used are steady-state selection, reedy over selection.

6.13 Crossover

Crossover is the main genetic operator. It operates on two chromosomes at a time and generates offspring by combining some features of both chromosomes. First the parents are selected and randomly mated constituting $\mu/2$ number of pairs. Two new child individuals are produced from a pair.

The simplest crossover type, the single point crossover (one-point crossover) chooses a random cutoff point and the portions after the cuts are swapped to form two child individuals (Hasançebi, 2001). One-point crossover is illustrated in the example below.

Example: A prespecified probability (p_c), which is also called crossover rate is determined. This is taken in the range of [0, 1.0]. For each pair of individuals, a uniform random number (r) is selected in the range of [0, 1] and if this is smaller than crossover rate ($r \leq p_c$) then crossover is performed, otherwise crossover is skipped. In this case, the child individuals duplicate their parents straightaway. This procedure carries a few parents to the next population and prevents to restrict the life span of parents to one generation only.



One-point Crossover

The other crossover approaches are two-point, multi-point, variable to variable, uniform crossover.

Two point crossover is applied by selecting two random positions in a chromosome and swapping the two corresponding parts of the parents. Good results are obtained in large populations.

In uniform crossover, a pattern (or template) is created randomly. If the gene of the pattern is 1, the same gene of the child 1 is taken from parent 1. The same procedure is done inversely for child 2. Two-point crossover and uniform crossover are presented below

Parent 1	1 0 0 0 1 0	
Parent 2	1 1 0 1 0 1	
Pattern	1 0 1 0 1 0	
Offspring 1	1 1 0 1 1 1	if pattern(i)=1 then offspring1[i]=parent1 [i] else offspring1[i]=parent2(i)
Offspring 2	1 0 0 0 0 0	if pattern(i)=1 then offspring2[i]=parent2 [i] else offspring2[i]=parent2(i)

Uniform Crossover

Parent 1	1 1 0 0 1 0 0 1 1 1 0	offspring 1	1 1 0 0 0 1 1 0 0 1 1 0
Parent 2	1 0 0 0 0 1 1 0 0 0 0 1	offspring 2	1 0 0 0 1 0 0 1 1 0 0 1

Two-point Crossover

Hasançebi (2001) proposed two newly developed crossover approaches named mixed crossover implementation and direct variable exchange.

The mixed crossover approach uses a combination of single, 2-point and 3-point crossovers for selected proportions of generations for a fixed generation number. In the direct design variable exchange approach, each design variable is directly and

separately exchanged between paired individuals according to an empirical probability function.

There are some experimental observations suggesting that two-point and uniform crossover exhibit better behaviour than other operators, but there is no theoretical proof as to which one is the best.

6.14 Mutation

Mutation is an operator, which produces spontaneous random changes in various chromosomes and it introduces some extra variability into the population in order to avoid local minima. It also prevents the population from genetic similarity. Although it is a secondary GA operator, it can play an important role in the search. It can be an explorative operator by moving the search into regions of the solution space it may never reached (Pezeshk et al. 2000).

Mutation rate (p_m) is kept less than 0.01 and typically is between 0.001 and 0.005. High mutation rate can cause the loss of information obtained so far, and damage on genetic structures of child individuals.

It controls the rate at which new genes are introduced into the population. If the mutation rate is too low, many genes that might be useful are never tried out. On the other hand, if the mutation rate is too high, there will be much random perturbation and the offspring will lose their resemblance to the parents. This means that the genetic algorithm will lose its ability to learn from the history of the search (Osyczka, 2002).

6.15 Elitist Strategy

This strategy is not a genetic operator, but it increases the productiveness of GAs. De Jong (1975) proposed to preserve the best individuals generated up to time t . In other words, elitist strategy depends on the basis of survival of the best feasible individual obtained so far. At the end of each generation, the best feasible individuals of the parent and child populations are determined with respect to their objective function values and feasibilities. For the constrained problems; best feasible individuals must be satisfied $Penalty(x_i^{(t)}) = 0$
 $W_c(x_i^{(t)}) = W(x_i^{(t)}) \longrightarrow \min.$

The feasible best of the parent population replaces the worst individual of the child population. By this way, the best feasible individual is kept on alive until a new but better one emerges. The most valuable search experience is prevented to be lost and it leads to a non-increasing curve of the best feasible individual during successive generations (Hasançebi, 2001).

In some resources, this strategy is presented as “leader of the population”. At each generation the member having the lowest cost function value (for minimization problems) among the entire population is defined as the “leader” of the population. This value is transferred to the next generation automatically. It is safe-guarded from extinction due to genetic operators. On benefit of using a leader is that the best cost function value of the population can never increase from one iteration to another, and some of the best “genes” can always survive (Huang and Arora, 1997).

6.16 Constraint Handling in GAs

GAs are used to solve unconstrained optimization problem, but generally, optimization problems are subject to constraints. The integration of constraints into GAs is accomplished by the use of penalty functions. The solutions which are out of the feasible domain are penalized using a penalty coefficient. In other words, a

constrained optimization problem is transformed to an unconstrained problem by associating penalty with all constraint violations.

6.17 Penalty Function Approach

The most widely used constraint handling method is penalty function approach. As previously discussed, the constrained problem is transformed into an unconstrained one by defining a new objective function. This technique is also commonly used in conventional optimization. In conventional optimization, the penalty technique is used to generate a sequence of infeasible points whose limit is an optimum solution to the original problem. In GAs this technique is used to keep a certain amount of infeasible solutions in each generation so as to enforce genetic search towards an optimal solution. In other words, infeasible solutions are not rejected (Gen and Cheng, 1997). But adding a penalty term to the fitness of an infeasible point causes that its fitness never attains that of a feasible point (Cheng and Li, 1997).

Many researchers believe that penalty functions should be harsh, so that the GA will avoid the forbidden spaces. However, the foundation of GA research states that a GA optimizes by combining partial information from the population. Therefore, infeasible solutions may provide some useful information. If the penalty is too large, the design process may converge too quickly, not allowing the GA to exploit various combinations of strings. If the penalty is too small, the convergence process may be too slow and computational costs could be high (Pezeshk et al 2000).

For maximization problems, penalty function results values less than zero to reduce the modified objective function. For minimization problems, the inverse is done. So the penalized solutions are maximized with respect to degree of violation.

In general, penalty functions can be classified into two classes: constant penalty and variable penalty.

The constant penalty approach is less effective for the complex problems and variable penalty approach is a much more promising strategy (Gen and Cheng, 1997).

In general, the variable penalty approach contains two components:

- (i) Variable penalty ratio,
- (ii) Penalty amount for the violation of constraints

The variable penalty ratio can be adjusted according to:

- (i) The degree of violation of constraints,
- (ii) The iteration number of genetic algorithms.

The degree of violation of constraints approach increases the penalty pressure as the violation becomes severe which leads to the class of static penalty. Second approach (the iteration number of genetic algorithms) increases the penalty pressure along with the growing of evolutionary process, which leads to the class of dynamic penalty.

Essentially, penalty is a function of the distance from feasible area. Some penalty function methods used in GAs for solving non-linear programming are introduced below:

6.17.1 Homaifar, Qi and Lai's Method

$$Penalty(x_i^{(t)}) = \begin{cases} 0 & \text{if } x_i^{(t)} \text{ is feasible} \\ \sum r_i \cdot g_i^2(x_i^{(t)}) & \text{otherwise} \end{cases}$$

$$\begin{aligned} & \min W(x_i^{(t)}) \\ & g_i(x_i^{(t)}) \geq 0 \quad i : 1, 2, \dots, m \quad (6.16) \\ & W_c(x_i^{(t)}) = W(x_i^{(t)}) + Penalty(x_i^{(t)}) \end{aligned}$$

The penalty function is constructed with two components

- (i) variable penalty factor
- (ii) penalty for the violation of constraints.

where

r_i : a variable penalty coefficient for the i-th constraint.

6.17.2 Joines and Houck's Method

Joines and Houck proposed the following penalty function model;

$$Penalty(x_i^{(t)}) = (r_0.t)^\alpha \sum_{k=1}^m g_k^\beta(x_i^{(t)}) \quad (6.17)$$

where

$x_i^{(t)}$: i-th individual of the population at t-th generation,

$g_k(x_i^{(t)})$: k-th constraint amongst a total number of m constraints (zero in case of no violation),

$(r_0.t)^\alpha$: Parameters used to adjust the scale of penalty value,

r_0 : Penalty coefficient,

α, β : Parameters used to adjust the scale of penalty value.

For r_0, α, β the values 0.5, 2 and 2 are recommended respectively.

6.17.3 Hasańebi Method

Hasańebi (2001) modified the Joines and Houck's penalty function as shown below:

$$Penalty(x_i^{(t)}) = (r_0.t)^2 \sum [g_k(x_i^{(t)}) . k] \quad (6.18)$$

k : Constraint multiplier parameter,

Such a modification is thought to be necessary since the normalized constraints are used in optimization problems in order to distribute equal and fair penalty for violation of constraints. The penalty given to individuals in Joines and Houck's method becomes very small due to normalized constraints. Hasańcebi (2001) suggested the value of 10 for k parameter. In this way, it was observed that the penalty function combines the two requirements of exploration and exploitation in a balanced manner.

6.18 Formulation of Size Optimum Design Problem of Truss Structures

A general discrete sizing structural optimization problem is mathematically defined as follows:

Find a vector of cross-sectional areas,

$$A^T = [A_1, A_2, \dots, A_{N_m}] \in S$$

to minimize

$$W(A) = \sum_{i=1}^{N_m} \rho_i \cdot A_i \cdot L_i \quad (6.19)$$

subject to

$$g_i(A) = |\sigma_i| - |\sigma_i^a| \leq 0 \quad i = 1, \dots, N_m$$

$$h_i(A) = |H_i| - |H_i^a| \leq 0 \quad i = 1, \dots, N_m$$

$$u_{j,k}(A) = |u_{j,k}| - |u_{i,k}^a| \leq 0 \quad j = 1, \dots, N_m$$

where

A : A vector of cross-sectional areas,

S : Available list,

$W(A)$: Objective function (weight of the structure),

- ρ_i : Unit weight of i-th member,
 L_i : Length of i-th member,
 A_s : Cross-sectional area of i-th member,
 N_m : Total number of structural members,
 N_j : Total number of nodes,
 $g_i(A)$: Stress constraint of i-th member,
 $h_i(A)$: Stability constraint of i-th member,
 $u_{i,k}(A)$: Displacement constraint at the j-th node in the k-th direction,
 σ_i : Stress in the i-th member,
 σ_i^a : Allowable stress in the i-th member,
 H_i : Slenderness ratio in the i-th member,
 H_i^a : Allowable slenderness ratio in the i-th member,
 $U_{j,k}$: Displacement at the j-th node in the k-th direction,
 $U_{j,k}^a$: Allowable displacement at the j-th node in the k-th direction,

It is stated before that the most preferred technique to handle constraints in GA optimization problems is penalizing strategy. In this technique, a modified objective function is defined by adding the penalty function into the original objective function. But the general approach is to use normalized constraints in order to provide an equal and fair penalty distribution for different types of constraint violations. So the constraints defined above are rearranged as below (Hasançebi, 2001):

$$g_i(A) = \max \left\{ 0, \left| \frac{\sigma_i}{\sigma_i^a} \right| - 1 \right\} \quad (6.20)$$

$$h_i(A) = \max\left\{0, \left|\frac{H_i}{H_i^a}\right| - 1\right\} \quad (6.21)$$

$$u_{j,k}(A) = \max\left\{0, \left|\frac{u_{j,k}}{u_{j,k}^a}\right| - 1\right\} \quad (6.22)$$

CHAPTER 7

SIMULATED ANNEALING

7.1 Introduction

Simulated annealing is a combinatorial optimization technique. The idea for simulated annealing method comes from thermodynamics and metallurgy. When the metal is cooled very slowly, it tends to solidify in a structure of minimum energy. Annealing is the physical process of heating up a solid and then cooling it down slowly until it crystallizes. The atoms in the material have high energies at high temperatures and have more freedom to arrange techniques. As the temperature is reduced, the atomic energies decrease. A crystal with regular structure is obtained at the state where the system has minimum energy (Pham and Karaboga, 2000).

So the analogy between physical state of atoms and optimization problem is established. In this method, the aim is to bring a physical system to a state of minimum energy level by rearranging its atomic configuration. If the cooling is carried out very quickly, rapid widespread irregularities and defects are formed in the (quenching) crystal structure. The system does not reach the minimum energy level. In order to make the system attain minimum energy, it has to be cooled down slowly.

“**The Metropolis Algorithm**”, a paper by Metropolis et al (1953), was published to simulate the cooling of material in a heat bath. He used the principles of statistical mechanics, Boltzman distribution and transition probability. In 1983 Kirkpatrick et al used the Metropolis algorithm to search for the best among feasible solutions of an optimization problem.

Although it is very simple to implement, it can be quite powerful. This technique has been used on a wide range of problems like traveling salesman problem, scheduling, storage optimization, circuit design problems, structural optimization, etc.

The implementation of simulated annealing is similar to traditional techniques; only one design point is generated at a time. It sometimes gives better ability to locate global optimum as compared to the GAs.

The most popular advantage of simulated annealing is the prevention of entrapment in a local optimum. It also has an enhanced capability to employ a very exploitative search in appropriate design regions. On the other hand, it is easier to be computerized as compared to other techniques (including GAs). Although it requires more evolutions on objective function, it is faster than GAs.

Some other features of simulated annealing are as follows:

- (i) The quality of the final solution does not depend on the initial guesses, but worse starting designs increase the computational effort.
- (ii) Similar to GAs, the convergence or transition characteristics are not affected by the continuity and differentiability of the functions, due to discrete nature of the function and constraint evaluations.
- (iii) The convergence is also not effected by the convexity of the feasible space.
- (iv) It is not necessary that the design variables are negative.

- (v) The method can be adapted to solve mixed-integer, discrete or continuous problems.
- (vi) For constrained problems, an equivalent unconstrained function can be formulated as in the case of GAs (Rao, 1996).

7.2 Simulated Annealing Process

Metropolis and his colleagues introduced a simple algorithm that was mimicked from annealing process in thermodynamics. Their proposed algorithm is based on Monte Carlo techniques which are explained below:

Assume a current state S_i of the solid with energy E_i . A new state with subsequent state S_j and energy E_j is generated by applying a perturbation mechanism. This perturbation causes to form a new energy state of the solid. This perturbation is done by randomly selecting a particle and displacing it by some random amount.

If the energy of the new state is lower than the energy of the current state ($\Delta E = E_j - E_i \leq 0$) then the displacement is accepted and the current state becomes the new state. If the energy of new state is higher ($\Delta E = E_j - E_i > 0$) then the state S_j accepted with a certain probability. This is given by:

$$Prob(accept) = e^{-\left(\frac{\Delta E}{K.t}\right)} \quad (7.1)$$

where

K : Boltzman constant,

t : Current temperature,

ΔE : Difference of energy levels, $E_j - E_i$

Boltzman constant is sometimes used as constant number but generally it is taken as average difference of energy levels, ΔE_{ave} .

This procedure is repeated a large number of times at the same temperature, in order to bring the system to thermal equilibrium. The acceptance criterion defined above is known as the Metropolis step and the procedure is known as the Metropolis algorithm. At high temperatures, the acceptance probability converges to 1 for all energy states according to equation (7.1). As seen from the equation, the probability of accepting a worse move is a function of both the temperature of the system and the change in the cost function. When the temperature drops, the probability of accepting a worse move is decreased. If the temperature drops to a value around 0, only better moves are accepted which effectively makes simulated annealing act like hill climbing.

30 years after the idea of Metropolis was introduced, a correspondence between annealing and optimization was established by Kirkpatrick et al (1983) and Cerny (1985) independently. They found the similarities listed below between these two different phenomena (Hasançebi, 2001):

- (i) The solutions in optimization are identical to the states in the physical system,
- (ii) Cost or objective function of an optimization problem is analogous to the energy level of a state,
- (iii) The current and candidate states are equivalent to the current and neighborhood solutions in an optimization problem,
- (iv) The temperature is a control parameter of optimization process,
- (v) The globally and locally minimum energy states correspond to global and local optimum respectively.

7.3 The Algorithm

The basic idea of the method is to generate a random point and evaluate the problem functions. If the trial point is infeasible, it is rejected and a new trial point close to the first one is generated. If this point is feasible and the cost function is smaller than the current best record, then the point is accepted as the best value. If

the trial point is feasible but the cost function is higher than the best value, it is not rejected immediately. A test called Metropolis test is executed. A random number is generated. If this number is smaller than the number found by Metropolis test, this value is accepted as the best value even though it is not actually. If the randomly generated number is higher than the number of Metropolis test, it is rejected. During the algorithm, a temperature parameter is used. Then this temperature is reduced slowly (called cooling schedule). Since the Metropolis test depends on this temperature value, the acceptance probability decreases to zero as the temperature is reduced. This means that the algorithm is likely to accept worse designs in the initial stages. But in the final stages, the worse designs are almost always rejected. So this strategy avoids getting trapped at a local optimum (Huang and Arora, 1997).

The main steps of SA are listed below:

- (i) Start with an initial solution and call it current solution.
- (ii) Generate a neighboring solution.
- (iii) If the new solution gives better objective cost, accept it and replace the current solution by the new one.
- (iv) Otherwise, accept it with a certain probability.
- (v) In the beginning, worse solutions are quite likely to be accepted.
- (vi) The chance of worse solutions being accepted reduces as the algorithm goes. Towards the end, worse solutions are less likely to be accepted.

In designing the cooling schedule, initial temperature, temperature reduction rule, number of iterations at each temperature and a stopping criterion must be specified.

7.4 Advantages of Simulated Annealing Over a Local Search Algorithm

SA handles only one possible solution at each time. So it is different from GAs which execute the individuals of a population. But SA is similar to local search algorithm to some extent. SA and local search algorithm both start with a randomly

created solution. The next trial (candidate solution) is generated in the close neighborhood of the current solution. The objective function values are calculated and compared for two possible solutions. If the candidate solution gives a better value of objective function then this solution is replaced to the current solution without any investigation. The procedure explained above is approximately the same with the local search algorithm. But the main difference starts from this point. If the candidate solution has a worse objective function value, this value is not rejected at first. On the contrary local search algorithm allows only downhill moves, so rejects the poorer solution. In SA, the candidate solution with a worse objective function value is tested by Metropolis test. In this test, the probability of accepting a poor candidate solution is given by $P = e^{-\Delta W / K.t}$ where K is the Boltzman parameter. The generated random number (r) in the range $[0,1]$ is compared with probability of acceptance. If the generated random number is lower (or equal to) than the acceptance probability ($P \leq r$), this poor design is accepted. Otherwise ($r > P$) it is rejected.

At early stages of the optimization process, the acceptance probability is high due to the high value of the temperature. This leads uphill moves and prevents getting stuck in local optima. As the temperature drops (cooling) the acceptance probability is lowered. At very low temperatures the algorithm becomes greedy which allows only downhill moves for minimization problems.

The main deficiencies of the method are the unknown rate at which the target level is to be reduced, and the uncertainty in the total number of trials and in the number of trials after which the target level needs to be reduced (Huang and Arora, 1997).

7.5 Stages of the Procedure

7.5.1 Cooling Procedure

Annealing (cooling) procedure of a simulated annealing algorithm consists of four components. These are listed below:

- (i) Starting temperature,
- (ii) Final temperature,
- (iii) Temperature decrement,
- (iv) Iterations at each temperature.

These components will be discussed below in detail.

7.5.2 Starting Temperature

The starting temperature must be hot enough to allow a move to almost any neighborhood state. If this is not done then the ending solution will be the same or very close to the starting solution.

On the other hand, if the starting temperature is too high then the search can move to any neighborhood and thus transform the search into a random search.

There is no specific method for finding a suitable starting temperature for a whole range of problems. Some different methods are offered for various cases in literature. One of the methods which is used widely is explained below:

Assume P^s as acceptance probability of candidate design at the start, then the acceptance probability:

$$t = t^s \quad P^s = e^{-\frac{\Delta E}{K.t^s}} \quad (7.2)$$

which is known as Metropolis test (explained before).

For the first poor candidates at the starting temperature, the Boltzman parameter will be equal to ΔE_{ave} . K is the running average of ΔE .

$$t = t_s \quad K = \Delta E \quad (7.3)$$

Substituting eq.(7.3) into eq.(7.4) leads to

$$P^s = e^{-1/t^s}$$

$$t^s = -\frac{1}{\text{Ln}(P^s)} \quad (7.4)$$

So the starting temperature depends on the starting acceptance probability, according to eq.(7.4). If larger values of starting acceptance probability are selected, the starting temperature will be high. It is generally chosen in the range of [0.5 , 0.9]. For value of $P^s=0.5$, t^s will be 1.44, and for $P^s=0.90$, $t^s = 19.49$.

Rayward- Smith (1996) suggested to start with a very high temperature and cool it rapidly until about 60 % of most solutions are being accepted. This forms the real starting temperature and it can now be cooled more slowly. A similar idea, suggested by Dowsland (1995) is to heat the system rapidly until a certain proportion of worse solutions are accepted and then slow cooling can start. This can be seen to be similar to how physical annealing works in that the material is heated until it is liquid and then cooling begins.

7.5.3 Final Temperature

The method used in deriving the starting temperature can be repeated to get the final temperature. Again the formulation is used as below:

$$t^f = -\frac{1}{\text{Ln}(P^f)} \quad (7.5)$$

The formula depends on the final acceptance probability. In this way, the final acceptance probability is equated to small values and it is found a value around 0. For example, $P^f=1 \times 10^{-6}$ leads a final temperature of $t^f=0.072$.

7.5.4 Temperature Decrement

When we decide the initial and final temperatures, the next step is to find the decrement of the temperature. For general optimization problems, temperature is an arbitrary parameter with the same units as the cost function. The way in which we decrease the temperature is critical to the success of the algorithm. SA theory states that enough iteration should be allowed at each temperature so that the system stabilizes at that temperature. Unfortunately, theory also states that the number of iterations at each temperature to achieve this might be exponential to the problem size which is impractical.

So there are some proposals to select the temperature increment. One way to decrease the temperature is a simple linear method.

$$t^{(c+1)} = f \cdot t^{(c)} \quad (7.6)$$

where

- $t^{(c+1)}$: Temperature of next cooling cycle,
- $t^{(c)}$: Temperature of previous cycle,
- f : A factor less than 1.

By the experience, f is used between 0.8 and 0.99 with better results being found in the higher end of the range. The higher the value of f , the longer it will take to decrease the temperature to the stopping criterion.

Assume that the total of N_c cooling cycles is preceded. This means that the temperature is reduced N_c-1 times throughout the process. So the equation is found;

$$t^f = t^s f^{N_c-1} \quad (7.7)$$

So substituting

$t^s = -\frac{1}{\text{Ln}(P^s)}$ and $t^f = -\frac{1}{\text{Ln}(P^f)}$ into this equation results:

$$f = \left[\frac{\text{Ln}(P^s)}{\text{Ln}(P^f)} \right]^{1/(N_c-1)} \quad (7.8)$$

From this equation, it is seen that temperature decrement is very sensitive to the number of cooling cycles. A small value of cooling factor obtained with low values for N_c can cause a rapid cooling schedule (quenching phenomenon in actual annealing analogue). On the contrary, a large value of N_c will give better result with careful annealing. But this can cause a heavy computational effort.

Balling (1991) and Bennage and Dhingra (1995) proposed that $N_c= 200$ and 300 are appropriate values for a careful annealing, preventing a premature solution.

Huang and Arora (1997) propose the following temperature reducing scheme; $t_s = \max(10000, \text{TCOST})$, if $K= 0$; and $t_K = 0.9 t_{K-1}$, if $K \geq 1$, where t_s and t_K are, respectively, the initial (starting) temperature and the temperature at the K -th iteration (an iteration here implies a design search process in which the temperature remains unchanged), K is the iteration number, and TCOST is the approximated value of the cost function which is estimated by the minimum cost of 10 randomly generated feasible points.

7.6 Candidate Design

In SA, only one point is generated at a time and the next point is generated within a certain neighbourhood of the current point. Thus, although SA randomly generates design points without the need for function or gradient information, it is not a pure random search within the entire design space. At early stage, a new point can be located far away from the current point to speed up the search process and to avoid getting trapped at a local minimum point. After the temperature decreases, the new

point is usually created nearby in order to focus on the local area (Huang and Arora, 1997).

In the original Metropolis algorithm, a candidate state is formed by changing the position of a single atom at random by a slight amount. This stage is stated as perturbation in SA. Since a severe perturbation may not result a neighboring solution, only a single variable of the current solution is randomly altered.

This is done for a selected variable as follows: First, it is decided a perturbation value. This value is chosen at random in an interval, which comprises the former and latter δ discrete neighbor values in the design set. If we name the current design set as V^c , the set of possible discrete values that the variable can assume in the candidate design will be in the interval,

$$V^a \in [V^c - \delta, \dots, V^c - 1, V^c + 1, \dots, V^c + \delta] \quad (7.9)$$

The candidate is formed by taking the new value of this variable and retaining the values of others same as in the current design.

The value of δ is under discussion. Balling (1991) has used a value of $\delta=2$ in a discrete optimization problem consisting of 81 and 46 discrete values. Bennage and Dhingra have used 6 and 9 for two design sets of 30 and 42 discrete values, respectively. Quinn and Izzuddin (1998) claim that the optimum design improves in case of δ is taken as half of the total number of discrete values in the design set.

Huang and Arora (1997) proposed the following method to generate a new design point:

Let z be a random number uniformly distributed in 0 and 1.

(i) For continuous variables;

$$x_i^{(a)} = \min(x_{iU}, x_i^{(c)} + \alpha(x_{iU} - x_{iL})), \quad \text{if } z \leq 0.5. \quad (7.10)$$

$$x_i^{(a)} = \max(x_{iL}, x_i^{(c)} + \alpha(x_{iU} - x_{iL})), \quad \text{if } z > 0.5. \quad (7.11)$$

where

$x_i^{(a)}$: The new (candidate) design for the i -th variable,

$x_i^{(c)}$: The current design for the i -th variable,

x_{iL} : The lower bound for the i -th variable,

x_{iU} : The upper bound for the i -th variable,

α : Step size calculated as $\alpha = \max(0.01, 0.2(0.9)^{K-1})$, where K is the iteration number.

(ii) For discrete variables;

If the current design point has the m -th discrete value for the i -th variable (i.e. $x_i^{(c)} = d_{im}$), then the new value for the i -th variable becomes $x_i^{(a)} = d_{ij}$, where $j = \min(q_i, m+J)$, if $z \leq 0.5$ or $j = \max(1, m-J)$, if $z > 0.50$. The integer J is calculated as $J = \max(1, \text{INT}(0.2(0.9)^{K-1} q_i))$, where $\text{INT}(x)$ denotes the integer part of x , and q_i is the number of discrete values for the i -th variable.

7.7 Iteration of Inner Loop

Another decision we have to make is how many iterations we have to make at each temperature. The success of SA algorithm depends on the attainment of thermal equilibrium at different temperatures during the cooling cycles. This thermal equilibrium is constituted with the iteration number. While a high number of iterations result in a very high degree of computational burden, a low number of iterations may not be sufficient to bring the system to the thermal equilibrium. Bennage and Dhingra (1995) noticed that the algorithm might easily avoid local

optima and reach thermal equilibrium under the influence of high values of acceptance probabilities in the early stages of optimization. However, especially towards the latest stages design transitions are quite restricted and escaping from local optima is only possible through an extensive neighborhood sampling. So the iteration number is kept low at the start, and it is increased gradually as cooling proceeds.

The formula proposed for iteration number is shown below:

$$I = \text{round} \left[I^f + (I^f - I^s) \left[\frac{t - t^f}{t^f - t^s} \right] \right] \quad (7.12)$$

where

I^s : Iteration number of the inner loop at the starting temperature,

I^f : Iteration number of the inner loop at the final temperature,

t^s : Starting temperature,

t^f : Final temperature,

$I^s = 1$ and $I^f \in [3,6]$ are recommended.

Using these values the iteration number I of the inner loop at a particular temperature (t) is calculated as in eq.(7.13).

Another method, first suggested by Lundy (1986) is to do only one iteration at each temperature, but to decrease the temperature very slowly. The formula used is;

$$t = t / (1 + \beta.t) \quad (7.13)$$

where

β : Suitably small number,

t : Temperature.

7.8 Constraint Handling

SA is an unconstrained optimization technique, similar to GAs. In order to solve a constraint optimization problem, two approaches are proposed. Balling (1991) proposed to disregard the infeasible designs automatically and to carry out only in the feasible regions of design space. Second approach as Bennage and Dhingra (1995) proposed is the use of a penalty function introducing to unconstrained objective function to define a modified (constrained) objective function. In this method, the search is not restricted to the feasible regions, but infeasible solutions are penalized. Penalty function method has superiorities over the first approach. These are listed below:

- (i) If the starting solution is far away from the optimum, using both feasible and infeasible regions makes the algorithm reach the optimum much faster.
- (ii) Diverting the search process temporarily to infeasible regions avoids getting trapped in a local optimum.
- (iii) For the case where the optimum is located very close to infeasible regions, approaching to the optimum from the infeasible regions is possible and sometimes more advantageous.

CHAPTER 8

NUMERICAL EXAMPLES

In this chapter, seven numerical examples are studied using genetic algorithm and simulated annealing techniques. Practical design load cases are used in the first three problems according to “ASCE 7-98 Minimum Design Loads for Buildings and Other Structures”. In fact, the use of five basic load combinations is stipulated in ASCE 7-98 for Allowable Stress Design (ASD), as follows:

$$1. D \quad (8.1)$$

$$2. D + L + F + H + T + (L_r \text{ or } S \text{ or } R) \quad (8.2)$$

$$3. D + (W \text{ or } 0.7 E) + L + (L_r \text{ or } S \text{ or } R) \quad (8.3)$$

$$4. 0.6 D + W + H \quad (8.4)$$

$$5. 0.6 D + 0.7 E + H \quad (8.5)$$

where

D : Dead load

E : Earthquake load

F : Load due to fluids with well-defined pressures and maximum heights

H : Load due to lateral earth pressure, ground water pressure, or pressure of bulk materials

L : Live load

L_r : Roof live load

- R : Rain load
- S : Snow load
- T : Self-straining force
- W : Wind load

The fourth test problem is taken from the literature for comparison purposes. Finally, in the last three examples, the effect of rise-to-span ratio on the optimum design is investigated, in addition to double layer domes.

8.1 354-Bar Dome (Height of 4.34 m.)

The design of an auditorium building with a capacity of 500 people, which is assumed to locate in Nebraska will be achieved. It is circular in plan view. It has a diameter of 40 m. The building consists of two parts; the main part which is reinforced concrete, and the roof part which is a pin-connected type steel dome with 354 members and 127 joints. The total height of the building is 14.34 m., and the height of the steel dome is only 4.34 m. The plan and side views of the building are shown in Figures 8.1 and 8.2. The top view, side view and 3-dimensional view of the steel dome are presented in Fig.8.3 through 8.5.

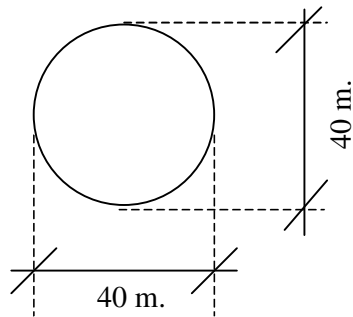


Fig.8.1. Top View (354-Bar)

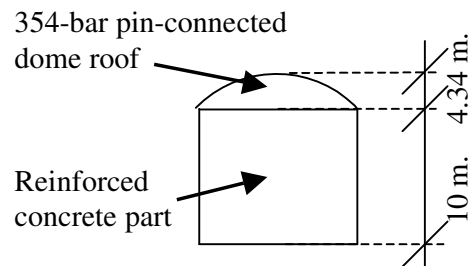


Fig.8.2. Side View (354-Bar)

As highlighted in the preceding chapters, two important loads for dome structures are wind and snow loads. Therefore, here these two loads will be calculated according to the design code, ASCE 7-98.

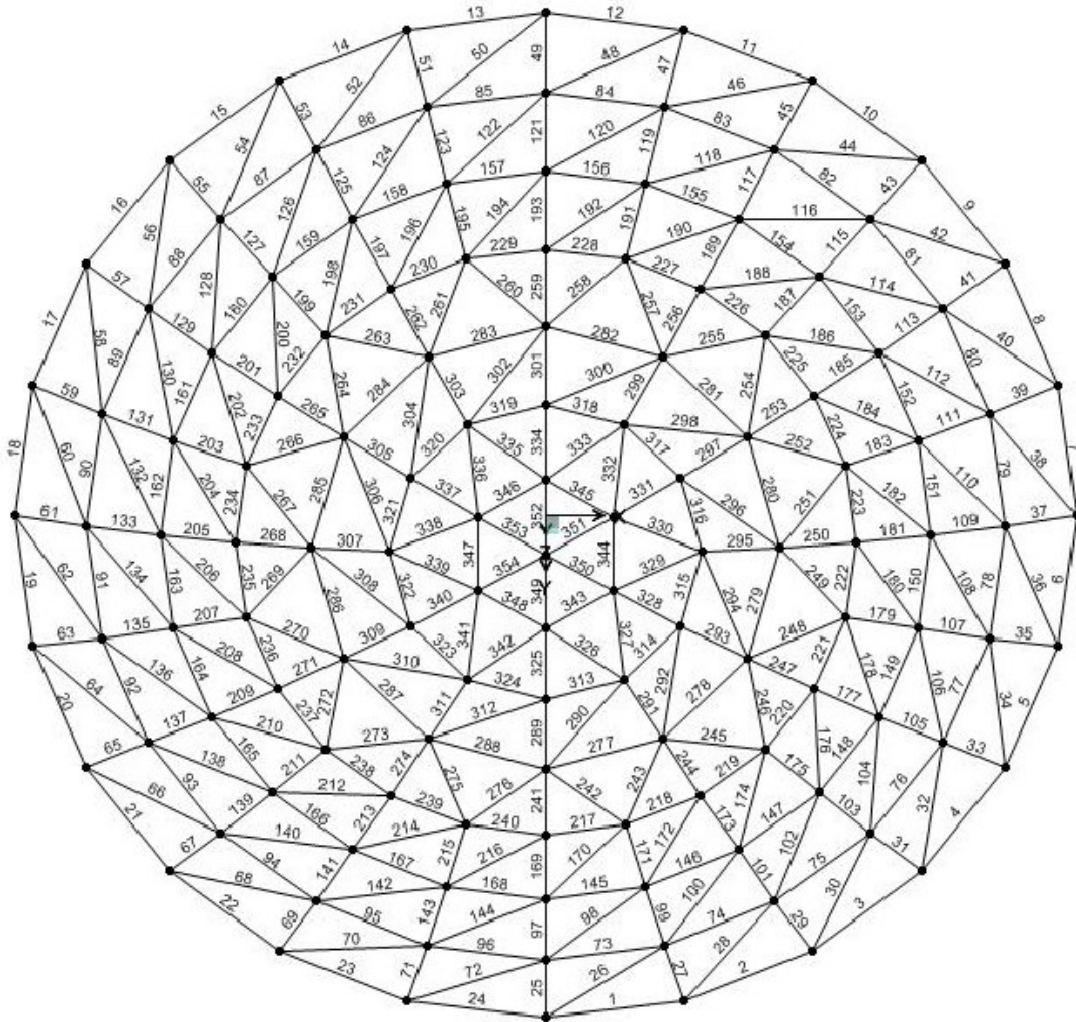


Fig.8.3. Top View of 354-Bar Dome (Given Member Numbers)

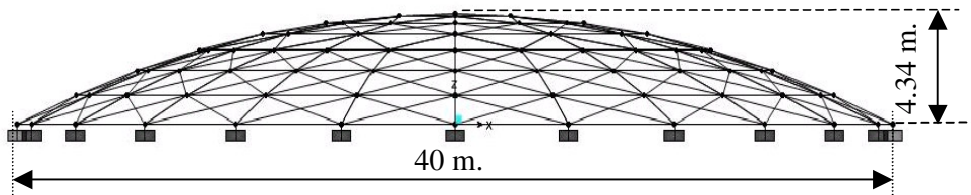


Fig.8.4. Side View of 354-Bar Dome

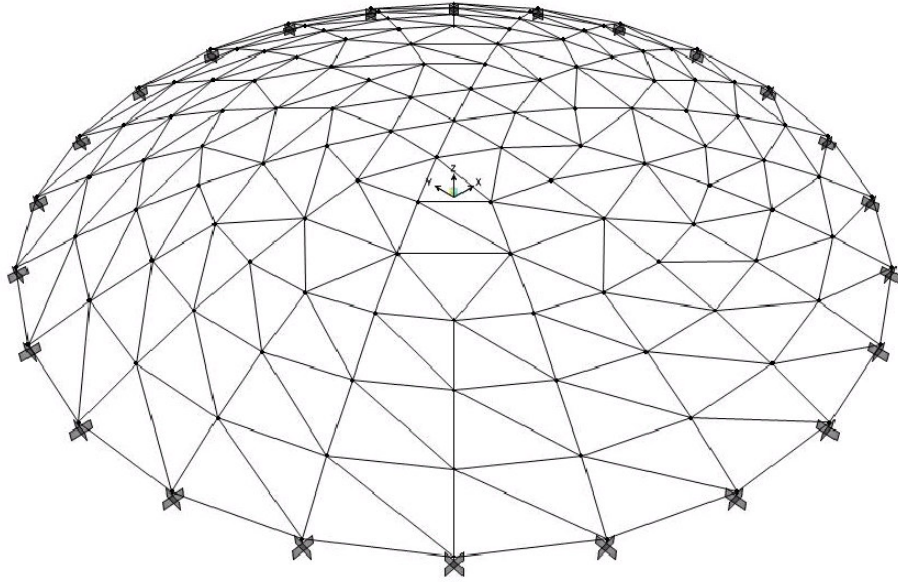


Fig.8.5. 3-D View of 354-Bar Dome

8.1.1 Wind Load (Analytical Procedure)

The design procedure explained in part 6.5.3. of ASCE 7-98 is followed.

Basic Wind Speed V for Nebraska is taken from Figure 6.1 of ASCE 7-98.

$$V = 40 \text{ m/s} \quad (90 \text{ mph})$$

Wind Directionality Factor K_d is taken from Table 6.6 of ASCE 7-98.

$$K_d = 0.85 \quad (\text{for arched roofs})$$

Importance Factor I for the building is determined as 1.15 from Table 6.1 of ASCE 7-98.

$$I = 1.15 \quad (\text{for building category III})$$

Exposure Category is assumed as C from the definitions given in part 6.5.6 of ASCE 7-98.

Velocity Pressure Exposure Coefficient K_z is taken from Table 6-5 of ASCE 7-98. The mean height of the roof is 12.17 m. (40 feet).

$$K_z = 1.04 \quad (\text{for exposure C and 40 ft height})$$

Topographic Factor K_{zt} is calculated from $K_{zt} = (1 + K_1 K_2 K_3)^2$ where K_1 , K_2 , K_3 are taken from Fig.6.2 of ASCE 7-98.

It is assumed that there are a 2-D ridge with $H/L_h = 0.30$, 3-D escarpment with $x/L_h = 1.00$ and 2-D ridge with $z/L_h = 0.40$ in the general topology, where

H : Height of the hill or escarpment relative to the upwind terrain, in meter,

L_h : Distance upwind of crest to where the difference in the ground elevation is half the height of the hill or escarpment, in meter,

K_1 : Factor to account for shape of topographic feature and maximum speed-up effect,

K_2 : Factor to account for reduction in speed-up with distance upwind or downwind of crest,

K_3 : Factor to account for reduction in speed-up with height above local terrain,

x : Distance (upwind or downwind) from the crest to the building site, in meter,

z : Height above local ground level, in meter,

$$K_1 = 0.43, \quad K_2 = 0.33, \quad K_3 = 0.30 \quad (\text{from Fig.6.2 of ASCE 7-98})$$

$$K_{zt} = (1 + 0.43 \times 0.33 \times 0.30)^2 = 1.087$$

Gust Effect Factor G is found as 0.85 directly by assuming the structure as rigid.

$$G = 0.85$$

Enclosure Classification is assumed as enclosed, since all lateral and upper parts of the building are closed and subjected to wind pressure directly.

Velocity Pressure is calculated by using the equation given in ASCE 7-98.

$$q_z = 0.613.K_z.K_{zt}.K_d V^2 I \text{ (N/m}^2\text{)} \quad \text{(8.6) (Eq. 6-13 of ASCE 7-98)}$$

$$q_z = 0.613 \times 1.04 \times 1.087 \times 0.85 \times (40)^2 \times 1.15$$

$$q_z = 1084 \text{ N/m}^2$$

Internal Pressure Coefficients GC_{pi} are found as +0.18 and -0.18 for enclosed buildings from Table 6.7 of ASCE 7-98. Two signed values (positive and negative) are used according to the code. Plus and minus signs signify pressures acting towards and away from the internal surfaces.

External Pressure Coefficients C_p are found from Table 6.8 of ASCE 7-98. The dome is assumed to be separated into three parts, such as windward quarter, center half and leeward quarter. Three different external pressure coefficients for these three parts of the dome are calculated with respect to rise-to-span ratio. The rise-to-ratio, r is $4.34/40=0.10$ for the building considered above.

$$C_p = -0.9 \quad \text{(for windward quarter)}$$

$$C_p = -0.7 - r = -0.7 - 0.1 = -0.8 \quad \text{(for center half)}$$

$$C_p = -0.5 \quad \text{(for leeward quarter)}$$

Main Force Resisting Systems

Design wind pressure is calculated as follows:

$$p = qGC_p - q_i(GC_{pi}) \quad \text{(N/m}^2\text{)} \quad \text{(8.7) (Eq.6-15 of ASCE 7-98)}$$

where

q = q_h for roofs, evaluated at height h ,

q_i = q_h for roofs of enclosed buildings,

G : Gust effect factor,

C_p : External pressure coefficient from Fig.6-3 or Table 6-8 of ASCE 7-98,

(GC_{pi}) : Internal pressure coefficient from Table 6-7 of ASCE 7-98.

For windward quarter

$$p = 1084 \times 0.85 \times (-0.90) - 1084 \times (\pm 0.18) = \begin{cases} -1024 \text{ N/m}^2 \\ -634 \text{ N/m}^2 \end{cases}$$

For center half

$$p = 1084 \times 0.85 \times (-0.80) - 1084 \times (\pm 0.18) = \begin{cases} -932 \text{ N/m}^2 \\ -542 \text{ N/m}^2 \end{cases}$$

For leeward quarter

$$p = 1084 \times 0.85 \times (-0.50) - 1084 \times (\pm 0.18) = \begin{cases} -656 \text{ N/m}^2 \\ -266 \text{ N/m}^2 \end{cases}$$

Notice that all the forces is negative, meaning that they act away from the surface (suction). This is due to the low height of the dome. According to Table 6-8 of ASCE 7-98, the domes which have rise-to-span ratios larger than 0.2 have positive wind pressure while the ones which have rise-to-span ratios less than 0.2 have negative wind pressures. These results are compatible with the wind tunnel test results presented in Fig.3.12 and 3.13.

8.1.2 Snow Loads

The equation given in ASCE 7-98 for snow load calculations is given below;

$$p_f = 0.7 \cdot C_e \cdot C_t \cdot I \cdot p_g \quad (8.8) \text{ (Eq.7-1 of ASCE 7-98)}$$

where

p_f : The snow load on a roof with a slope equal to or less than 5°,

C_e : Exposure factor, determined from Table 7-2 of ASCE 7-98,

C_t : Thermal factor, determined from Table 7-3 of ASCE 7-98,

I : Importance factor, determined from Table 7-4 of ASCE 7-98,

p_g : Ground snow load, determined from Fig.7-1 and Table 7-1 of ASCE 7-98.

$$C_e = 0.9 \quad (\text{for exposure category C and fully exposed roof})$$

$$C_t = 1.0 \quad (\text{for structures except as indicated in Table 7.3})$$

$$I = 1.10 \quad (\text{for building category III})$$

$$p_g = 25 \text{ lb/ft}^2 \quad (1.1975 \text{ kN/m}^2) \quad (\text{for Nebraska})$$

$$p_f = 0.7 \times 0.90 \times 1.0 \times 1.10 \times 1.1975 = 0.830 \text{ kN/m}^2$$

Tangent of vertical angle from eaves to crown= $4.34 / 20 = 0.217$ Angle= 12.2°
 Since the vertical angle exceeds 10° , the minimum allowable values of p_f do not apply. Using $p_f = 0.830 \text{ kN/m}^2$ and formulation for sloped-roof load yields;

$$p_s = C_s p_f \quad (8.9) \text{ (Eq.7-2 of ASCE 7-98)}$$

where

p_s : The sloped-roof snow load,

C_s : Roof slope factor,

p_f : The snow load on a roof with a slope equal to or less than 5° .

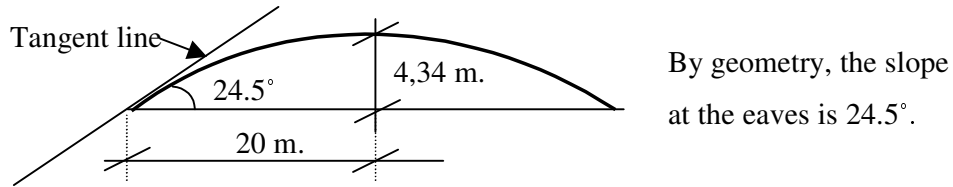


Fig.8.6. Side View of The Dome (354-Bar)

From Fig.7.2a of ASCE 7-98, $C_s = 1.0$ until slope exceeds 30° (total length of the roof in this problem).

$$C_s = 1.0 \quad (\text{from Fig.7-2 and Fig.7-3 of ASCE 7-98 for a roof slope of } 24.5^\circ)$$

$$p_s = 0.830 \text{ kN/m}^2 \quad (\text{balanced load})$$

Unbalanced Snow Load (from Fig.7-3 of ASCE 7-98)

Since the vertical angle from the eaves to the crown is greater than 10° and less than 60° , the unbalanced snow loads must be considered. The unbalanced loads are calculated according to the formulation for case 1 (slope at eaves $< 30^\circ$) given in Fig.7-3 of ASCE 7-98.

Unbalanced load at crown;

$$= 0.5 * p_f = 0.5 * 0.830 = 0.415 \text{ kN/m}^2$$

Unbalanced load at eaves;

$$= 2 * p_f = 2 * 0.830 = 1.660 \text{ kN/m}^2$$

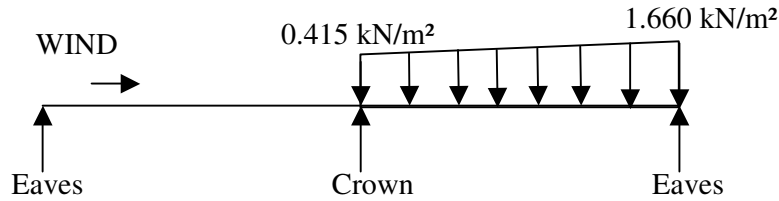


Fig.8.7. Unbalanced Snow Load (354-Bar)

8.1.3 Dead Load

Sandwich type aluminium cladding is used. The dead load of this cladding (including frame elements to be used for girts) is taken as 200 N/m².

8.1.4 Roof Live Load

Roof live load can be taken as 900 N/m² to take into account the weight of the men climbing on the roof. But this load is compensated by snow load since roof live load and snow load cannot be acted at the same time.

8.1.5 Combined Loaded Case

Six load cases are considered as shown below;

1. D + S (balanced)
2. D + S (unbalanced)
3. D + W (taken internal pressure coefficient as positive) + S (balanced)
4. D + W (taken internal pressure coefficient as negative) + S (balanced)
5. D + W (taken internal pressure coefficient as positive) + S (unbalanced)
6. D + W (taken internal pressure coefficient as negative) + S (unbalanced)

These load cases are shown schematically in Fig.8.8 through Fig.8.11. Note that these figures are not to scale.

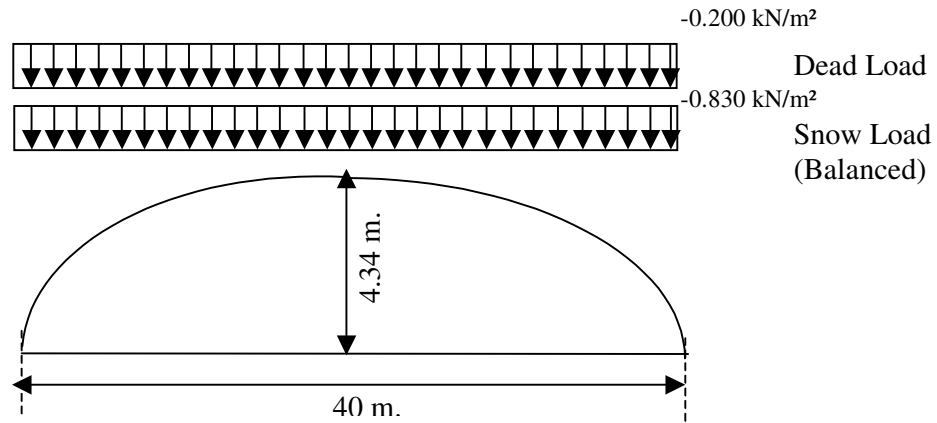


Fig.8.8 Load Case 1 of 354-Bar Dome (h=4.34 m)

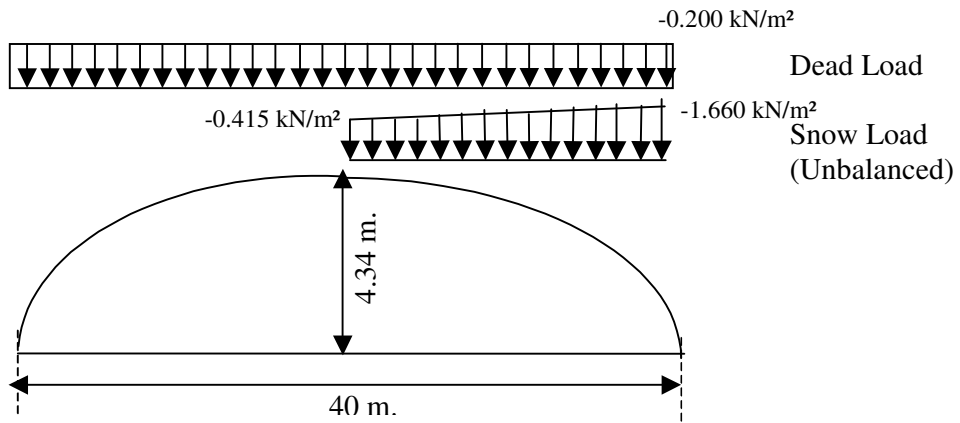


Fig.8.9 Load Case 2 of 354-Bar Dome (h=4.34 m)

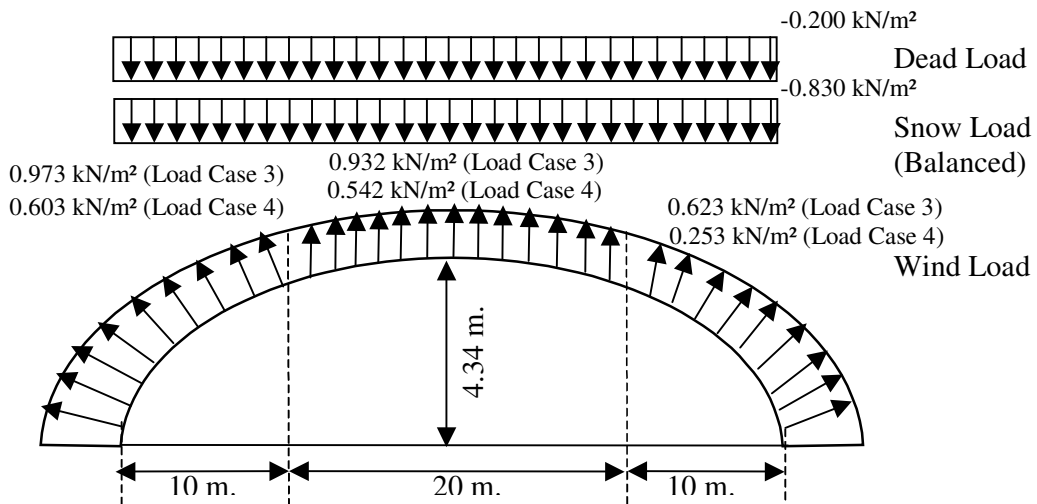


Fig.8.10 Load Case 3-4 of 354-Bar Dome (h=4.34 m)

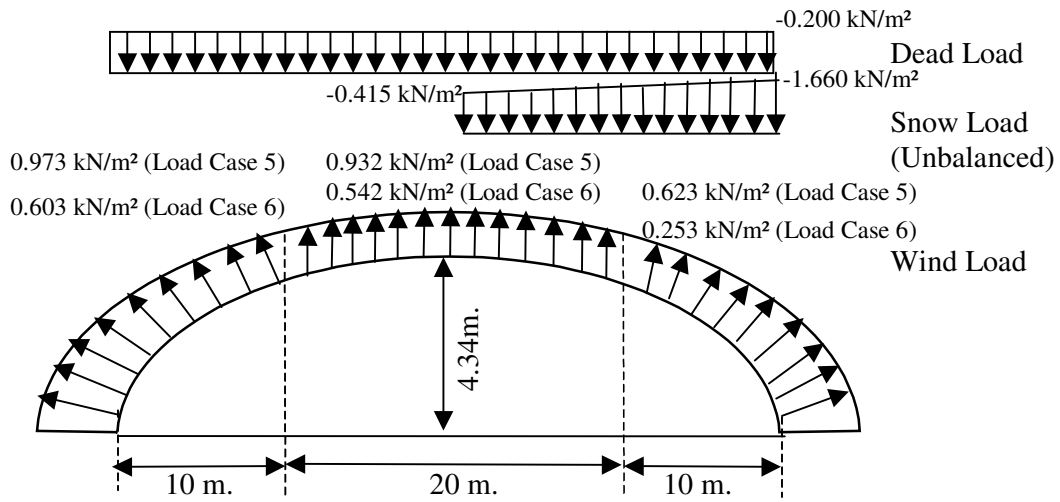


Fig.8.11 Load Case 5-6 of 354-Bar Dome (h=4.34 m)

As stated before, according to ASCE 7-98 the dome is divided into three pieces such as windward quarter, center half and leeward quarter, as shown in Fig.8.12. Hence, the loads acting on these pieces are calculated separately.

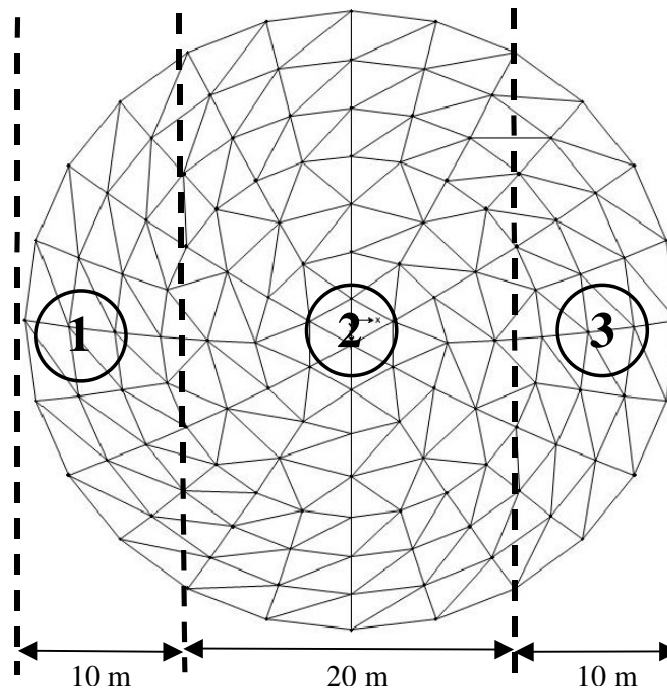


Fig.8.12. Pieces of 354-Bar Dome (h=4.34 m)

Whole Structure	}	Number of Total Joints	:127
		Number of Total Members	:354
		Total Area (Curved)	:1301 m ²
		Projected Area	:1257 m ²
Piece 1		Piece 2	Piece 3
Number of Joints:27		Number of Joints :73	Number of Joints:27
Curved Area :254.4 m ²		Curved Area :792.2 m ²	Curved Area :254.4 m ²
Projected Area:245.85 m ²		Projected Area :765.41 m ²	Projected Area :245.85 m ²

8.1.6 Load Combinations

It is assumed that dead and snow loads act on the projected area, while wind load acts on the curved surface area.

Load Case 1 (Dead Load + Balanced Snow)

-0.200 kN/m² (Dead Load)

-0.830 kN/m² (Snow Load)

-1.030 kN/m² (↓) (Dead + Snow Load)

Load Case 2 (Dead Load + Unbalanced Snow)

For Left Half

-0.200 kN/m² (↓) (Dead Load)

For Right Half

-0.200 kN/m² (Dead Load)

-1.0375 kN/m² (Average Unbalanced Snow Load)

-1.238 kN/m² (↓) (Dead + Snow Load)

Load Case 3 (Dead Load + Balanced Snow + Wind Load with Positive Internal Pressure Coefficient)

For Windward Quarter

-0.200 kN/m² (Dead Load)

-0.830 kN/m² (Snow Load)

-1.030 kN/m² (↓) (Dead + Snow Load)

0.973 kN/m² (↑) (Wind Load) (1.024 x Cos 18.10°)

-0.318 kN/m² (←) (Lateral Load Due to Wind) (1.024 x Sin 18.10°)

For Center Half

-0.200 kN/m² (Dead Load)

-0.830 kN/m² (Snow Load)

-1.030 kN/m² (↓) (Dead + Snow Load)

0.932 kN/m² (↑) (Wind Load)

For Leeward Quarter

-0.200 kN/m² (Dead Load)

-0.830 kN/m² (Snow Load)

-1.030 kN/m² (↓) (Dead + Snow Load)

0.623 kN/m² (↑) (Wind Load) (0.656 x Cos 18.10°)

0.204 kN/m² (→) (Lateral Load Due to Wind) (0.656 x Sin 18.10°)

Load Case 4 (Dead Load + Balanced Snow + Wind Load with Negative Internal Pressure Coefficient)

For Windward Quarter

-0.200 kN/m² (Dead Load)

-0.830 kN/m² (Snow Load)

-1.030 kN/m² (↓) (Dead + Snow Load)

0.603 kN/m² (↑) (Wind Load) (0.634 x Cos 18.10°)

-0.197 kN/m² (←) (Lateral Load Due to Wind) (0.634 x Sin 18.10°)

For Center Half

-0.200 kN/m² (Dead Load)

-0.830 kN/m² (Snow Load)

-1.030 kN/m² (↓) (Dead + Snow Load)

0.542 kN/m² (↑) (Wind Load)

For Leeward Quarter

-0.200 kN/m² (Dead Load)

-0.830 kN/m² (Snow Load)

-1.030 kN/m² (↓) (Dead + Snow Load)

0.253 kN/m² (↑) (Wind Load) (0.266 x Cos 18.10°)

0.083 kN/m² (→) (Lateral Load Due to Wind) (0.266 x Sin 18.10°)

Load Case 5 (Dead Load + Unbalanced Snow + Wind Load with Positive Internal Pressure Coefficient)

For Windward Quarter

-0.200 kN/m² (Dead Load)

0 kN/m² (Snow Load)

-0.200 kN/m² (↓) (Dead + Snow Load)

0.973 kN/m² (↑) (Wind Load) (1.024 x Cos 18.10°)

-0.318 kN/m² (←) (Lateral Load Due to Wind) (1.024 x Sin 18.10°)

For Center Half (Left Part)

-0.200 kN/m² (Dead Load)

0 kN/m² (Snow Load)

-0.200 kN/m² (↓) (Dead + Snow Load)

0.932 kN/m² (↑) (Wind Load)

For Center Half (Right Part)

-0.200 kN/m² (Dead Load)

-0.726 kN/m² (Average Unbalanced Snow Load)

-0.926 kN/m² (↓) (Dead + Snow Load)

0.932 kN/m² (↑) (Wind Load)

For Leeward Quarter

-0.200 kN/m² (Dead Load)

-1.348 kN/m² (Average Unbalanced Snow Load)

-1.548 kN/m² (↓) (Dead + Snow Load)

0.623 kN/m² (↑) (Wind Load) (0.656 x Cos 18.10°)

0.204 kN/m² (→) (Lateral Load Due to Wind) (0.656 x Sin 18.10°)

Load Case 6 (Dead Load + Unbalanced Snow + Wind Load with Negative Internal Pressure Coefficient))

For Windward Quarter

-0.200 kN/m² (Dead Load)

0 kN/m² (Snow Load)

-0.200 kN/m² (↓) (Dead + Snow Load)

0.603 kN/m² (↑) (Wind Load) (0.634 x Cos 18.10°)

-0.197 kN/m^2 (\leftarrow) (Lateral Load Due to Wind) ($0.634 \times \sin 18.10^\circ$)

For Center Half (Left Part)

-0.200 kN/m^2 (Dead Load)

0 kN/m^2 (Snow Load)

-0.200 kN/m^2 (\downarrow) (Dead + Snow Load)

0.542 kN/m^2 (\uparrow) (Wind Load)

For Center Half (Right Part)

-0.200 kN/m^2 (Dead Load)

-0.726 kN/m^2 (Average Unbalanced Snow Load)

-0.926 kN/m^2 (\downarrow) (Dead + Snow Load)

0.542 kN/m^2 (\uparrow) (Wind Load)

For Leeward Quarter

-0.200 kN/m^2 (Dead Load)

-1.348 kN/m^2 (Average Unbalanced Snow Load)

-1.548 kN/m^2 (\downarrow) (Dead + Snow Load)

0.253 kN/m^2 (\uparrow) (Wind Load) ($0.266 \times \cos 18.10^\circ$)

0.083 kN/m^2 (\rightarrow) (Lateral Load Due to Wind) ($0.266 \times \sin 18.10^\circ$)

8.1.7 Loads Acting On Joints

Load Case 1 (D + S_{Balanced})

$(-1.030 \text{ kN/m}^2 * 1257 \text{ m}^2)/(127 \text{ joints}) = -10.195 \text{ kN/joint} = \underline{-2.291 \text{ kip/joint}}$ (\downarrow)

Load Case 2 (D + S_{Unbalanced})

For Left Half

$(-0.200 \text{ kN/m}^2 * 1257 \text{ m}^2/2)/(127 \text{ joints}/2) = -1.980 \text{ kN/joint} = \underline{-0.445 \text{ kip/joint}}$ (\downarrow)

For Right Half

$(-1.238 \text{ kN/m}^2 * 1257 \text{ m}^2/2)/(127 \text{ joints}/2) = -12.253 \text{ kN/joint} = \underline{-2.754 \text{ kip/joint}}$ (\downarrow)

Load Case 3 (D + S_{Balanced} + W_{Positive Internal Pressure Coefficient})

For Windward Quarter

$(-1.030 \text{ kN/m}^2 * 245.85 \text{ m}^2 + 0.973 \text{ kN/m}^2 * 254.40 \text{ m}^2)/(27 \text{ joints}) = -0.211 \text{ kN/joint} = \underline{-0.047 \text{ kip/joint}}$ (\downarrow)

Lateral Load

$$(-0.318 \text{ kN/m}^2 * 254.4 \text{ m}^2) / (27 \text{ joints}) = -2.996 \text{ kN/joint} = \underline{\underline{-0.673 \text{ kip/joint}}} \leftarrow$$

For Center Half

$$(-1.030 \text{ kN/m}^2 * 765.41 \text{ m}^2 + 0.932 \text{ kN/m}^2 * 792.2 \text{ m}^2) / (73 \text{ joints}) = -0.686 \text{ kN/joint} = \underline{\underline{-0.154 \text{ kip/joint}}} \downarrow$$

For Leeward Quarter

$$(-1.030 \text{ kN/m}^2 * 245.85 \text{ m}^2 + 0.623 \text{ kN/m}^2 * 254.4 \text{ m}^2) / (27 \text{ joints}) = -3.509 \text{ kN/joint} = \underline{\underline{-0.789 \text{ kip/joint}}} \downarrow$$

Lateral Load

$$(0.204 \text{ kN/m}^2 * 254.4 \text{ m}^2) / (27 \text{ joints}) = 1.922 \text{ kN/joint} = \underline{\underline{0.432 \text{ kip/joint}}} \rightarrow$$

Load Case 4 (D + S_{Balanced} + W_{Negative Internal Pressure Coefficient})

For Windward Quarter

$$(-1.030 \text{ kN/m}^2 * 245.85 \text{ m}^2 + 0.603 \text{ kN/m}^2 * 254.4 \text{ m}^2) / (27 \text{ joints}) = -3.697 \text{ kN/joint} = \underline{\underline{-0.831 \text{ kip/joint}}} \downarrow$$

Lateral Load

$$(-0.197 \text{ kN/m}^2 * 254.4 \text{ m}^2) / (27 \text{ joints}) = -1.856 \text{ kN/joint} = \underline{\underline{-0.417 \text{ kip/joint}}} \leftarrow$$

For Center Half

$$(-1.030 \text{ kN/m}^2 * 765.41 \text{ m}^2 + 0.542 \text{ kN/m}^2 * 792.2 \text{ m}^2) / (73 \text{ joints}) = -4.918 \text{ kN/joint} = \underline{\underline{-1.106 \text{ kip/joint}}} \downarrow$$

For Leeward Quarter

$$(-1.030 \text{ kN/m}^2 * 245.85 \text{ m}^2 + 0.253 \text{ kN/m}^2 * 254.4 \text{ m}^2) / (27 \text{ joints}) = -6.995 \text{ kN/joint} = \underline{\underline{-1.573 \text{ kip/joint}}} \downarrow$$

Lateral Load

$$(0.083 \text{ kN/m}^2 * 254.4 \text{ m}^2) / (27 \text{ joints}) = 0.782 \text{ kN/joint} = \underline{\underline{0.176 \text{ kip/joint}}} \rightarrow$$

Load Case 5 (D + S_{Unbalanced} + W_{Positive Internal Pressure Coefficient})

For Windward Quarter

$$(-0.200 \text{ kN/m}^2 * 245.85 \text{ m}^2 + 0.973 \text{ kN/m}^2 * 254.4 \text{ m}^2) / (27 \text{ joints}) = 7.347 \text{ kN/joint} = \underline{\underline{1.652 \text{ kip/joint}}} \uparrow$$

Lateral Load

$$(-0.318 \text{ kN/m}^2 * 254.4 \text{ m}^2) / (27 \text{ joints}) = -2.996 \text{ kN/joint} = \underline{\underline{-0.674 \text{ kip/joint}}} \leftarrow$$

For Center Half (Left Part)

$$(-0.200 \text{ kN/m}^2 * (765.41 \text{ m}^2/2) + 0.542 \text{ kN/m}^2 * (792.2 \text{ m}^2/2)) / (73/2 \text{ joints}) = 3.785 \text{ kN/joint} = \underline{\mathbf{0.851 \text{ kip/joint}}} (\uparrow)$$

For Center Half (Right Part)

$$(-0.926 \text{ kN/m}^2 * (765.41 \text{ m}^2/2) + 0.932 \text{ kN/m}^2 * (792.2 \text{ m}^2/2)) / (73/2 \text{ joints}) = 0.405 \text{ kN/joint} = \underline{\mathbf{0.091 \text{ kip/joint}}} (\uparrow)$$

For Leeward Quarter

$$(-1.548 \text{ kN/m}^2 * 245.85 \text{ m}^2 + 0.623 \text{ kN/m}^2 * 254.4 \text{ m}^2) / (27 \text{ joints}) = -8.225 \text{ kN/joint} = \underline{\mathbf{-1.850 \text{ kip/joint}}} (\downarrow)$$

Lateral Load

$$(0.204 \text{ kN/m}^2 * 254.4 \text{ m}^2) / (27 \text{ joints}) = 1.922 \text{ kN/joint} = \underline{\mathbf{0.432 \text{ kip/joint}}} (\rightarrow)$$

Load Case 6 (D + S_{Unbalanced} + W_{Negative Internal Pressure Coefficient})

For Windward Quarter

$$(-0.200 \text{ kN/m}^2 * 245.85 \text{ m}^2 + 0.603 \text{ kN/m}^2 * 254.4 \text{ m}^2) / (27 \text{ joints}) = 3.860 \text{ kN/joint} = \underline{\mathbf{0.868 \text{ kip/joint}}} (\uparrow)$$

Lateral Load

$$(-0.197 \text{ kN/m}^2 * 254.4 \text{ m}^2) / (27 \text{ joints}) = -1.856 \text{ kN/joint} = \underline{\mathbf{-0.417 \text{ kip/joint}}} (\leftarrow)$$

For Center Half (Left Part)

$$(-0.200 \text{ kN/m}^2 * (765.41 \text{ m}^2/2) + 0.542 \text{ kN/m}^2 * (792.2 \text{ m}^2/2)) / (73/2 \text{ joints}) = 3.785 \text{ kN/joint} = \underline{\mathbf{0.851 \text{ kip/joint}}} (\uparrow)$$

For Center Half (Right Part)

$$(-0.926 \text{ kN/m}^2 * (765.41 \text{ m}^2/2) + 0.542 \text{ kN/m}^2 * (792.2 \text{ m}^2/2)) / (73/2 \text{ joints}) = -3.827 \text{ kN/joint} = \underline{\mathbf{-0.860 \text{ kip/joint}}} (\downarrow)$$

For Leeward Quarter

$$(-1.548 \text{ kN/m}^2 * 245.85 \text{ m}^2 + 0.253 \text{ kN/m}^2 * 254.4 \text{ m}^2) / (27 \text{ joints}) = -11.712 \text{ kN/joint} = \underline{\mathbf{-2.633 \text{ kip/joint}}} (\downarrow)$$

Lateral Load

$$(0.083 \text{ kN/m}^2 * 254.4 \text{ m}^2) / (27 \text{ joints}) = 0.782 \text{ kN/joint} = \underline{\mathbf{0.176 \text{ kip/joint}}} (\rightarrow)$$

8.1.8 Results

American circular hollow pipes are used in the design. As stated before, two different softwares (SSTOGA and SSTOSA) which utilize two techniques (Genetic Algorithms and Simulated Annealing) are made use of in the analysis. Since these techniques are probabilistic, the programs are run three times in order to ensure the reliability of the results. The result which is tabulated in Table 8.1 was located by both programs. Four different ready sections (P2+1/2, P3, P3+1/2,P4) are used in the design.

Table 8.1. Result of 354-Bar Dome

Member Type	Number of Members (From Fig.8.3)	Ready Section	Cross Sectional Area (in ²)
A ₁	1:24	P3	2.23
A ₂	25,27,29,.....,67,69,71	P3	2.23
A ₃	26,28,30,.....,68,70,72	P4	3.17
A ₄	73:96	P4	3.17
A ₅	97,99,101,.....,139,141,143	P3	2.23
A ₆	98,100,102,.....,140,142,144	P3+1/2	2.68
A ₇	145:168	P3+1/2	2.68
A ₈	169,171,173,.....,211,213,215	P3	2.23
A ₉	170,172,174,.....,212,214,216	P3+1/2	2.68
A ₁₀	217:240	P3+1/2	2.68
A ₁₁	241,244,247,250,253,256, 259,262,265,268,271,274	P2+1/2	1.70
A ₁₂	242 ,245,248,251,254,257, 260,263,266,269,272,275	P2+1/2	1.70
A ₁₃	243 ,246,249,252,255,258, 261,264,267,270,273,276	P2+1/2	1.70
A ₁₄	277:288	P3	2.23
A ₁₅	289,291,293,.....,307,309,311	P3	2.23
A ₁₆	290,292,294,.....,308,310,312	P3	2.23
A ₁₇	313:324	P2+1/2	1.70
A ₁₈	325,328,331,334,337,340	P2+1/2	1.70
A ₁₉	326,329,332,335,338,341	P2+1/2	1.70
A ₂₀	327,330,333,336,339,342	P2+1/2	1.70
A ₂₁	343:348	P2+1/2	1.70
A ₂₂	349:354	P2+1/2	1.70
	Total Volume		132208.06 in²
	Total Weight		37471.47 lb

As seen from the Table 8.1, the optimum design is 37471 lb. The graphs of evolution towards to optimum design for both softwares (SSTOGA using Genetic Algorithm and SSTOSA using Simulated Annealing) are presented graphically in Fig.8.13.

In SSTOGA, 1000 generations each having 100 structural analyses are performed. This means that the software uses totally 100,000 structural analyses to converge the optimum solution (blue line).

In SSTOSA, 30,279 structural analyses in 300 cooling cycles are performed in order to find the optimum design (red line). This is fewer as compared to the number of the SSTOGA software. So this effects the CPU time. While SSTOSA performs 30,279 structural analyses to converge the optimum solution in about 4 hours (with a computer of AMD 1700 and 128 Mb RAM), SSTOGA converges the same optimum design by performing 100,000 structural analyses in about 20 hours. This shows that CPU times are very distinctive where SSTOSA converges very earlier than SSTOGA.

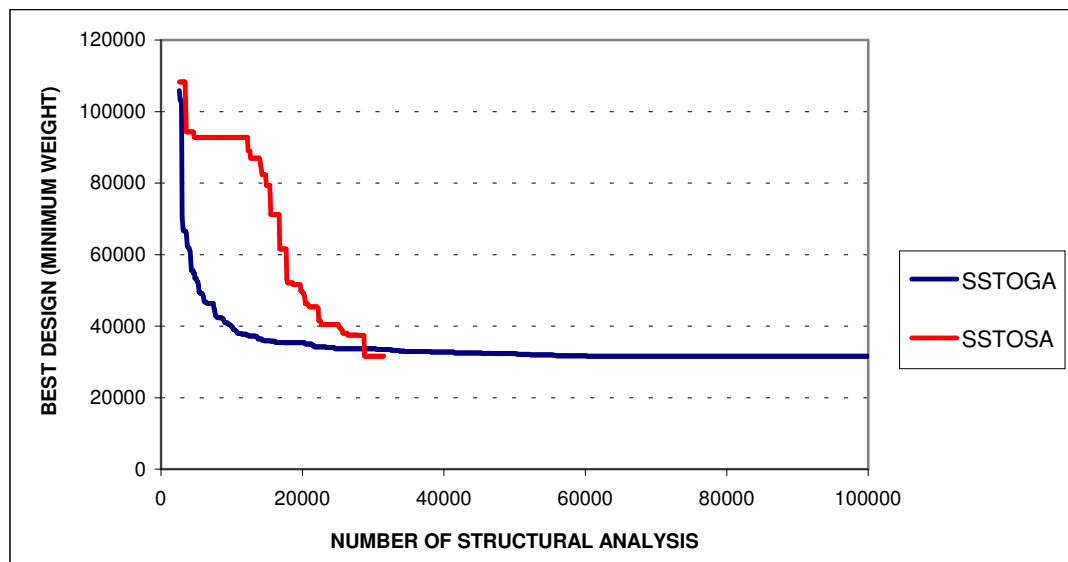


Fig.8.13. Graph of Number of Structural Analysis vs. Feasible Best Design of 354-Bar Dome (h=4.34 m) Using SSTOGA and SSTOSA.

8.2 354-Bar Dome (Height of 8.28 m.)

The same structure of first dome is assumed to design for a height of 8.28 m. The other design considerations (diameter, number of joints, number of members) are same as the first one. The total height of the building is 18.28 m. in this problem. The plan and side views of the building are shown in Figures 8.14 and 8.15. The side view of the steel dome, distinct from the first test problem, is presented in Fig.8.16.

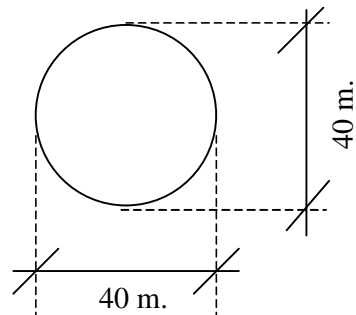


Fig.8.14. Top View (354-Bar)

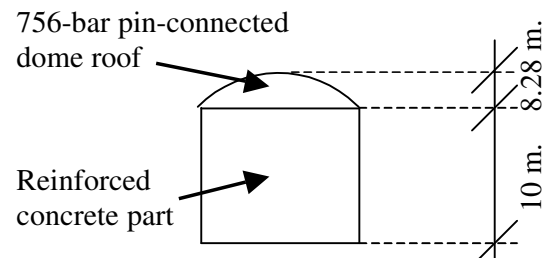


Fig.8.15. Side View (354-Bar)

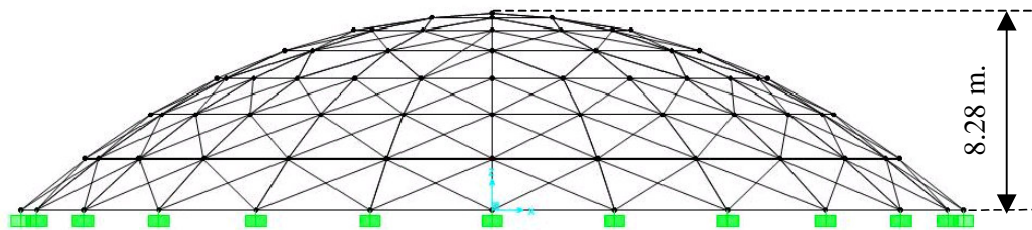


Fig.8.16. Side View of 354-Bar Dome

8.2.1. Wind Load (Analytical Procedure)

The design procedure explained in part 6.5.3. of ASCE 7-98 is followed.

Basic Wind Speed V for Nebraska is taken from Figure 6.1 of ASCE 7-98.

$$V = 40 \text{ m/s} \quad (90 \text{ mph})$$

Wind Directionality Factor K_d is taken from Table 6.6 of ASCE 7-98.

$$K_d = 0.85 \quad (\text{for arched roofs})$$

Importance Factor I for the building is determined as 1.15 from Table 6.1 of ASCE 7-98.

$$I = 1.15 \quad (\text{for building category III})$$

Exposure Category is assumed as C from the definitions given in part 6.5.6. of ASCE 7-98.

Velocity Pressure Exposure Coefficient K_z is taken from Table 6-5 of ASCE 7-98.

The mean height of the roof is 14.14 m. (46.4 feet).

$$K_z = 1.07 \quad (\text{for exposure C and 46 ft height})$$

Topographic Factor K_{zt} is calculated from $K_{zt} = (1 + K_1 K_2 K_3)^2$ where K_1 , K_2 , K_3 are taken from Fig.6.2 of ASCE 7-98.

It is assumed that there are a 2-D ridge with $H/L_h = 0.30$, 3-D escarpment with $x/L_h = 1.00$ and 2-D ridge with $z/L_h = 0.40$ in the general topology, where

H : Height of the hill or escarpment relative to the upwind terrain , in meter,

L_h : Distance upwind of crest to where the difference in the ground elevation is half the height of the hill or escarpment, in meter,

K_1 : Factor to account for shape of topographic feature and maximum speed-up effect,

K_2 : Factor to account for reduction in speed-up with distance upwind or downwind of crest,

K_3 : Factor to account for reduction in speed-up with height above local terrain,

x : Distance (upwind or downwind) from the crest to the building site, in meter,

z : Height above local ground level, in meter,

$$K_1 = 0.43, \quad K_2 = 0.33, \quad K_3 = 0.30 \quad (\text{from Fig.6.2 of ASCE 7-98})$$

$$K_{zt} = (1 + 0.43 \times 0.33 \times 0.30)^2 = 1.087$$

Gust Effect Factor G is found as 0.85 directly by assuming the structure as rigid.

$$G = 0.85$$

Enclosure Classification is assumed as enclosed, since the all lateral and upper parts of the building are closed and subjected to wind pressure directly.

Velocity Pressure is calculated by using the equation below;

$$q_z = 0.613 \cdot K_z \cdot K_{zt} \cdot K_d \cdot V^2 I \text{ (N/m}^2\text{)} \quad \mathbf{(8.10)} \quad (\text{Eq. 6-13 of ASCE 7-98})$$

$$q_z = 0.613 \times 1.07 \times 1.087 \times 0.85 \times (40)^2 \times 1.15$$

$$q_z = 1115 \text{ N/m}^2 = 111,5 \text{ kg/m}^2$$

Internal Pressure Coefficients GC_{pi} are found as +0.18 and -0.18 for enclosed buildings from Table 6.7 of ASCE 7-98. As stated before, ASCE 7-98 advises to use two values which are positive and negative.

External Pressure Coefficients C_p are found from Table 6.8 of ASCE 7-98. The dome is assumed to be separated into three parts, such as windward quarter, center half and leeward quarter. Three different external pressure coefficients for these three parts of the dome are with respect to rise-to-span ratio. The rise-to-ratio, r is $8.28/40=0.207$ for the building considered above.

$$C_p = 1.5 r - 0.3 = 1.5 * 0.207 - 0.3 = 0.0105 \quad (\text{for windward quarter})$$

$$C_p = -0.7 - r = -0.7 - 0.207 = -0.907 \quad (\text{for center half})$$

$$C_p = -0.5 \quad (\text{for leeward quarter})$$

Main Force Resisting Systems

$$p = qGC_p - q_i(GC_{pi}) \quad (\text{N/m}^2) \quad (8.11)$$

where

q = q_h for roofs, evaluated at height h ,

q_i = q_h for roofs of enclosed buildings,

G : Gust effect factor,

C_p : External pressure coefficient from Fig.6-3 or Table 6-8 of ASCE 7-98,

(GC_{pi}) : Internal pressure coefficient from Table 6-7 of ASCE 7-98.

For windward quarter

$$p = 1115 \times 0.85 \times (0.0105) - 1115 \times (\pm 0.18) = \begin{cases} 211 \text{ N/m}^2 \\ -191 \text{ N/m}^2 \end{cases}$$

For center half

$$p = 1115 \times 0.85 \times (-0.907) - 1115 \times (\pm 0.18) = \begin{cases} -1060 \text{ N/m}^2 \\ -659 \text{ N/m}^2 \end{cases}$$

For leeward quarter

$$p = 1115 \times 0.85 \times (-0.50) - 1115 \times (\pm 0.18) = \begin{cases} -674 \text{ N/m}^2 \\ -273 \text{ N/m}^2 \end{cases}$$

In this case, a positive pressure is detected acting on the windward quarter. Wind effects create negative pressure (suction) on the other parts of the dome. This is also compatible with the results presented in Fig.3.12 and 3.13.

8.2.2. Snow Loads

The same equation as in the first problem is used;

$$p_f = 0.7.C_e.C_t.I.p_g \quad (8.12) \text{ (Eq.7-1 of ASCE 7-98)}$$

where

p_f : The snow load on a roof with a slope equal to or less than 5° ,

- C_e : Exposure factor, determined from Table 7-2 of ASCE 7-98,
- C_t : Thermal factor, determined from Table 7-3 of ASCE 7-98,
- I : Importance factor, determined from Table 7-4 of ASCE 7-98,
- p_g : Ground snow load, determined from Fig.7-1 and Table 7-1 of ASCE 7-98.

$$C_e = 0.9 \quad (\text{for exposure category C and fully exposed roof})$$

$$C_t = 1.0 \quad (\text{for structures except as indicated in Table 7.3})$$

$$I = 1.10 \quad (\text{for building category III})$$

$$p_g = 25 \text{ lb/ft}^2 \quad (1.1975 \text{ kN/m}^2) \quad (\text{for Nebraska})$$

$$p_f = 0.7 \times 0.9 \times 1.0 \times 1.10 \times 1.1975 = 0.830 \text{ kN/m}^2$$

Tangent of vertical angle from eaves to crown = $8.28 / 20 = 0.217$ Angle = 24.4°

Since the vertical angle exceeds 10° , the minimum allowable values of p_f do not apply. Use $p_f = 0.830 \text{ kN/m}^2$

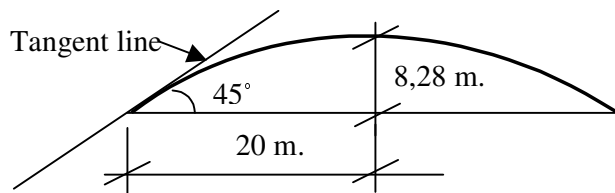
$$p_s = C_s p_f \quad (8.13) \quad (\text{Eq.7-2 of ASCE 7-98})$$

where

p_s : The sloped-roof snow load,

C_s : Roof slope factor,

p_f : The snow load on a roof with a slope equal to or less than 5° .



By geometry, the slope at the eaves is 45° .

Fig.8.17. Side View of The Dome (354-Bar)

From Fig.7.2a of ASCE 7-98, $C_s = 1.0$ until slope exceeds 30° which is (by geometry) 14.15 m. from the centerline. In this area $p_s = 1 * 0.830 = 0.830 \text{ kN/m}^2$ is found. At the eaves, where the slope is 45° , for $C_s = 0.65$, $p_s = 0.65 * 0.830 = 0.540 \text{ kN/m}^2$ is obtained.

$$C_s = 1.0 \quad (\text{from Fig.7-2 and Fig.7-3 of ASCE 7-98 for a roof slope of } 12^\circ)$$

Unbalanced Snow Load (from Fig.7-3 of ASCE 7-98)

Since the vertical angle from the eaves to the crown is greater than 10° and less than 60° , the unbalanced snow loads must be considered. The same procedure explained in the first problem is repeated.

Unbalanced load at crown;

$$= 0.5 * p_f = 0.5 * 0.830 = 0.415 \text{ kN/m}^2$$

Unbalanced load at 30-degree point

$$= 2 * p_f C_s / C_e = 2 * 0.830 * 1.0 / 0.9 = 1.844 \text{ kN/m}^2$$

Unbalanced load at eaves;

$$= 2 * p_f = 2 * 0.830 = 1.660 \text{ kN/m}^2$$

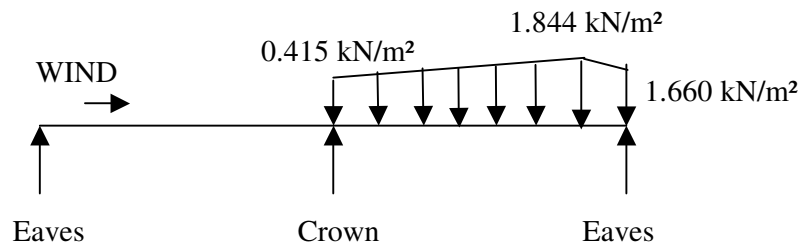


Fig.8.18. Unbalanced Snow Load (354-Bar)

8.2.3. Dead Load

Sandwich type aluminium cladding is used. The dead load of this cladding (including frame elements to be used for girts) is taken as 200 N/m².

8.2.4. Roof Live Load

Roof live load can be taken as 900 N/m² to take into account the weight of the men climbing on the roof for various purposes such as cleaning. But this load is compensated by snow load since roof live load and snow load cannot be acted at the same time.

8.2.5. Combined Loaded Case

The six load cases are considered as shown below;

1. D + S (balanced)
2. D + S (unbalanced)
3. D + W (taken internal pressure coefficient as positive) + S (balanced)
4. D + W (taken internal pressure coefficient as negative) + S (balanced)
5. D + W (taken internal pressure coefficient as positive) + S (unbalanced)
6. D + W (taken internal pressure coefficient as negative) + S (unbalanced)

These load cases are shown schematically in Fig.8.19 through Fig.8.24.

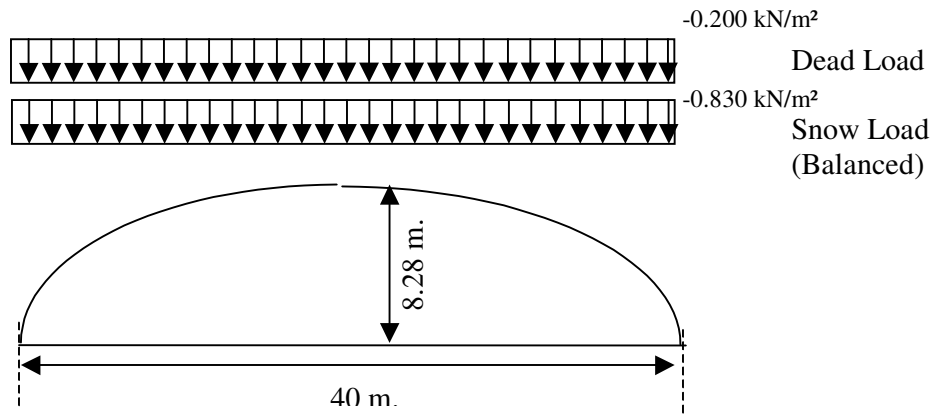


Fig.8.19. Load Case 1 of 354-Bar Dome (h=8.28 m.)

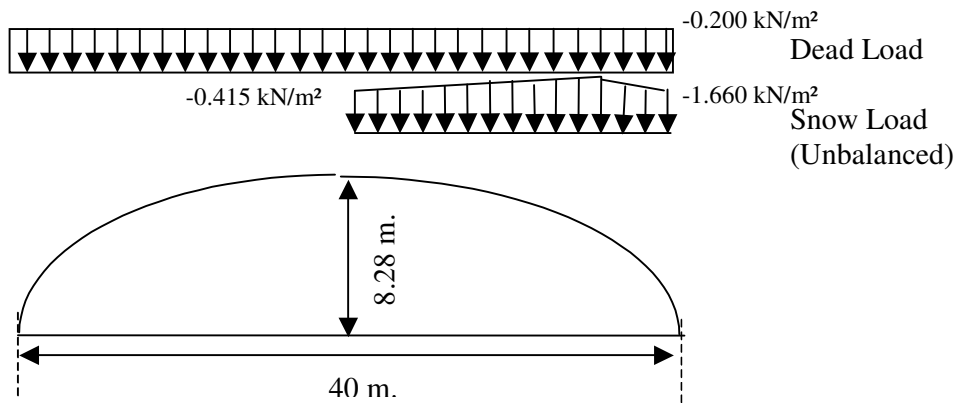


Fig.8.20. Load Case 2 of 354-Bar Dome (h=8.28 m.)

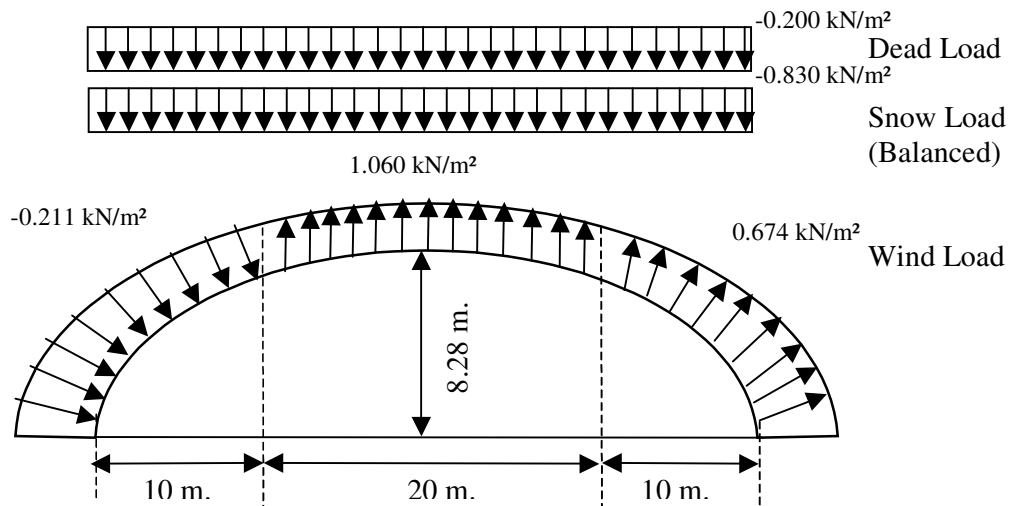


Fig.8.21. Load Case 3 of 354-Bar Dome (h=8.28 m.)

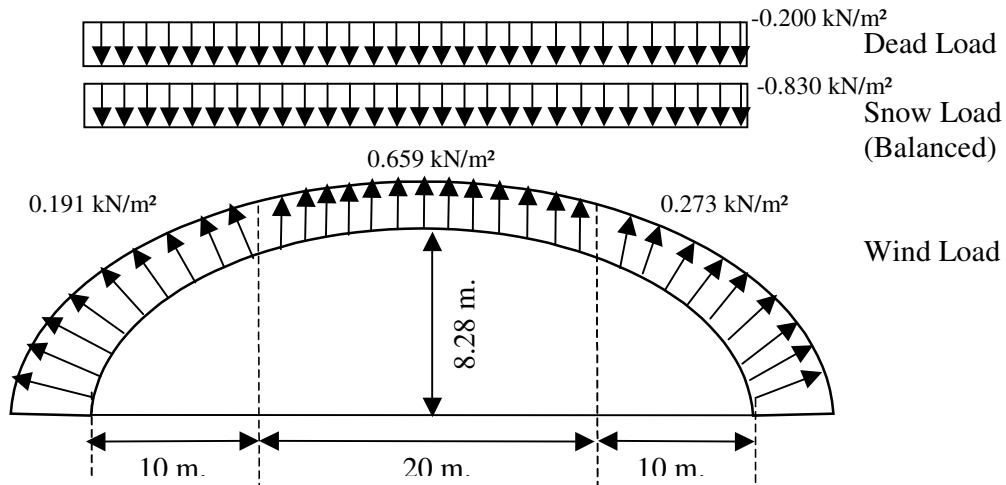


Fig.8.22. Load Case 4 of 354-Bar Dome (h=8.28 m.)

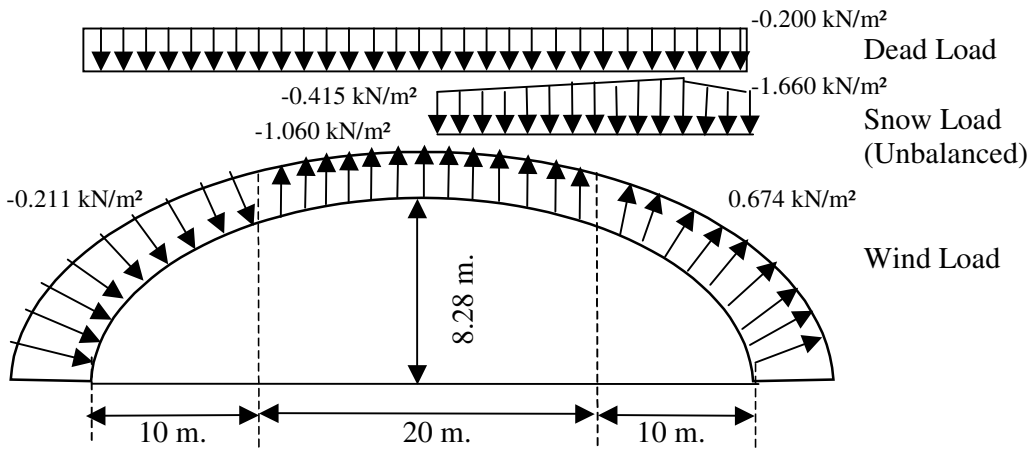


Fig.8.23. Load Case 5 of 354-Bar Dome (h=8.28 m.)

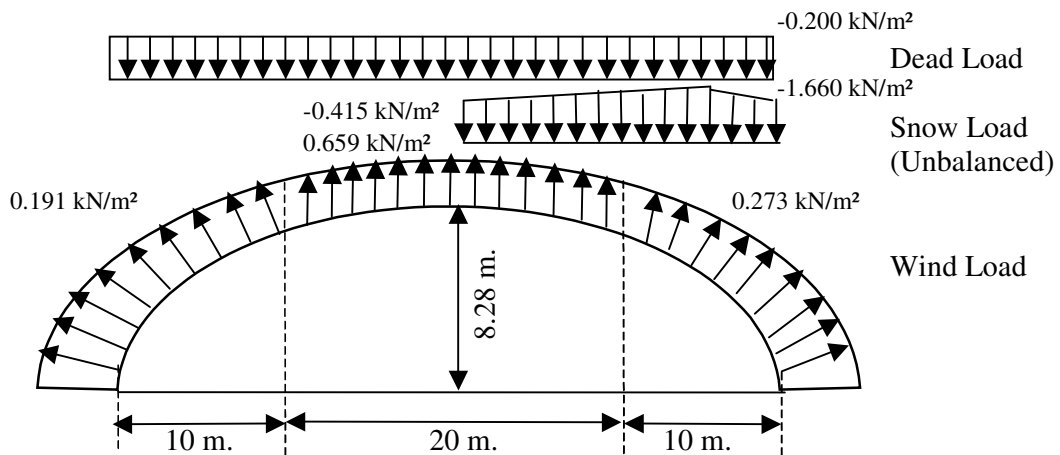


Fig.8.24. Load Case 1 of 354-Bar Dome (h=8.28 m.)

Since the rise-to-span ratio is not low as compared to the one in example 1, the wind loads acting on the windward quarter is positive (compression) and the loads which act the other parts of the dome is negative (suction).

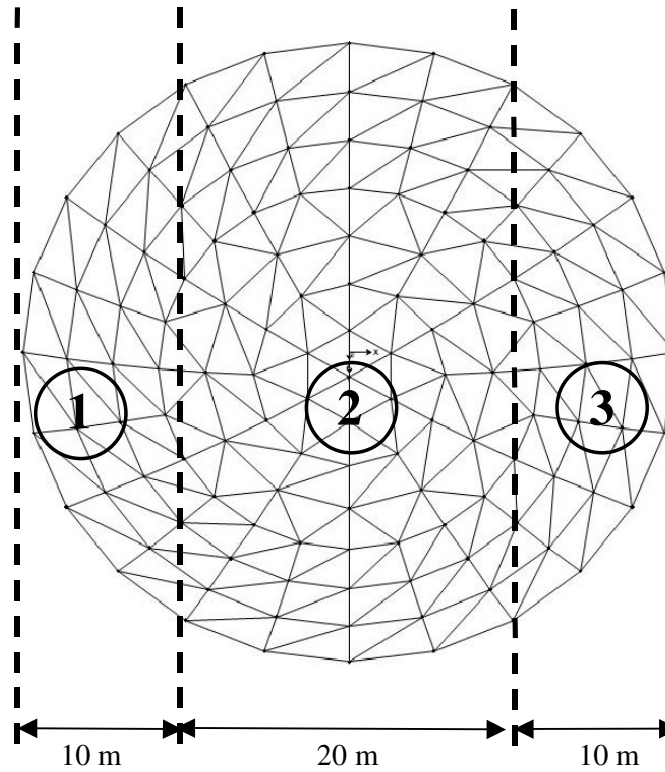


Fig.8.25. Pieces of 354- Bar Dome (h=8.28 m)

Whole Structure	{ Number of Total Joints :127 Number of Total Members :354 Total Area :1467.4 m ² Projected Area :1257 m ²		
	Piece 1	Piece 2	Piece 3
	Number of Joints:27	Number of Joints :73	Number of Joints:27
	Total Area :303 m ²	Total Area :861.4 m ²	Total Area :303 m ²
Projected Area:245.85 m ²	Projected Area :765.41 m ²	Projected Area :245.85 m ²	

8.2.6 Load Combinations

Load Case 1 (Dead Load + Balanced Snow)

-0.200 kN/m² (Dead Load)

-0.830 kN/m² (Snow Load)

-1.030 kN/m² (↓) (Dead + Snow Load)

Load Case 2 (Dead Load + Unbalanced Snow)

For Left Half

-0.200 kN/m² (↓) (Dead Load)

For Right Half

-0.200 kN/m² (Dead Load)

-1.130 kN/m² (Average Unbalanced Snow Load)

-1.330 kN/m² (↓) (Dead + Snow Load)

Load Case 3 (Dead Load + Balanced Snow + Wind Load with Positive Internal Pressure Coefficient)

For Windward Quarter

-0.200 kN/m² (Dead Load)

-0.830 kN/m² (Snow Load)

-1.030 kN/m² (↓) (Dead + Snow Load)

-0.179 kN/m² (↑) (Wind Load) (-0.211 x Cos 32.02°)

0.112 kN/m² (→) (Lateral Load Due to Wind) (0.211 x Sin 32.02°)

For Center Half

-0.200 kN/m² (Dead Load)

-0.830 kN/m² (Snow Load)

-1.030 kN/m² (↓) (Dead + Snow Load)

1.060 kN/m² (↑) (Wind Load)

For Leeward Quarter

-0.200 kN/m² (Dead Load)

-0.830 kN/m² (Snow Load)

-1.030 kN/m² (↓) (Dead + Snow Load)

0.572 kN/m² (↑) (Wind Load) (0.674 x Cos 32.02°)

0.357 kN/m^2 (\rightarrow) (Lateral Load Due to Wind) ($0.674 \times \sin 32.02^\circ$)

Load Case 4 (Dead Load + Balanced Snow + Wind Load with Negative Internal Pressure Coefficient)

For Windward Quarter

-0.200 kN/m^2 (Dead Load)

-0.830 kN/m^2 (Snow Load)

-1.030 kN/m^2 (\downarrow) (Dead + Snow Load)

0.162 kN/m^2 (\uparrow) (Wind Load) ($0.191 \times \cos 32.02^\circ$)

-0.101 kN/m^2 (\leftarrow) (Lateral Load Due to Wind) ($0.191 \times \sin 32.02^\circ$)

For Center Half

-0.200 kN/m^2 (Dead Load)

-0.830 kN/m^2 (Snow Load)

-1.030 kN/m^2 (\downarrow) (Dead + Snow Load)

0.659 kN/m^2 (\uparrow) (Wind Load)

For Leeward Quarter

-0.200 kN/m^2 (Dead Load)

-0.830 kN/m^2 (Snow Load)

-1.030 kN/m^2 (\downarrow) (Dead + Snow Load)

0.231 kN/m^2 (\uparrow) (Wind Load) ($0.273 \times \cos 32.02^\circ$)

0.145 kN/m^2 (\rightarrow) (Lateral Load Due to Wind) ($0.273 \times \sin 32.02^\circ$)

Load Case 5 (Dead Load + Unbalanced Snow + Wind Load with Positive Internal Pressure Coefficient)

For Windward Quarter

-0.200 kN/m^2 (Dead Load)

0 kN/m^2 (Snow Load)

-0.200 kN/m^2 (\downarrow) (Dead + Snow Load)

-0.179 kN/m^2 (\downarrow) (Wind Load) ($-0.211 \times \cos 32.02^\circ$)

0.112 kN/m^2 (\rightarrow) (Lateral Load Due to Wind) ($0.211 \times \sin 32.02^\circ$)

For Center Half (Left Part)

-0.200 kN/m^2 (Dead Load)

0 kN/m^2 (Snow Load)

-0.200 kN/m² (↓) (Dead + Snow Load)

1.060 kN/m² (↑) (Wind Load)

For Center Half (Right Part)

-0.200 kN/m² (Dead Load)

-0.726 kN/m² (Average Unbalanced Snow Load)

-0.926 kN/m² (↓) (Dead + Snow Load)

1.060 kN/m² (↑) (Wind Load)

For Leeward Quarter

-0.200 kN/m² (Dead Load)

-1.348 kN/m² (Average Unbalanced Snow Load)

-1.548 kN/m² (↓) (Dead + Snow Load)

0.571 kN/m² (↑) (Wind Load) (0.674 x Cos 32.02°)

0.357 kN/m² (→) (Lateral Load Due to Wind) (0.674 x Sin 32.02°)

Load Case 6 (Dead Load + Unbalanced Snow + Wind Load with Negative Internal Pressure Coefficient))

For Windward Quarter

-0.200 kN/m² (Dead Load)

0 kN/m² (Snow Load)

-0.200 kN/m² (↓) (Dead + Snow Load)

0.162 kN/m² (↑) (Wind Load) (0.191 x Cos 32.02°)

-0.101 kN/m² (←) (Lateral Load Due to Wind) (0.191 x Sin 32.02°)

For Center Half (Left Part)

-0.200 kN/m² (Dead Load)

0 kN/m² (Snow Load)

-0.200 kN/m² (↓) (Dead + Snow Load)

0.659 kN/m² (↑) (Wind Load)

For Center Half (Right Part)

-0.200 kN/m² (Dead Load)

-0.726 kN/m² (Average Unbalanced Snow Load)

-0.926 kN/m² (↓) (Dead + Snow Load)

0.659 kN/m² (↑) (Wind Load)

For Leeward Quarter

-0.200 kN/m² (Dead Load)

-1.348 kN/m² (Average Unbalanced Snow Load)

-1.548 kN/m² (↓) (Dead + Snow Load)

0.231 kN/m² (↑) (Wind Load) (0.273 x Cos 32.02°)

0.083 kN/m² (→) (Lateral Load Due to Wind) (0.266 x Sin 18.10°)

8.2.7 Loads Acting On Joints

Load Case 1 (D + S_{Balanced})

$(-1.030 \text{ kN/m}^2 * 1257 \text{ m}^2)/(127 \text{ joints}) = -10.195 \text{ kN/joint} = \underline{\underline{-2.291 \text{ kip/joint}}}$ (↓)

Load Case 2 (D + S_{Unbalanced})

For Left Half

$(-0.200 \text{ kN/m}^2 * 1257 \text{ m}^2/2)/(127 \text{ joints}/2) = -1.980 \text{ kN/joint} = \underline{\underline{-0.445 \text{ kip/joint}}}$ (↓)

For Right Half

$(-1.330 \text{ kN/m}^2 * 1257 \text{ m}^2/2)/(127 \text{ joints}/2) = -13.164 \text{ kN/joint} = \underline{\underline{-2.959 \text{ kip/joint}}}$ (↓)

Load Case 3 (D + S_{Balanced} + W_{Positive Internal Pressure Coefficient})

For Windward Quarter

$(-1.030 \text{ kN/m}^2 * 245.85 \text{ m}^2 + (-0.179 \text{ kN/m}^2) * 303 \text{ m}^2)/(27 \text{ joints}) = -11.388 \text{ kN/joint}$
 $= \underline{\underline{-2.560 \text{ kip/joint}}}$ (↓)

Lateral Load

$(0.112 \text{ kN/m}^2 * 303 \text{ m}^2)/(27 \text{ joints}) = 1.257 \text{ kN/joint} = \underline{\underline{0.283 \text{ kip/joint}}}$ (→)

For Center Half

$(-1.030 \text{ kN/m}^2 * 765.41 \text{ m}^2 + 1.060 \text{ kN/m}^2 * 861.4 \text{ m}^2)/(73 \text{ joints}) = 1.708 \text{ kN/joint} =$
 $\underline{\underline{0.384 \text{ kip/joint}}}$ (↑)

For Leeward Quarter

$(-1.030 \text{ kN/m}^2 * 245.85 \text{ m}^2 + 0.572 \text{ kN/m}^2 * 303 \text{ m}^2)/(27 \text{ joints}) = -2.960 \text{ kN/joint} =$
 $\underline{\underline{-0.665 \text{ kip/joint}}}$ (↓)

Lateral Load

$(0.357 \text{ kN/m}^2 * 303 \text{ m}^2)/(27 \text{ joints}) = 4.006 \text{ kN/joint} = \underline{\underline{0.901 \text{ kip/joint}}}$ (→)

Load Case 4 (D + S_{Balanced} + W_{Negative Internal Pressure Coefficient})

For Windward Quarter

$$(-1.030 \text{ kN/m}^2 * 245.85 \text{ m}^2 + 0.162 \text{ kN/m}^2 * 303 \text{ m}^2) / (27 \text{ joints}) = -7.561 \text{ kN/joint} = \underline{\underline{-1.700 \text{ kip/joint}}} (\downarrow)$$

Lateral Load

$$(-0.101 \text{ kN/m}^2 * 303 \text{ m}^2) / (27 \text{ joints}) = -1.133 \text{ kN/joint} = \underline{\underline{-0.255 \text{ kip/joint}}} (\leftarrow)$$

For Center Half

$$(-1.030 \text{ kN/m}^2 * 765.41 \text{ m}^2 + 0.659 \text{ kN/m}^2 * 861.4 \text{ m}^2) / (73 \text{ joints}) = -3.023 \text{ kN/joint} = \underline{\underline{-0.679 \text{ kip/joint}}} (\downarrow)$$

For Leeward Quarter

$$(-1.030 \text{ kN/m}^2 * 245.85 \text{ m}^2 + 0.231 \text{ kN/m}^2 * 303 \text{ m}^2) / (27 \text{ joints}) = -6.786 \text{ kN/joint} = \underline{\underline{-1.526 \text{ kip/joint}}} (\downarrow)$$

Lateral Load

$$(0.145 \text{ kN/m}^2 * 303 \text{ m}^2) / (27 \text{ joints}) = 1.627 \text{ kN/joint} = \underline{\underline{0.366 \text{ kip/joint}}} (\rightarrow)$$

Load Case 5 (D + S_{Unbalanced} + W_{Positive Internal Pressure Coefficient})

For Windward Quarter

$$(-0.200 \text{ kN/m}^2 * 245.85 \text{ m}^2 + (-0.179 \text{ kN/m}^2) * 303 \text{ m}^2) / (27 \text{ joints}) = -3.830 \text{ kN/joint} = \underline{\underline{-0.861 \text{ kip/joint}}} (\uparrow)$$

Lateral Load

$$(-0.112 \text{ kN/m}^2 * 303 \text{ m}^2) / (27 \text{ joints}) = -1.257 \text{ kN/joint} = \underline{\underline{-0.283 \text{ kip/joint}}} (\leftarrow)$$

For Center Half (Left Part)

$$(-0.200 \text{ kN/m}^2 * (765.41 \text{ m}^2 / 2) + 1.060 \text{ kN/m}^2 * (861.40 \text{ m}^2 / 2)) / (73 / 2 \text{ joints}) = 10.411 \text{ kN/joint} = \underline{\underline{2.341 \text{ kip/joint}}} (\uparrow)$$

For Center Half (Right Part)

$$(-0.926 \text{ kN/m}^2 * (765.41 \text{ m}^2 / 2) + 1.060 \text{ kN/m}^2 * (861.4 \text{ m}^2 / 2)) / (73 / 2 \text{ joints}) = 2.799 \text{ kN/joint} = \underline{\underline{0.629 \text{ kip/joint}}} (\uparrow)$$

For Leeward Quarter

$$(-1.548 \text{ kN/m}^2 * 245.85 \text{ m}^2 + 0.571 \text{ kN/m}^2 * 303 \text{ m}^2) / (27 \text{ joints}) = -7.688 \text{ kN/joint} = \underline{\underline{-1.728 \text{ kip/joint}}} (\downarrow)$$

Lateral Load

$$(0.357 \text{ kN/m}^2 * 303 \text{ m}^2) / (27 \text{ joints}) = 4.006 \text{ kN/joint} = \underline{\underline{0.901 \text{ kip/joint}}} (\rightarrow)$$

Load Case 6 (D + S_{Unbalanced} + W_{Negative Internal Pressure Coefficient})

For Windward Quarter

$$(-0.200 \text{ kN/m}^2 * 245.85 \text{ m}^2 + 0.162 \text{ kN/m}^2 * 303 \text{ m}^2) / (27 \text{ joints}) = -0.003 \text{ kN/joint} = \underline{\underline{-0.0007 \text{ kip/joint}}} (\downarrow)$$

Lateral Load

$$(-0.101 \text{ kN/m}^2 * 303 \text{ m}^2) / (27 \text{ joints}) = -1.133 \text{ kN/joint} = \underline{\underline{-0.255 \text{ kip/joint}}} (\leftarrow)$$

For Center Half (Left Part)

$$(-0.200 \text{ kN/m}^2 * (765.41 \text{ m}^2/2) + 0.659 \text{ kN/m}^2 * (861.4 \text{ m}^2/2)) / (73/2 \text{ joints}) = 5.679 \text{ kN/joint} = \underline{\underline{1.277 \text{ kip/joint}}} (\uparrow)$$

For Center Half (Right Part)

$$(-0.926 \text{ kN/m}^2 * (765.41 \text{ m}^2/2) + 0.659 \text{ kN/m}^2 * (861.4 \text{ m}^2/2)) / (73/2 \text{ joints}) = -1.933 \text{ kN/joint} = \underline{\underline{-0.435 \text{ kip/joint}}} (\downarrow)$$

For Leeward Quarter

$$(-1.548 \text{ kN/m}^2 * 245.85 \text{ m}^2 + 0.231 \text{ kN/m}^2 * 303 \text{ m}^2) / (27 \text{ joints}) = -11.503 \text{ kN/joint} = \underline{\underline{-2.586 \text{ kip/joint}}} (\downarrow)$$

Lateral Load

$$(0.145 \text{ kN/m}^2 * 303 \text{ m}^2) / (27 \text{ joints}) = 1.627 \text{ kN/joint} = \underline{\underline{0.366 \text{ kip/joint}}} (\rightarrow)$$

8.2.8 Results

American circular hollow pipes are used in the design. As stated before, two different softwares (SSTOGA and SSTOSA) which utilize two techniques (Genetic Algorithms and Simulated Annealing) are made use of in the analysis. Each program is run three times as in problem 1. The design result which is tabulated in Table 8.2 was found by running both programs three times. Four different ready sections (P2+1/2, P3, P3+1/2, EP3) are used in this design.

Table 8.2. Result of 354-Bar Dome

Member Type	Number of Members (From Fig.8.3)	Ready Section	Cross Sectional Area (in²)
A ₁	1:24	P3	2.23
A ₂	25,27,29,.....,67,69,71	EP3	3.02
A ₃	26,28,30,.....,68,70,72	P3+1/2	2.68
A ₄	73:96	P3	2.23
A ₅	97,99,101,.....,139,141,143	P3	2.23
A ₆	98,100,102,.....,140,142,144	P3	2.23
A ₇	145:168	P3	2.23
A ₈	169,171,173,.....,211,213,215	P3	2.23
A ₉	170,172,174,.....,212,214,216	P3	2.23
A ₁₀	217:240	P3	2.23
A ₁₁	241,244,247,250,253,256,259,262,265,268,271,274	P3	2.23
A ₁₂	242 ,245,248,251,254,257,260,263,266,269,272,275	P3	2.23
A ₁₃	243 ,246,249,252,255,258,261,264,267,270,273,276	P3	2.23
A ₁₄	277:288	P2+1/2	1.70
A ₁₅	289,291,293,.....,307,309,311	P3	2.23
A ₁₆	290,292,294,.....,308,310,312	P3	2.23
A ₁₇	313:324	P2+1/2	1.70
A ₁₈	325,328,331,334,337,340	P3	2.23
A ₁₉	326,329,332,335,338,341	P2+1/2	1.70
A ₂₀	327,330,333,336,339,342	P2+1/2	1.70
A ₂₁	343:348	P2+1/2	1.70
A ₂₂	349:354	P2+1/2	1.70
	Total Volume		127957 in²
	Total Weight		36247 lb

As seen from the Table 8.2, the optimum design is 36247 lb. The graphs of evolution to optimum design for both techniques (SSTOGA using Genetic Algorithm and SSTOSA using Simulated Annealing) are presented in Fig.8.26.

In SSTOGA, 1000 generations each having 100 structural analyses are performed. This software uses totally 100,000 structural analyses to converge the optimum solution as seen from the graph (blue line).

In SSTOSA, 30,259 structural analyses in 300 cooling cycles are performed in order to find the optimum design, as seen from the graph (red line). This is fewer as compared to the number of the SSTOGA software. So this effects the CPU time. While SSTOSA performs 30,259 structural analyses to converge the optimum solution in about 4 hours (with a computer of AMD 1700 and 128 Mb RAM), SSTOGA converges the same optimum design by performing 100,000 structural analyses in about 21 hours. This shows that CPU times are very distinctive where SSTOSA converges very earlier than SSTOGA.

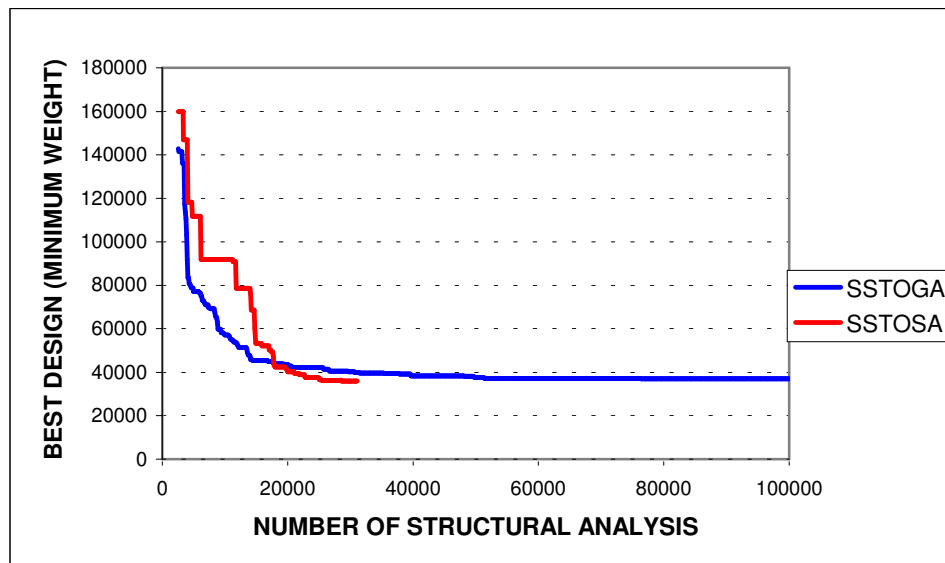


Fig.8.26. Graph of Number of Structural Analysis vs. Feasible Best Design of 354-Bar Dome (h=8.28 m) Using SSTOGA and SSTOSA.

8.3 756-Bar Dome

The roof of the same auditorium building with a capacity of 500 people which is located in Nebraska, is assumed to be made up of 756-bar dome. It is circular in plan view, too. It has the same diameter of 40 m. Again, the building consists of two parts, the main part which is reinforced concrete, and the roof part which is pin-connected steel dome with 756 members and 271 joints. The total height of the building is 18.28 m. in this problem and the height of the steel dome is 8.28 m. as in the second problem. The plan and side views of the building are shown in Figures 8.27 and 8.28. The top view, side view and 3-dimensional view of the steel dome are presented in Fig.8.29 through 8.31.

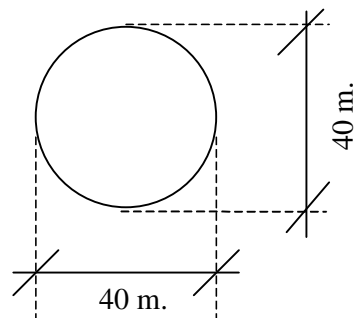


Fig.8.27. Top View (756-Bar)

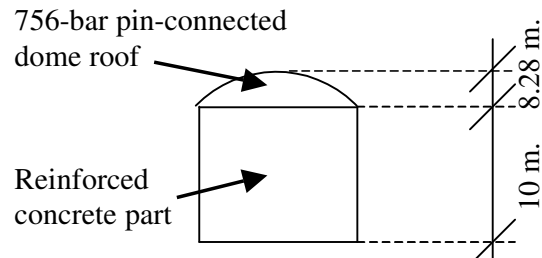


Fig.8.28. Side View (756-Bar)

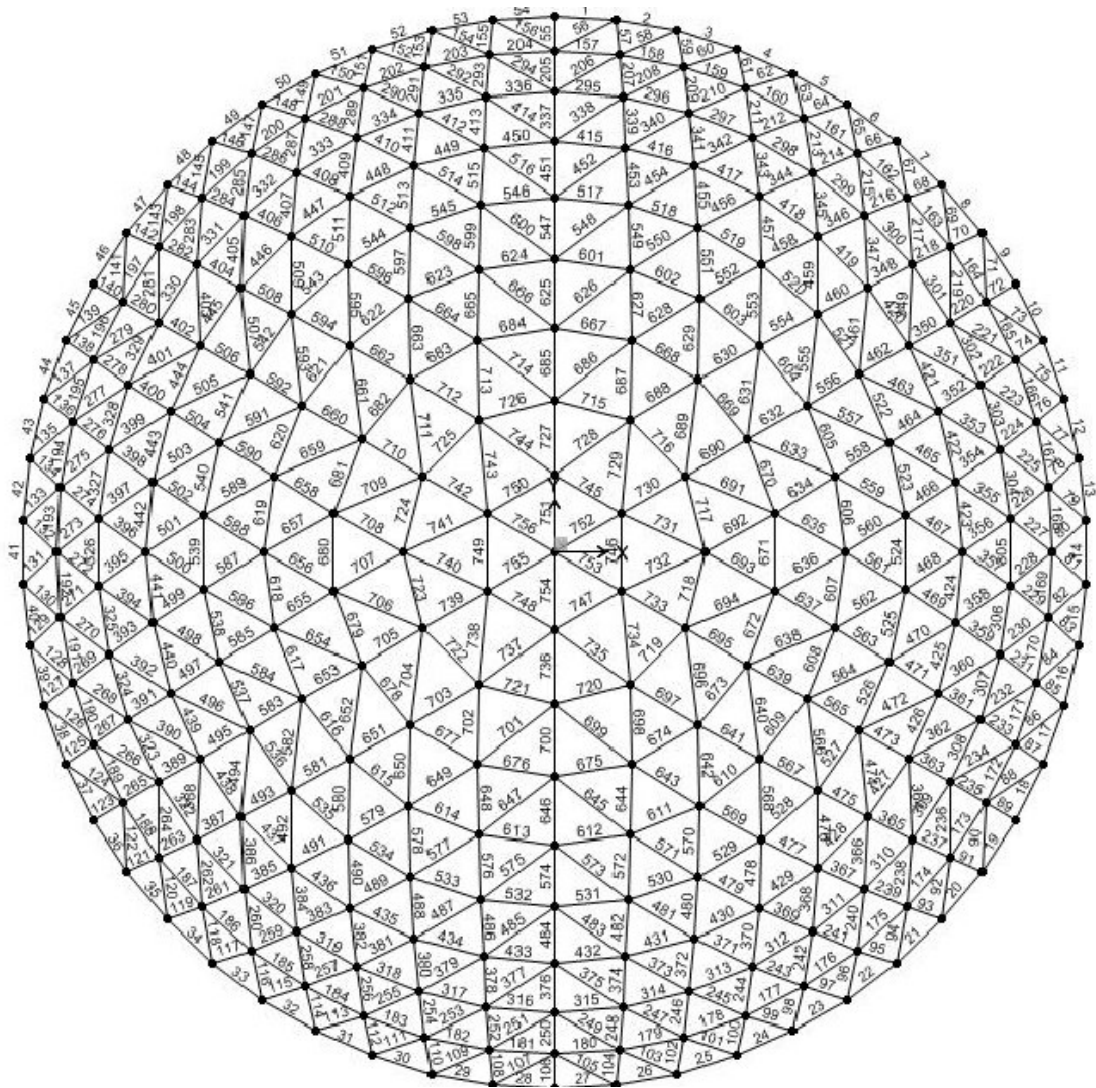


Fig.8.29. Top View of 756-Bar Dome

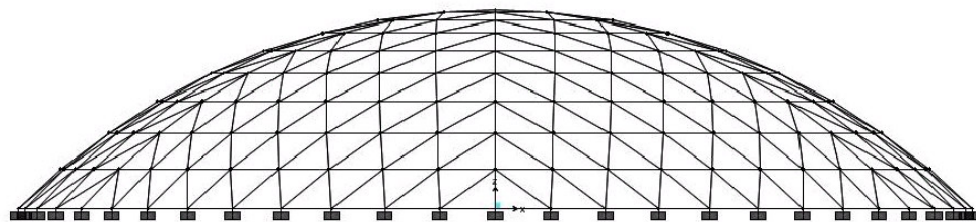


Fig.8.30. Side View of 756-Bar Dome

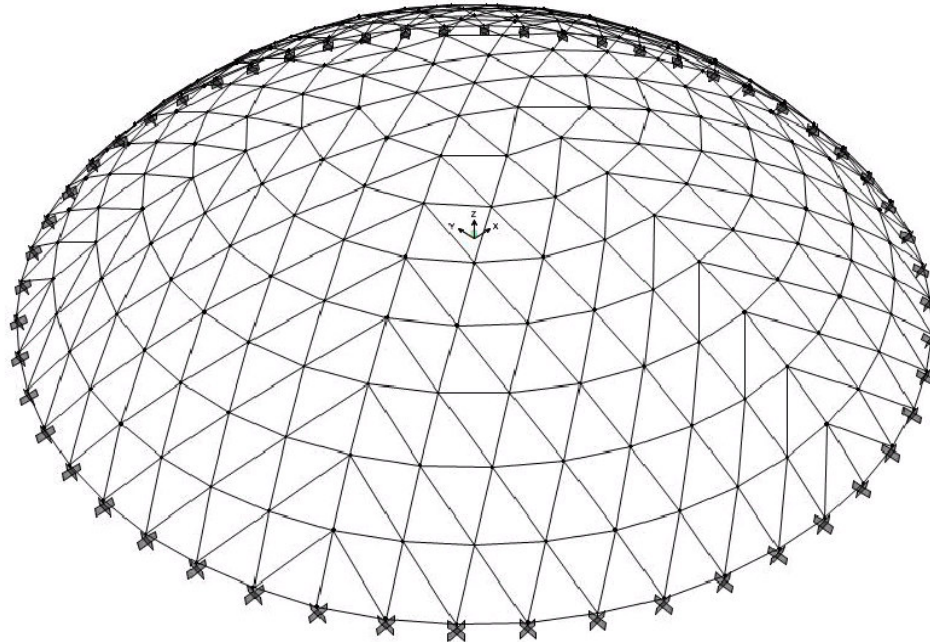


Fig.8.31. 3-D View of 756-Bar Dome

8.3.1. Wind Load (Analytical Procedure)

Since the dimensions of the dome is the same as the second problem, the design procedure explained in 8.2.1 is achieved again.

For windward quarter

$$p = 1115 \times 0.85 \times (0.0105) - 1115 \times (\pm 0.18) = \begin{cases} 211 \text{ N/m}^2 \\ -191 \text{ N/m}^2 \end{cases}$$

For center half

$$p = 1115 \times 0.85 \times (-0.907) - 1115 \times (\pm 0.18) = \begin{cases} -1060 \text{ N/m}^2 \\ -659 \text{ N/m}^2 \end{cases}$$

For leeward quarter

$$p = 1115 \times 0.85 \times (-0.50) - 1115 \times (\pm 0.18) = \begin{cases} -674 \text{ N/m}^2 \\ -273 \text{ N/m}^2 \end{cases}$$

8.3.2. Snow Loads

Since the same design procedure outlined in 8.2.2 is done, the same design snow loads for the balanced and unbalanced cases are found as stated in 8.2.2.

Unbalanced load at crown;

$$= 0.5 * p_f = 0.5 * 0.830 = 0.415 \text{ kN/m}^2$$

Unbalanced load at 30-degree point

$$= 2 * p_f C_s/C_e = 2 * 0.830 * 1.0 / 0.9 = 1.844 \text{ kN/m}^2$$

Unbalanced load at eaves;

$$= 2 * p_f = 2 * 0.830 = 1.660 \text{ kN/m}^2$$

8.3.3. Dead Load

Sandwich type aluminium cladding is used. The dead load of this cladding (including frame elements to be used for girts) is taken as 200 N/m².

8.3.4. Roof Live Load

Roof live load can be taken as 900 N/m² to take into account the weight of the men climbing on the roof for various purposes. But this load is compensated by snow load since roof live load and snow load cannot be acted at the same time.

8.3.5. Combined Loaded Case

The six load cases are considered as shown below;

1. D + S (balanced)
2. D + S (unbalanced)
3. D + W (taken internal pressure coefficient as positive) + S (balanced)
4. D + W (taken internal pressure coefficient as negative) + S (balanced)
5. D + W (taken internal pressure coefficient as positive) + S (unbalanced)
6. D + W (taken internal pressure coefficient as negative) + S (unbalanced)

These load cases are shown schematically in Fig.8.19 through Fig.8.24.

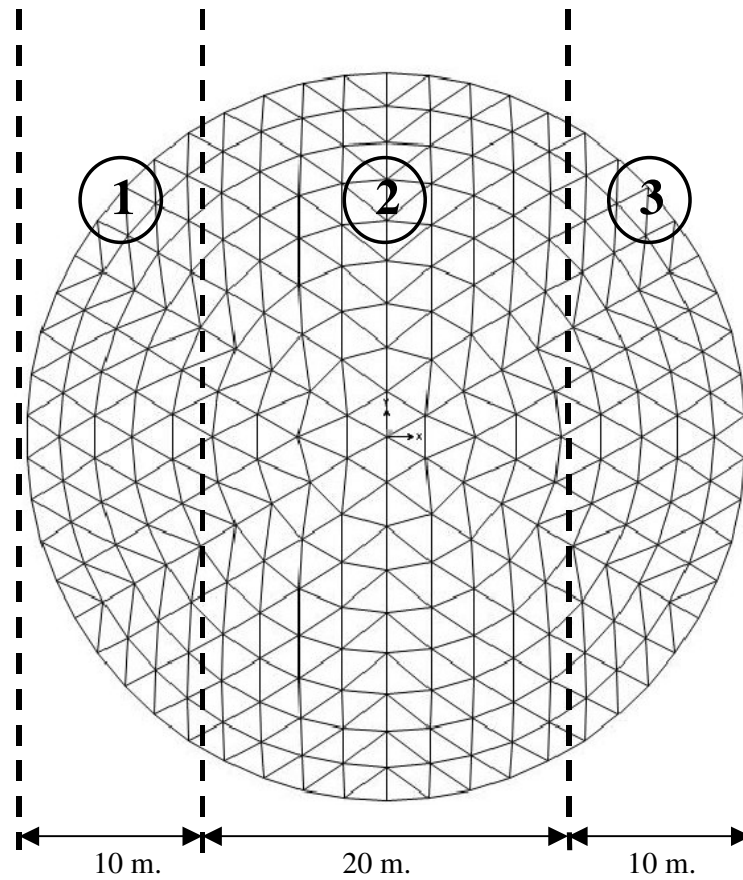


Fig.8.32. Pieces of 756-Bar Dome

Whole Structure	Number of Total Joints	:271			
	Number of Total Members	:756			
	Total Area	:1467.4 m ²			
	Projected Area	:1257 m ²			
Piece 1	Piece 2	Piece 3			
Number of Joints	:60	Number of Joints	:151	Number of Joints	:60
Total Area	:303 m ²	Total Area	:861.4 m ²	Total Area	:303 m ²
Projected Area	:245.85 m ²	Projected Area	:765.41 m ²	Projected Area	:245.85 m ²

8.3.6 Load Combinations

Load Case 1 (Dead Load + Balanced Snow)

-0.200 kN/m² (Dead Load)

-0.830 kN/m² (Snow Load)

-1.030 kN/m² (↓) (Dead + Snow Load)

Load Case 2 (Dead Load + Unbalanced Snow)

For Left Half

-0.200 kN/m² (↓) (Dead Load)

For Right Half

-0.200 kN/m² (Dead Load)

-1.130 kN/m² (Average Unbalanced Snow Load)

-1.330 kN/m² (↓) (Dead + Snow Load)

Load Case 3 (Dead Load + Balanced Snow + Wind Load with Positive Internal Pressure Coefficient)

For Windward Quarter

-0.200 kN/m² (Dead Load)

-0.830 kN/m² (Snow Load)

-1.030 kN/m² (↓) (Dead + Snow Load)

-0.179 kN/m² (↑) (Wind Load) (-0.211 x Cos 32.02°)

0.112 kN/m² (→) (Lateral Load Due to Wind) (0.211 x Sin 32.02°)

For Center Half

-0.200 kN/m² (Dead Load)

-0.830 kN/m² (Snow Load)

-1.030 kN/m² (↓) (Dead + Snow Load)

1.060 kN/m² (↑) (Wind Load)

For Leeward Quarter

-0.200 kN/m² (Dead Load)

-0.830 kN/m² (Snow Load)

-1.030 kN/m² (↓) (Dead + Snow Load)

0.572 kN/m² (↑) (Wind Load) (0.674 x Cos 32.02°)

0.357 kN/m² (→) (Lateral Load Due to Wind) (0.674 x Sin 32.02°)

Load Case 4 (Dead Load + Balanced Snow + Wind Load with Negative Internal Pressure Coefficient)

For Windward Quarter

-0.200 kN/m² (Dead Load)

-0.830 kN/m² (Snow Load)

-1.030 kN/m² (↓) (Dead + Snow Load)

0.162 kN/m² (↑) (Wind Load) (0.191 x Cos 32.02°)

-0.101 kN/m² (←) (Lateral Load Due to Wind) (0.191 x Sin 32.02°)

For Center Half

-0.200 kN/m² (Dead Load)

-0.830 kN/m² (Snow Load)

-1.030 kN/m² (↓) (Dead + Snow Load)

0.659 kN/m² (↑) (Wind Load)

For Leeward Quarter

-0.200 kN/m² (Dead Load)

-0.830 kN/m² (Snow Load)

-1.030 kN/m² (↓) (Dead + Snow Load)

0.231 kN/m² (↑) (Wind Load) (0.273 x Cos 32.02°)

0.145 kN/m² (→) (Lateral Load Due to Wind) (0.273 x Sin 32.02°)

Load Case 5 (Dead Load + Unbalanced Snow + Wind Load with Positive Internal Pressure Coefficient)

For Windward Quarter

-0.200 kN/m² (Dead Load)

0 kN/m² (Snow Load)

-0.200 kN/m² (↓) (Dead + Snow Load)

-0.179 kN/m² (↓) (Wind Load) (-0.211 x Cos 32.02°)

0.112 kN/m² (→) (Lateral Load Due to Wind) (0.211 x Sin 32.02°)

For Center Half (Left Part)

-0.200 kN/m² (Dead Load)

0 kN/m² (Snow Load)

-0.200 kN/m² (↓) (Dead + Snow Load)

1.060 kN/m² (↑) (Wind Load)

For Center Half (Right Part)

-0.200 kN/m² (Dead Load)

-0.726 kN/m² (Average Unbalanced Snow Load)

-0.926 kN/m² (↓) (Dead + Snow Load)

1.060 kN/m² (↑) (Wind Load)

For Leeward Quarter

-0.200 kN/m² (Dead Load)

-1.348 kN/m² (Average Unbalanced Snow Load)

-1.548 kN/m² (↓) (Dead + Snow Load)

0.571 kN/m² (↑) (Wind Load) (0.674 x Cos 32.02°)

0.357 kN/m² (→) (Lateral Load Due to Wind) (0.674 x Sin 32.02°)

Load Case 6 (Dead Load + Unbalanced Snow + Wind Load with Negative Internal Pressure Coefficient))

For Windward Quarter

-0.200 kN/m² (Dead Load)

0 kN/m² (Snow Load)

-0.200 kN/m² (↓) (Dead + Snow Load)

0.162 kN/m² (↑) (Wind Load) (0.191 x Cos 32.02°)

-0.101 kN/m² (←) (Lateral Load Due to Wind) (0.191 x Sin 32.02°)

For Center Half (Left Part)

-0.200 kN/m² (Dead Load)

0 kN/m² (Snow Load)

-0.200 kN/m² (↓) (Dead + Snow Load)

0.659 kN/m² (↑) (Wind Load)

For Center Half (Right Part)

-0.200 kN/m² (Dead Load)

-0.726 kN/m² (Average Unbalanced Snow Load)

-0.926 kN/m² (↓) (Dead + Snow Load)

0.659 kN/m² (↑) (Wind Load)

For Leeward Quarter

-0.200 kN/m² (Dead Load)

-1.348 kN/m² (Average Unbalanced Snow Load)

-1.548 kN/m² (↓) (Dead + Snow Load)

0.231 kN/m² (↑) (Wind Load) (0.273 x Cos 32.02°)

0.083 kN/m² (→) (Lateral Load Due to Wind) (0.266 x Sin 18.10°)

8.3.7 Loads Acting On Joints

Load Case 1 (D + S_{Balanced})

$(-1.030 \text{ kN/m}^2 * 1257 \text{ m}^2)/(271 \text{ joints}) = -4.778 \text{ kN/joint} = \underline{\underline{-1.074 \text{ kip/joint}}}$ (↓)

Load Case 2 (D + S_{Unbalanced})

For Left Half

$(-0.200 \text{ kN/m}^2 * 1257 \text{ m}^2/2)/(271 \text{ joints}/2) = -0.928 \text{ kN/joint} = \underline{\underline{-0.209 \text{ kip/joint}}}$ (↓)

For Right Half

$(-1.330 \text{ kN/m}^2 * 1257 \text{ m}^2/2)/(271 \text{ joints}/2) = -6.169 \text{ kN/joint} = \underline{\underline{-1.387 \text{ kip/joint}}}$ (↓)

Load Case 3 (D + S_{Balanced} + W_{Positive Internal Pressure Coefficient})

For Windward Quarter

$(-1.030 \text{ kN/m}^2 * 245.85 \text{ m}^2 + (-0.179 \text{ kN/m}^2) * 303 \text{ m}^2)/(60 \text{ joints}) = -5.124 \text{ kN/joint} = \underline{\underline{-1.152 \text{ kip/joint}}}$ (↓)

Lateral Load

$(0.112 \text{ kN/m}^2 * 303 \text{ m}^2)/(60 \text{ joints}) = 0.566 \text{ kN/joint} = \underline{\underline{0.127 \text{ kip/joint}}}$ (→)

For Center Half

$(-1.030 \text{ kN/m}^2 * 765.41 \text{ m}^2 + 1.060 \text{ kN/m}^2 * 861.4 \text{ m}^2)/(151 \text{ joints}) = 0.826 \text{ kN/joint} = \underline{\underline{0.186 \text{ kip/joint}}}$ (↑)

For Leeward Quarter

$(-1.030 \text{ kN/m}^2 * 245.85 \text{ m}^2 + 0.572 \text{ kN/m}^2 * 303 \text{ m}^2)/(60 \text{ joints}) = -1.332 \text{ kN/joint} = \underline{\underline{-0.299 \text{ kip/joint}}}$ (↓)

Lateral Load

$(0.357 \text{ kN/m}^2 * 303 \text{ m}^2)/(60 \text{ joints}) = 1.803 \text{ kN/joint} = \underline{\underline{0.405 \text{ kip/joint}}}$ (→)

Load Case 4 (D + S_{Balanced} + W_{Negative Internal Pressure Coefficient})

For Windward Quarter

$$(-1.030 \text{ kN/m}^2 * 245.85 \text{ m}^2 + 0.162 \text{ kN/m}^2 * 303 \text{ m}^2) / (60 \text{ joints}) = -3.402 \text{ kN/joint} = \underline{\underline{-0.765 \text{ kip/joint}}} (\downarrow)$$

Lateral Load

$$(-0.101 \text{ kN/m}^2 * 303 \text{ m}^2) / (60 \text{ joints}) = -0.510 \text{ kN/joint} = \underline{\underline{-0.115 \text{ kip/joint}}} (\leftarrow)$$

For Center Half

$$(-1.030 \text{ kN/m}^2 * 765.41 \text{ m}^2 + 0.659 \text{ kN/m}^2 * 861.4 \text{ m}^2) / (151 \text{ joints}) = -1.462 \text{ kN/joint} = \underline{\underline{-0.329 \text{ kip/joint}}} (\downarrow)$$

For Leeward Quarter

$$(-1.030 \text{ kN/m}^2 * 245.85 \text{ m}^2 + 0.231 \text{ kN/m}^2 * 303 \text{ m}^2) / (60 \text{ joints}) = -3.054 \text{ kN/joint} = \underline{\underline{-0.687 \text{ kip/joint}}} (\downarrow)$$

Lateral Load

$$(0.145 \text{ kN/m}^2 * 303 \text{ m}^2) / (60 \text{ joints}) = 0.732 \text{ kN/joint} = \underline{\underline{0.165 \text{ kip/joint}}} (\rightarrow)$$

Load Case 5 (D + S_{Unbalanced} + W_{Positive Internal Pressure Coefficient})

For Windward Quarter

$$(-0.200 \text{ kN/m}^2 * 245.85 \text{ m}^2 + (-0.179 \text{ kN/m}^2) * 303 \text{ m}^2) / (60 \text{ joints}) = -1.723 \text{ kN/joint} = \underline{\underline{-0.387 \text{ kip/joint}}} (\downarrow)$$

Lateral Load

$$(-0.112 \text{ kN/m}^2 * 303 \text{ m}^2) / (60 \text{ joints}) = -0.566 \text{ kN/joint} = \underline{\underline{-0.127 \text{ kip/joint}}} (\leftarrow)$$

For Center Half (Left Part)

$$(-0.200 \text{ kN/m}^2 * (765.41 \text{ m}^2 / 2) + 1.060 \text{ kN/m}^2 * (861.40 \text{ m}^2 / 2)) / (151 / 2 \text{ joints}) = 5.033 \text{ kN/joint} = \underline{\underline{1.132 \text{ kip/joint}}} (\uparrow)$$

For Center Half (Right Part)

$$(-0.926 \text{ kN/m}^2 * (765.41 \text{ m}^2 / 2) + 1.060 \text{ kN/m}^2 * (861.4 \text{ m}^2 / 2)) / (151 / 2 \text{ joints}) = 1.353 \text{ kN/joint} = \underline{\underline{0.304 \text{ kip/joint}}} (\uparrow)$$

For Leeward Quarter

$$(-1.548 \text{ kN/m}^2 * 245.85 \text{ m}^2 + 0.571 \text{ kN/m}^2 * 303 \text{ m}^2) / (60 \text{ joints}) = -3.459 \text{ kN/joint} = \underline{\underline{-0.778 \text{ kip/joint}}} (\downarrow)$$

Lateral Load

$$(0.357 \text{ kN/m}^2 * 303 \text{ m}^2) / (60 \text{ joints}) = 1.803 \text{ kN/joint} = \underline{\underline{0.405 \text{ kip/joint}}} (\rightarrow)$$

Load Case 6 (D + S_{Unbalanced} + W_{Negative Internal Pressure Coefficient})

For Windward Quarter

$$(-0.200 \text{ kN/m}^2 * 245.85 \text{ m}^2 + 0.162 \text{ kN/m}^2 * 303 \text{ m}^2) / (60 \text{ joints}) = -0.001 \text{ kN/joint} = \underline{\underline{-0.0003 \text{ kip/joint}}} (\downarrow)$$

Lateral Load

$$(-0.101 \text{ kN/m}^2 * 303 \text{ m}^2) / (60 \text{ joints}) = -0.510 \text{ kN/joint} = \underline{\underline{-0.115 \text{ kip/joint}}} (\leftarrow)$$

For Center Half (Left Part)

$$(-0.200 \text{ kN/m}^2 * (765.41 \text{ m}^2/2) + 0.659 \text{ kN/m}^2 * (861.4 \text{ m}^2/2)) / (151/2 \text{ joints}) = 2.746 \text{ kN/joint} = \underline{\underline{0.617 \text{ kip/joint}}} (\uparrow)$$

For Center Half (Right Part)

$$(-0.926 \text{ kN/m}^2 * (765.41 \text{ m}^2/2) + 0.659 \text{ kN/m}^2 * (861.4 \text{ m}^2/2)) / (151/2 \text{ joints}) = -0.934 \text{ kN/joint} = \underline{\underline{-0.210 \text{ kip/joint}}} (\downarrow)$$

For Leeward Quarter

$$(-1.548 \text{ kN/m}^2 * 245.85 \text{ m}^2 + 0.231 \text{ kN/m}^2 * 303 \text{ m}^2) / (60 \text{ joint}) = -5.176 \text{ kN/joint} = \underline{\underline{-1.164 \text{ kip/joint}}} (\downarrow)$$

Lateral Load

$$(0.145 \text{ kN/m}^2 * 303 \text{ m}^2) / (60 \text{ joint}) = 0.732 \text{ kN/joint} = \underline{\underline{0.164 \text{ kip/joint}}} (\rightarrow)$$

8.3.8 Results

American circular hollow pipes are used in the design. As stated before, two different softwares (SSTOGA and SSTOSA) which utilize two techniques (Genetic Algorithms and Simulated Annealing) are made use of in the analysis. Each program is run three times as in problem 1. The design result which is tabulated in Table 8.3 was found by running both programs three times. Four different ready sections (P1+1/4, P2, P2+1/2, EP2) are used in this design.

Table 8.3. Result of 756-Bar Dome

Member Type	Number of Members (From Fig.8.13)	Ready Section	Cross Sectional Area (in²)
A ₁	1:54	P1+1/4	0.67
A ₂	55:156	P2+1/2	1.70
A ₃	157:204	P2	1.07
A ₄	205:294	EP2	1.48
A ₅	295:336	P2	1.07
A ₆	337:414	EP2	1.48
A ₇	415:450	P2	1.07
A ₈	451:516	EP2	1.48
A ₉	517:546	P2	1.07
A ₁₀	547:600	EP2	1.48
A ₁₁	601:624	P2	1.07
A ₁₂	625:666	EP2	1.48
A ₁₃	667:684	P2	1.07
A ₁₄	685:714	P2	1.07
A ₁₅	715:726	P2+1/2	1.70
A ₁₆	727:744	EP2	1.48
A ₁₇	745:750	P2+1/2	1.70
A ₁₈	751:756	P2	1.07
	Total Volume		107826.26 in²
	Total Weight		30487 lb

As seen from the Table 8.3, the optimum design is 30487 lb. The graphs of evolution to optimum design for both techniques (SSTOGA using Genetic Algorithm and SSTOSA using Simulated Annealing) are presented in Fig.8.33.

In SSTOGA, 1000 generations each having 100 structural analyses are performed. This software uses totally 100,000 structural analyses to converge the optimum solution as seen from the graph (blue line).

In SSTOSA, 31694 structural analyses in 300 cooling cycles are performed in order to find the optimum design, as seen from the graph (red line). This is fewer as compared to the number of the SSTOGA software. So this effects the CPU time.

While SSTOSA performs 31694 structural analyses to converge the optimum solution in about 26 hours (with a computer of AMD 1700 and 128 Mb RAM), SSTOGA converges the same optimum design by performing 100,000 structural analyses in about 73 hours (more than 3 days). This shows that CPU times are very distinctive where SSTOSA converges very earlier than SSTOGA.

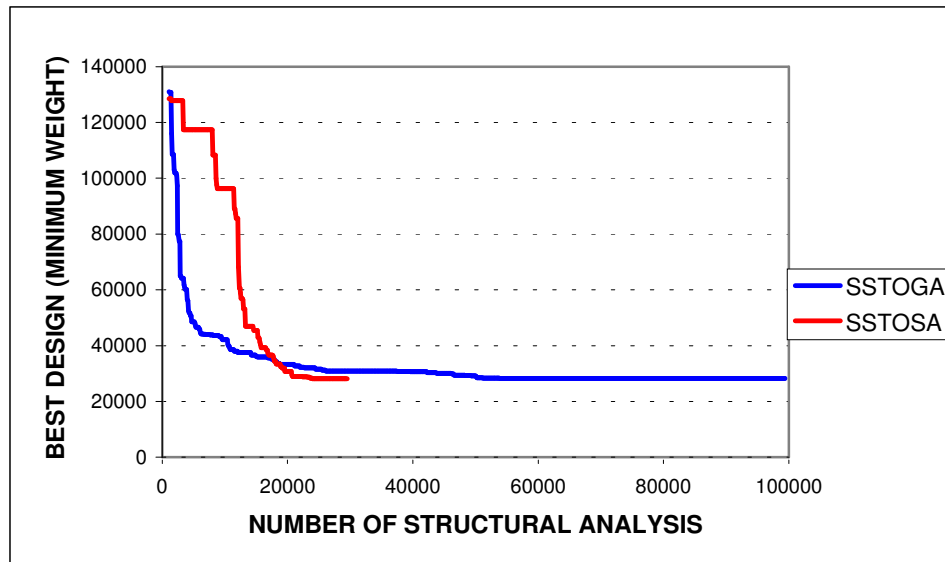
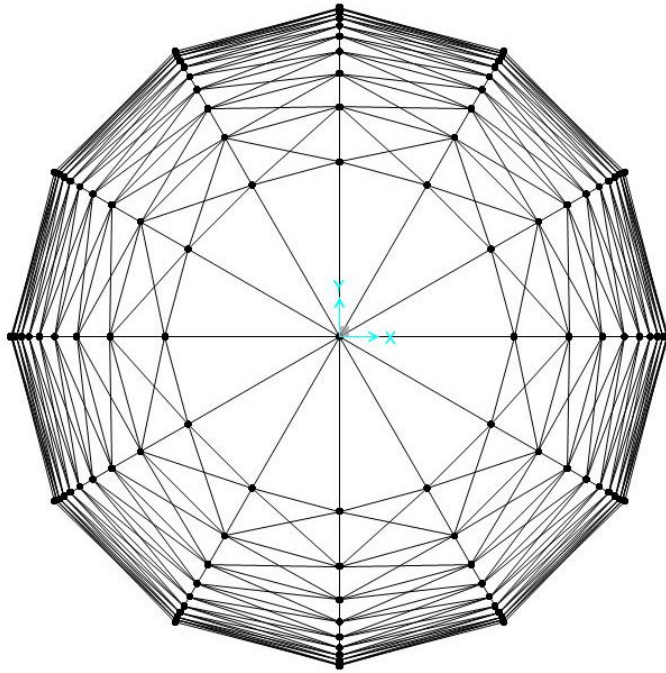


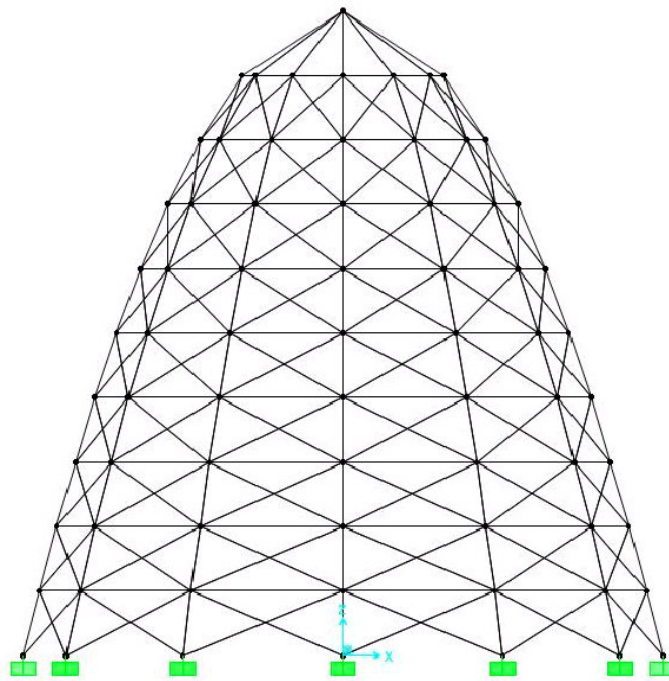
Fig.8.33. Graph of Number of Structural Analysis vs. Feasible Best Design of 756-Bar Dome Using SSTOGA and SSTOSA.

8.4 444-Bar Dome

The dome structure which has 444 elements and 121 nodes is presented below. This example is taken from literature. It was solved by Lamberti and Papapalettere in 2003. The top, side and 3-D views of the structure are presented in Fig. 8.34 through Fig.8.36 respectively.



8.34. Top View of 444-Bar Dome



8.35. Side View of 444-Bar Dome

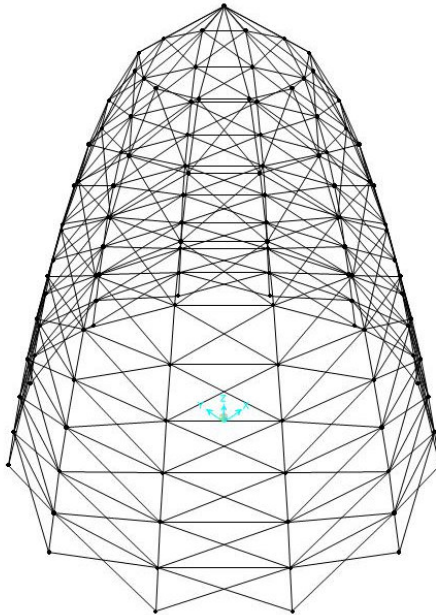


Fig.8.36. 3-D View of 444-Bar Dome

The structure has nine repeating modules each of which is comprised of 48 elements and a group of 12 elements on the top of these modules. The height of the structure is 20 m. and the radius at the ground level ($z=0$) is 10 m. The bars are grouped into 28 groups, 27 of them from nine repeating modules (vertical, horizontal and diagonal bars) and the one from the outermost module. The download vertical loads are assumed to apply to the structure; 100,000 lbf (45,359.24 kgf) at node 1 and 10,000 lbf (4535.924 kgf) at each other free node. The structure is restrained by 12 joints in the bottom layer. The continuous cross-sectional areas are used in this design. The lower bound of the cross-sectional areas is 0.1 in². The allowable tensile stress is 10,000 psi (7.031 kgf/mm²), the stress limit in compression is Euler buckling load. The displacements of the free nodes must be less than 0.25 in. (0.635 cm).

The same design conditions stated in the related article are used in order to make a comparison between results. As stated above, real load conditions and code-based

design are not used. Besides, predetermined point loads and stress check for tensile and compression members are made use of.

8.4.1 Results

Since the continuous cross-sections are used, different results are obtained for each trial. The results are tabulated for both SA and GAs techniques in Table 8.4.

Table 8.4. Results of 444-Bar Dome

Technique	Trial No	Best Design(lb)	Best Design(kg)
SA	1	20425.79	9264.97
SA	2	20403.23	9254.74
SA	3	20449.30	9275.64
SA	4	20419.12	9261.95
SA	5	20375.33	9242.09
SA	6	20424.07	9264.19
GA	1	22068.68	10010.18
GA	2	21913.01	9939.57
GA	3	21717.17	9850.74
GA	4	22093.23	10021.31
GA	5	21609.39	9801.85

The comparison of the results of the current work and the works from literature is shown in Table 8.5.

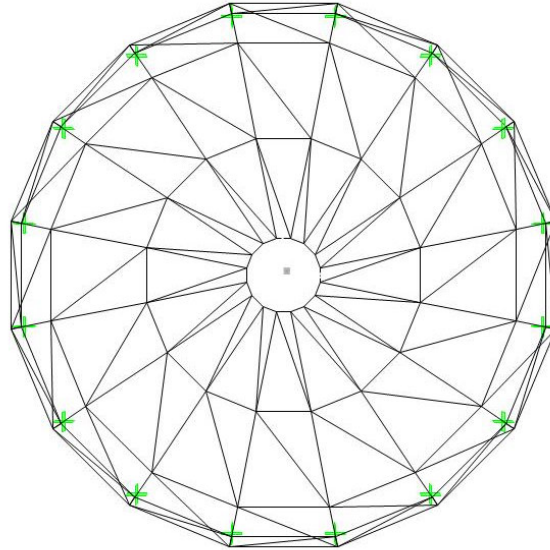
Table 8.5. Comparison of the Results

Technique Used	Related Article	Weight (kg)
Sequential Linear Programming (LESLP)	Lamberti and Pappalettere, 2003	9202.308
Sequential Linear Programming (Yu Chen's Technique)	Yu Chen, 1998	9202.308
Sequential Linear Programming (Commercial Optimizer DOT)	Vanderplaats, 1995	9308.650
Simulated Annealing (SSTOSA)	Current Work	9242.09
Genetic Algorithms (SSTOGA)	Current Work	9801.85

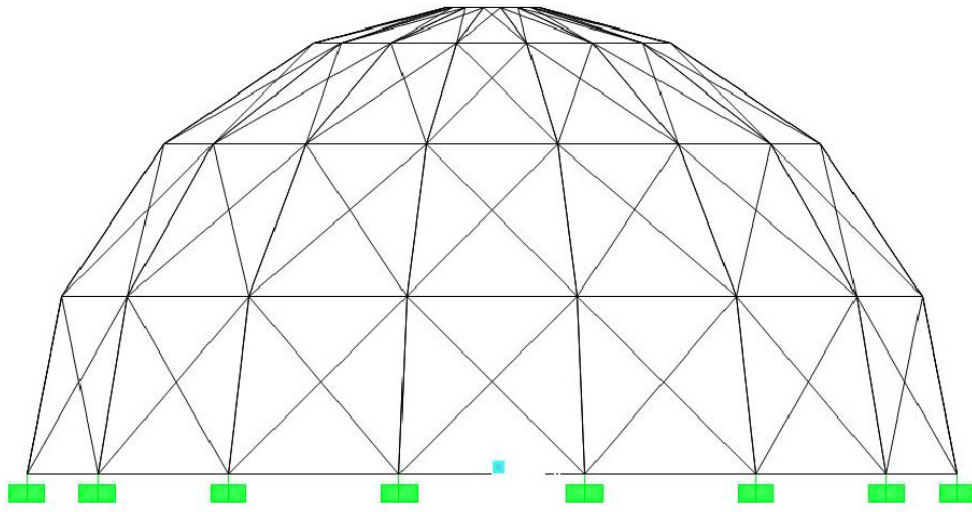
As seen from Table 8.5, SSTOSA converges better than SSTOGA. This is due to deflection criteria. In this problem (apart from the first three problems) deflection is very critical (0.635 cm.), so stress and displacement criteria must be fulfilled together. This prevents GAs converge better. But the value found by SSTOSA in the current work is very near the one found by Lamberti and Pappalettere, 2003

8.5 208-Bar Dome

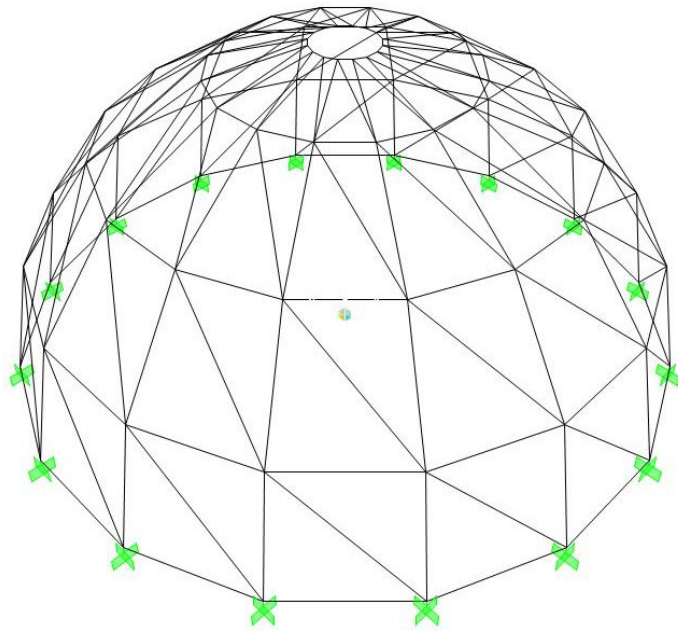
208-bar dome structure presented below is used to find the optimum rise-to-span ratio of dome structures. The rise-to-span ratios are increased gradually starting from 0.10 to 0.50 in order to find the value which gives the lowest weight. The same loading and design conditions are applied to all consecutive trials. Top, side and 3-D views of 208-bar dome is shown in Fig.8.37 through Fig.8.39. Member numbers of one half of the dome are given in Fig.8.40.



8.37. Top View of 208-Bar Dome



8.38. Side View of 208-Bar Dome



8.39. 3-D View of 208-Bar Dome

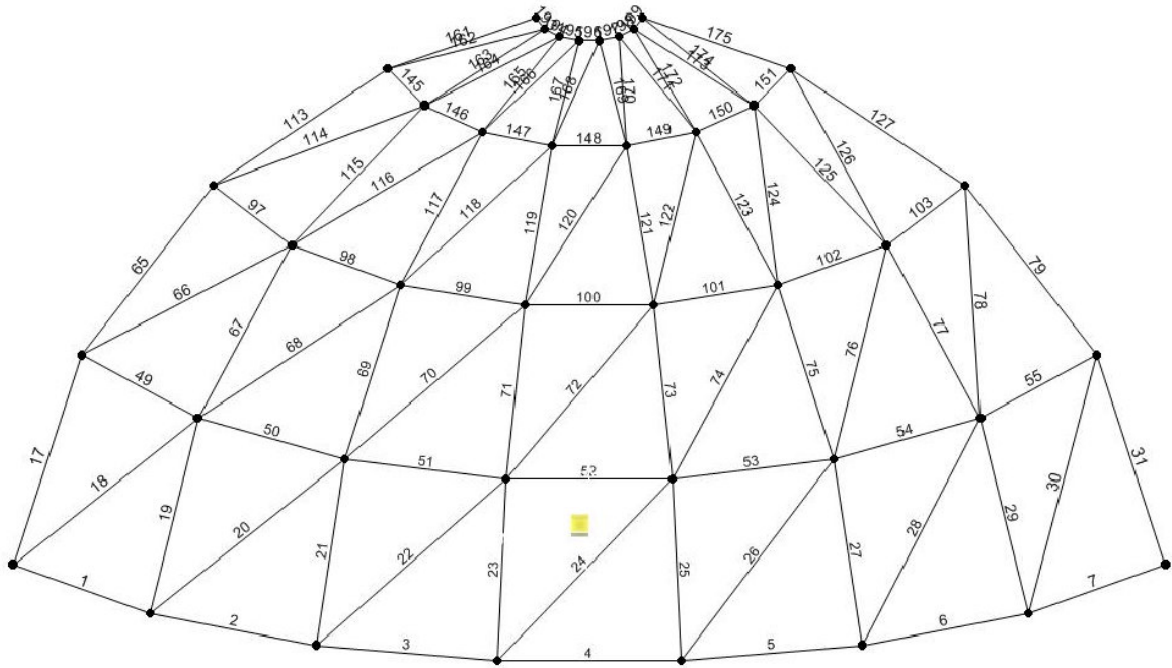


Fig.8.40. Half View of 208-Bar Dome (Given Member Numbers)

The load of 1 kip is assumed to effect at each free joint (joints from 17 to 80). Allowable Stress Design (ASD) of American Steel Standard is used in the design process and a displacement constraint is considered as $L/360$. The diameter is assumed to be 20 m. (787.40 in.) and the height is changed from 2 m. (78.74 in.) to 10 m. (393.70 in.). Nine consecutive trials are solved for the rise-to-span ratios, 0.10, 0.15, 0.20, 0.25, 0.30, 0.35, 0.40, 0.45, 0.50.

8.5.1. Results

The results obtained from utilizing the problems for different rise-to-span ratios are tabulated in Table 8.6. Each problem is solved for three times in order to be sure that global optimum results are found. As seen from the results, 0.20 is the optimum rise-to-span ratio for this problem.

Table 8.6. Results of 208-Bar Dome For Different Rise-to-Span Ratios

Rise-to-Span Ratio	Optimum Design (Minimum Weight) lb
0.10	6601.31
0.15	6111.38
0.20	5980.33
0.25	5990.97
0.30	6368.58
0.35	6463.08
0.40	6744.29
0.45	7593.95
0.50	8638.69

The results are presented graphically in Fig.8.41.

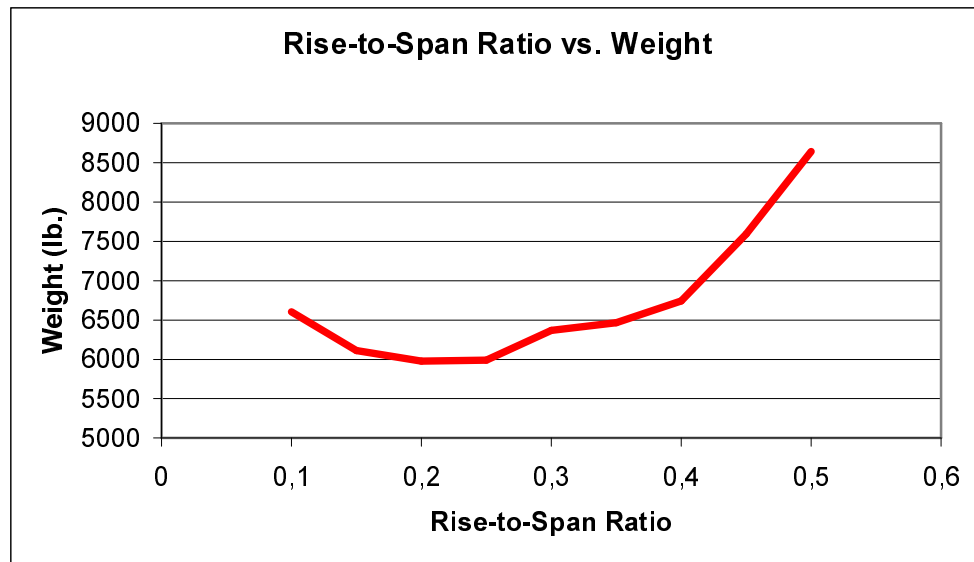


Fig.8.41. Rise-to-Span Ratio vs. Weight Graph (208-Bar)

8.6 354-Bar Dome

The dome structure which is presented in part 8.1 of this study, is used for the search of optimum rise-to-span ratio. This 354-bar dome is solved for different rise-to-span ratios varying from 0.10 to 0.50. The top, side and 3-D views of this structure are presented in Fig.8.3 through Fig.8.5. The same loading and design conditions are considered as stated for 208-bar dome.

8.6.1. Results

The results obtained from utilizing the problem for different rise-to-span ratios are tabulated in Table 8.7. Each problem is solved for three times in order to be sure that global optimum results are found. As seen from the results, 0.25 is found as the optimum rise-to-span ratio for this time.

Table 8.7. Results of 354-Bar Dome For Different Rise-to-Span Ratios

Rise-to-Span Ratio	Optimum Design (Minimum Weight) lb
0.10	28753.65
0.15	26602.90
0.20	26549.76
0.25	25903.64
0.30	26377.71
0.35	27976.20
0.40	28608.76
0.45	28891.85
0.50	32208.19

The results are presented graphically in Fig.8.42. It can be concluded that, for a single layer dome which has a circular base area, the optimum rise-to-span ratio is between 0.20 and 0.25.

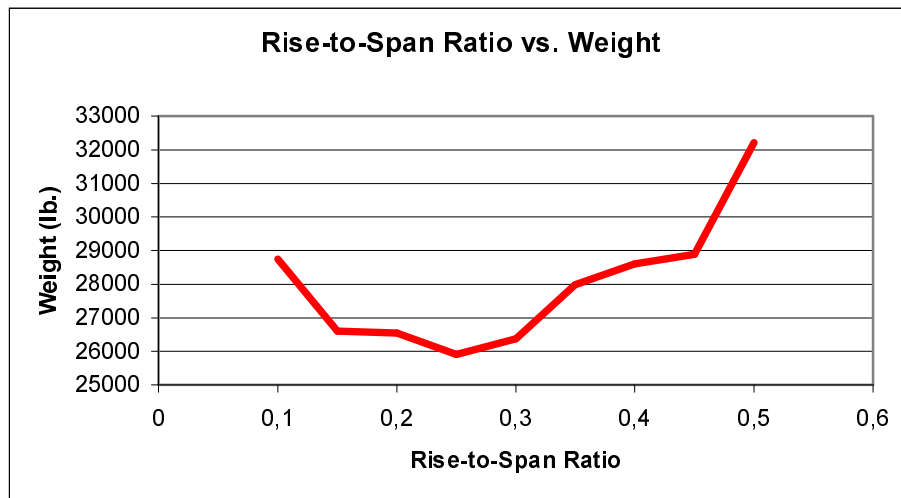
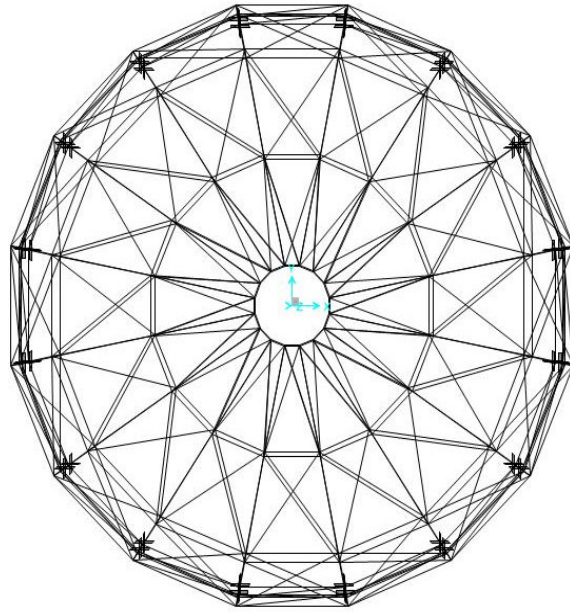


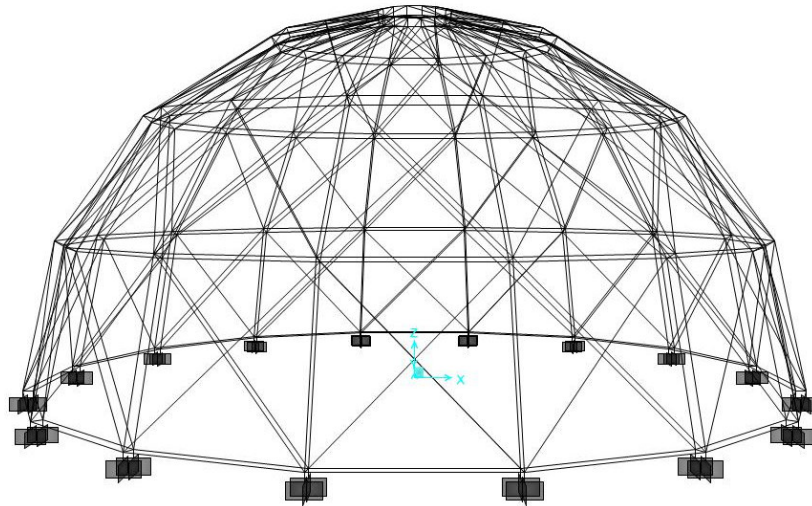
Fig.8.42 Rise-to-Span Ratio vs. Weight Graph (354-Bar)

8.7 560-Bar Dome

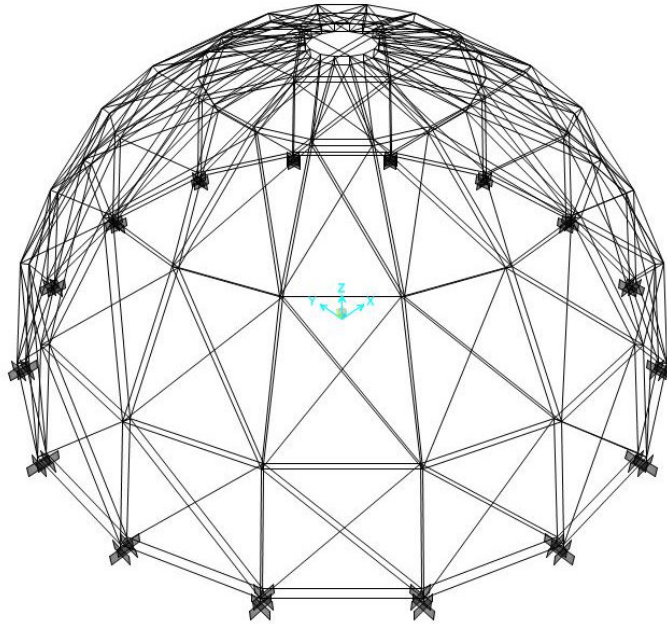
In the preceding chapters, it was mentioned that double layer domes are used in order to enclose larger spans more than 200 m span lengths and they are exceptionally rigid. In this problem, the 208-bar dome problem is assumed to have double layer. So, the effect of double-layer will be tried to investigate through this problem. A double layer dome which has a diameter of 20 m. and a height of 10 m. is investigated. The top, side and 3-D views of 560-bar dome are presented in Fig.8.43 through Fig.8.45. The load of 1 kip is assumed to effect at each free joint (joints from 17 to 80) and ASD-ASCE is used in the design process.



8.43. Top View of 560-Bar Dome



8.44. Side View of 560-Bar Dome



8.45. 3-D View of 560-Bar Dome

8.7.1 Results

A single layer dome (208-bar dome) which has the same dimensions with 560-bar dome is used in order to make a comparison. The results of single layer dome designed by using ASD-ASCE is presented in Table 8.8. The results of 560-bar double layer dome is shown in Table 8.9.

As seen from the tables, while eight different ready sections (EP1, EP1+1/2, P1/2, P1, P1+1/4, P1+1/2, P2, P2+1/2, P3) are used in the design of 208-bar dome, nine different ready section (EP1+1/4, P1/2, P1, P1+1/4, P1+1/2, P2, P2+1/2, P3, P3+1/2) are selected in the design of 560-bar dome.

Table 8.8. Result of 208-Bar Dome (Member numbers are given in Fig.8.40)

Member Type	No of Members	Ready Section	Cross Sectional Area (in ²)
A ₁	1:16	P2+1/2	1.70
A ₂	17:48	P3	2.23
A ₃	49:64	P1+1/4	0.67
A ₄	65,67,.....,93,95	P2+1/2	1.70
A ₅	66,68,.....,94,96	P3	2.23
A ₆	97:112	P1	0.49
A ₇	113:144	P2+1/2	1.70
A ₈	145:160	P1/2	0.25
A ₉	161,163,.....,189,191	EP1+1/2	1.07
A ₁₀	162,164,.....,190,192	P1+1/2	0.80
A ₁₁	193:208	EP1	0.64
	Total Volume		44378.57 in²
	Total Weight		12579.42 lb

Table 8.9. Result of 560-Bar Dome

Member Type	No of Members	Ready Section	Cross Sectional Area (in ²)
A ₁	1:16	P1+1/4	0.67
A ₂	17,19,.....,45,47	P2	1.07
A ₃	18,20,.....,46,48	P3	2.23
A ₄	49:64	P1+1/4	0.67
A ₅	65:96	P2	1.07
A ₆	97:112	P1	0.49
A ₇	113,115,.....,141,143	P2	1.07
A ₈	114,116,.....,142,144	P1+1/2	0.80
A ₉	145:160	P1/2	0.25
A ₁₀	161:192	P1+1/2	0.80
A ₁₁	193:208	P1/2	0.25
A ₁₂	209:224	P1+1/4	0.67
A ₁₃	225,227,.....,253,255	P3+1/2	2.68
A ₁₄	226,228,.....,254,256	P2	1.07
A ₁₅	257:272	P1+1/4	0.67
A ₁₆	273:304	P2	1.07
A ₁₇	305:320	P1	0.49
A ₁₈	321:352	P2+1/2	1.70
A ₁₉	353:368	P1/2	0.25
A ₂₀	369:400	P1+1/2	0.80
A ₂₁	401:416	EP1+1/4	0.88
A ₂₂	417:496	P1/2	0.25
A ₂₃	497:528	P2	1.07
A ₂₄	529:560	P1+1/2	0.80
	Total Volume		72203.30 in²
	Total Weight		20487.98 lb

While the number of members are almost tripled, the weight is increased just about 60 %. If the member end forces are investigated, it can be seen that the member end forces of double layer dome are almost one third of the ones of single layer dome. This shows that double layer domes must be preferred for very large spans or they can be used for the cases where the deflection limits are critical. The member forces of members 1 to 208 (elements of single layer dome and corresponding elements of inner layer of double-layer dome) are presented in Fig. 8.46 graphically in order to compare the forces. It can be noticed that the loads of the double-layer dome are very low as compared to the ones of single-layer dome. This shows the high rigidity of the double-layer domes.

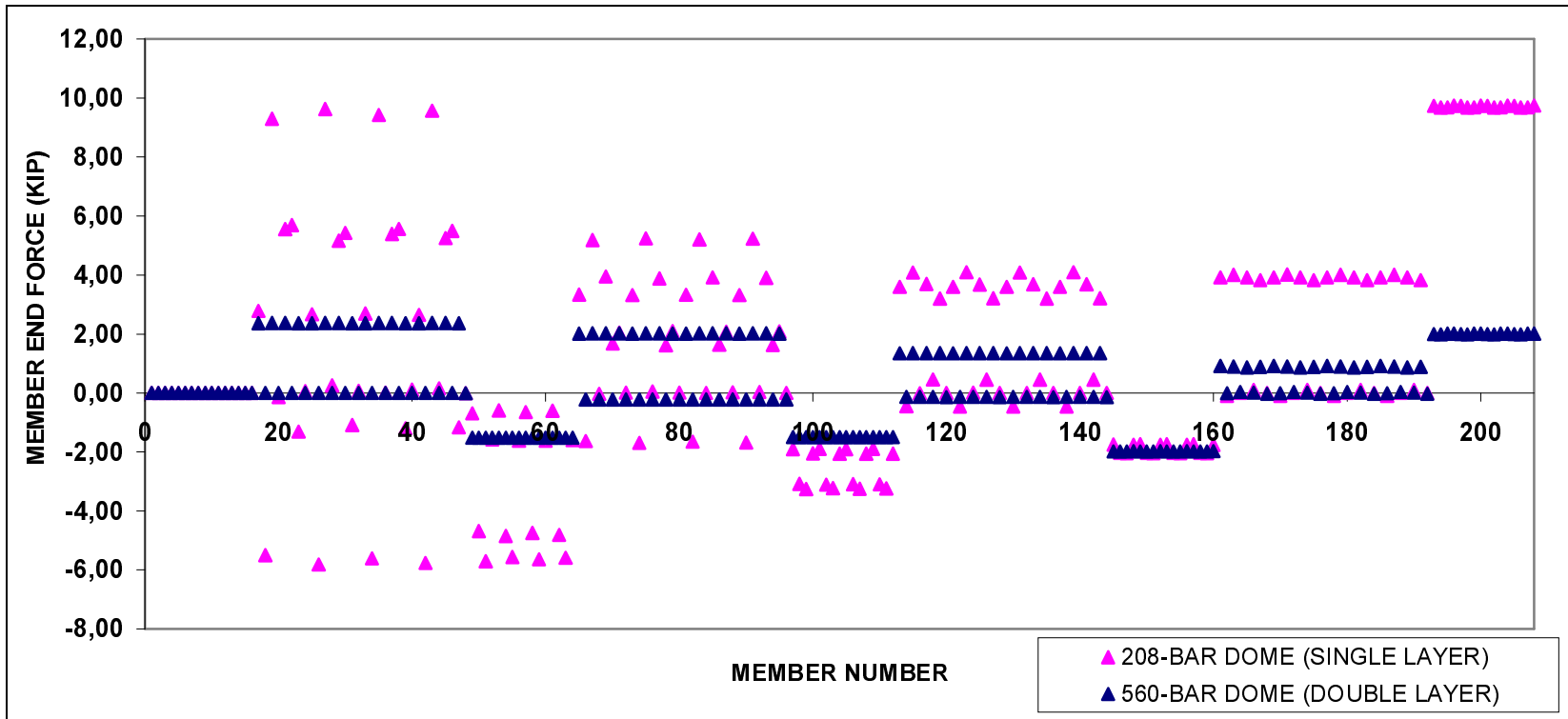


Fig.8.46 Comparison of Member Forces of Single and Double-Layer Domes

8.8 Discussion of the Results

In this chapter, seven design problems are investigated. The first three problems are assumed to be in real life case and the diameter of these three structures are kept constant in order to make a comparison. The detailed results are presented in the related parts, but a general schema is shown in Table 8.10 to compare the results.

Table 8.10 Comparison of the Results of Problems 8.1, 8.2, 8.3.

Type of Problem	No of Joints	No of Members	Height of the Dome	Minimum Weight	Total Length of the Members	Average Length of the Members	Average Weight of the Members
	A	B	C	D	E	E/B	D/E
354-Bar Dome	127	354	4.34 m.	16997 kg.	1386 m.	3.92 m.	12.263 kg/m.
354-Bar Dome	127	354	8.28 m.	16442 kg.	1441 m.	4.07 m.	11.410 kg/m.
756-Bar Dome	271	756	8.28 m.	13829 kg.	2029 m.	2.68 m.	6.816 kg/m.

As seen from the table above, the most economical design is the third one. At a first glance, this result may seem to be surprising since total length of the members in the third dome is the highest one. The reason leading to this result lies in the buckling strength of the members. That is, since the average length of the members is the lowest in the third dome, it turns out that buckling is less critical for the third dome. The fact that buckling is less critical for the third dome leads to selection of lighter cross-sections for the members, resulting in more economical design.

When the first and second domes are compared, it is seen that the second dome offers a more economical design, although the overall length of whole members is higher. This is because the rise-to-span ratio in the second dome, which is 0.2 allows the structure to exhibit a more efficient arch action which increases the strength against compression. This is also observed in test problems 5 and 6.

Although the third design leads to the least weight of the structure, its only shortcoming is the use of a high number of joints, which might be critical as far as cost optimization is concerned, rather than weight optimization.

The fourth problem is taken from the literature and point loads are assumed to act as stated in the corresponding articles. The results found in the current work are approximately the same as compared to the ones presented in the related articles. It concludes that softwares SSTOSA and SSTOGA can be used in the optimum design with confidence.

Fifth and sixth problems show that the optimum rise-to-span ratio for domes which have circular base area is between 0.20 and 0.25. The domes with rise-to-span ratios larger or smaller than these values do not result in economical solutions. As stated in the previous chapters, very shallow or deep domes are subjected to more severe loads and susceptible design problems such as snap-through buckling, local buckling.

Seventh problem is aimed to find the effect of double-layer. The results of this problem prove that double layer domes must be used in case of very large spans or for the cases where the deflection is critical. One other result obtained from the investigation of number forces in double layer domes show that these structures are very rigid as compared to the single layer domes.

CHAPTER 9

SUMMARY AND CONCLUSIONS

9.1 Overview of the Thesis

The use of two modern optimization techniques (GAs and SA) in the optimum structural design applications of pin-jointed 3-D dome structures has been explored in this thesis. These techniques have been investigated in terms of their applicability, efficiency and success to the problems of dome structures. Two practical software packages (e.g. SSTOGA and SSTOSA) developed by Hasańcebi (2001) have been used in the design process meeting requirements imposed by real life applications. A practical optimum design of domes is emphasized such that various loads (wind, snow etc.) acting on these structures are considered according to provisions of design codes.

Both techniques (GAs and SA) have been applied separately to the test problems in order to identify the differences in the search characteristics of the techniques, as well as their efficiencies. The emphasis is not only laid on the two global optimization techniques, but also the dome structures are extensively discussed. The various types of domes have been identified from the real life applications and literature survey. After getting a sound knowledge about two global optimization techniques and domes, the weight optimization of these structures have been studied considering various aspects of designs, such as shape, connection, form and dimension.

After this brief overview of the thesis, a more comprehensive discussion is presented in the following section to summarize and conclude the chapters.

9.2 Summary of the Thesis

In chapter 2, introductory information about dome structures is presented in order to clarify the attributes of these structures both from a theoretical and practical points of view. The types of dome structures which have been used widely in the world are discussed. The examples of domes constructed in Turkey and in the world are presented. Various components and details of the dome structures are also explained briefly in this chapter.

Chapter 3 covers the analysis aspect of dome structures. Although chapter 2 gives general information about this type structures, chapter 3 focuses on the issue of analysis (both linear and non-linear). The stiffness method (displacement method) is introduced as linear analysis tool in detail. The stiffness and transformation matrices are presented for 3-D truss type elements. The loads that act on these structures are briefly mentioned in this chapter since a separate chapter is devoted for design loads. Wind tunnel tests and test results obtained from wind tunnel tests are also presented in order to give a sound knowledge about the real load conditions.

Chapter 4 is devoted to design loads according to ASCE 7-98 “Minimum Design Loads for Buildings and Other Structures”. The wind and snow loads are highlighted since these two loads are the most critical loads for dome structures as experienced from the past tragic events (collapses of dome structures in the past). The design code of ASCE 7-98 is explained in detail in order to improve the understanding of the real load conditions such as wind and snow loads. The load conditions presented in this chapter are also utilized in the design of test problems discussed in chapter 8. The design loads, especially wind and snow loads are described in step-by-step manner.

Chapter 5 gives a brief outline of optimization techniques. A classification of optimization techniques is performed and the descriptions of classical and modern techniques are given briefly. Stochastic search techniques (global optimization techniques) are given a particular emphasis because GAs and SA belong to this specific category of optimization techniques. Extensive information about GAs and SA is avoided in this chapter, since they are broadly discussed in chapters 6 and 7.

In chapter 6, detailed information on genetic algorithms is presented in order to clarify the working principles of the technique, both from theoretical and practical points of view. Following a general algorithmic outline of a GA, the components of this algorithm are explicated, referring to some alternative approaches adopted to implement them. It is worthwhile to mention that the relative effectiveness of such approaches is still an ongoing research area due to a lack of theoretically supported concrete findings. The main steps of GAs and genetic operators used in the technique are explained in detail. Then the formulation of size optimum design problem of truss structures and constraint handling in GAs are presented in order to give the necessary background for the design process.

A comprehensive discussion on the simulated annealing technique is presented in chapter 7, clarifying the powerful parallelisms between its algorithmic realization and thermodynamical background. It has been emphasized that the robustness of SA primarily lies in its ability to effectively combine useful characteristics of both the global and random search strategies. It is worthwhile to mention that there are plenty of different algorithmic versions of SA in the literature. The SA algorithm discussed in chapter 7 rests on the use of Boltzman parameter, and thus exhibits certain superiorities in comparison to other versions. This is, in fact, closely related to the functionality and usefulness of Boltzman parameter during the optimization process. Because, apart from (i) enabling a fruitful implementation of the algorithm irrespective of problem type; and (ii) storing the search experience to govern the acceptance criteria of next candidates, this parameter contributes to the formation of an appropriate annealing schedule. However, in some other versions this task is

carried out by assigning arbitrary values to the annealing schedule parameters, and due to a lack of normalization of objective function values, a lot of trials has to be performed to determine the most efficient annealing schedule for a particular problem. Thus, it can be concluded that the use of Boltzman parameter in annealing algorithm is not a trivial task and should be favored to create an efficiently working algorithm.

Chapter 8 reports numerical experiments concerning the applications of GAs and SA to weight optimum design of dome structures. Seven test problems are solved here using both techniques, making use of real load conditions. Two different computer softwares prepared by Hasaebi (2001) were used; SSTOGA (Size, Shape and Topology Using Genetic Algorithms) and SSTOSA (Size, Shape and Topology Using Simulated Annealing). The first problem is 354-bar dome structure which is designed to be used as the roof of an auditorium building. Two techniques yielded the same result. In order to achieve a comparability of the techniques, the evolution of the best design during the course of optimization process was graphically presented for both of the techniques. The second test problem is similar to the first one, except the height of the dome is increased to 8.28 m. Third test problem has the same dimensions with the second dome, yet its topological configuration is different such that it has 756 bars and 271 joints. Real load conditions according to ASCE 7-98 “Minimum Design Loads for Buildings and Other Structures” were applied to all these three problems. Next, a problem taken from the literature was studied and the results found were compared in order to explore the efficiency of the algorithms. The last three problems were used to investigate the effect of rise-to-span ratio and double layer to the optimum design. A further discussion about the results is presented in the end of the chapter so as to give practical tips to the designers.

9.3 Conclusion

In the light of the experience gained through the test problems, it can be said that both optimization techniques (SA and GAs) generally converge the same optimum solution for the problems where design space is not heavily dominated by displacement constraints (test problems 1-3). However, SA finds the solution much faster (with a less number of structural analyses) than GAs.

The optimum rise-to-span ratio for domes was found to be between 0.20 and 0.25. This ratio has a significant influence on the optimum design of domes. Especially, for problems where shape optimization is not involved, it is recommended that the rise-to-span ratio of the domes be chosen between 0.20 and 0.25 for an effective design of the structures. As depicted from the graphs in Chapter 8, the domes having rise-to-span ratios above and below this range give rise to non-optimum solutions.

Another significant criterion governing the design of domes is the requirement of fully triangulation of the geometry. Since these types of structures have a high stiffness in all directions and are kinematically stable, triangulation must be used in the design of domes unless making rigid connection designs. For pin-connected dome design, the dome area must be formed from the triangular parts. Otherwise stability problem can be encountered.

Although the double layer dome used in the test problem 7 didn't produce any less weight than a single layer dome, it is a well-known fact that they should be used for larger spans (especially more than 100 m.) and for the cases where deflection criterion is critical. Since these structures have a higher rigidity, they can be used for the design of unobstructed large spans. The load analysis of the member forces in chapter 8 shows that when a single layer dome is replaced with a double layer dome, the member end forces can be decreased to one third and sometimes one fourth of their initial values. Because of this reason, in the design of the large spans,

double-layer design is preferred. There are numerous examples of double-layer domes which cover the spans more than 200 m. in the world.

The numerical examples discussed in the thesis indicate that as far as the load analysis of domes is concerned, snow load plus dead load should be considered. When calculating snow load, its symmetrical distribution over the entire dome should be considered together with its unsymmetrical distribution accumulated on one half of the dome. For some members, other load combinations such as DL + WL + SL are also observed to be critical.

Since the most of the dome structures are symmetrical, grouping of the members is essential for a practical design process. Besides, grouping of the symmetric members reduces the CPU time during the optimization process, especially when SA is employed.

In Turkey, dome structures are not used as commonly as in the world. As stated before, dome structures enclose a maximum amount of space with a minimum surface, so they are the most economical structures for the need of unobstructed closed places. For this reason, especially in USA, large unobstructed spans such as sports stadia, swimming pools, baseball pitches, gymnasiums, etc. are enclosed by using pin-connected or rigid type dome structures. From this standpoint, it is hoped that this thesis plays an encouraging role about the common use of this type structures in Turkey.

9.4 Recommendations for Future Works

Although genetic algorithm is very powerful technique, it leads to a massive computational effort, reducing the speed of the algorithm as compared to traditional optimization techniques. This discussion also holds for the simulated annealing, where the optimum is located via a high number of candidate sampling. Especially, the most time-consuming part of a structural optimization algorithm is the structural

analysis phase required to obtain the structural response of designs. There are several ways to avoid such an intensive computational task, and thus to enhance the efficiency of the solution algorithm in terms of computing time. One way is to make use of the natural parallelism inherent in these algorithms through an implementation in parallel computing environment. For instance, in GAs it is possible to divide a design population into a number of n sub-populations on a computer system of n -processors, such that each processor is held responsible for evolving its own sub-population. By this time, the computational effort may be reduced proportion to the number of processors used. A second and more efficient approach is to use the other artificial intelligence techniques, such as neural network or genetic programming, to provide computationally inexpensive estimates of structural response quantities. This is accomplished by establishing a functional relation between a set of input and output data.

This thesis conducted a research on the use of GAs and SA techniques in the optimum design of pin-jointed 3-D dome structures. The testing of other evolutionary algorithm techniques; evolutionary strategies (ESs) and evolutionary programming (EP), in some mathematical optimization problems indicates a strong evidence of their robustness and superiorities over GAs. Thus, it is essential to investigate the efficiency and effectiveness of ESs and EP in optimum structural design. However, this requires the development of their more powerful discrete versions, which will allow them to maintain their enhanced search capabilities in searching the design spaces of discrete optimization problems.

Rigidly jointed dome structures are also used widely in the world. Especially ribbed domes and geodesic domes can be analyzed by using the same techniques (GAs and SA) in the future works. Moreover, Eurocode 3 (code for steel structures in European Community) can be included to the design process for more realistic and economic designs.

REFERENCES

- Adeli, H., and Kumar, S. (1995). Distributed Genetic Algorithm for Structural Optimization. Journal of Aerospace Engineering, 156-163.
- Altınyaldız, Technical Specification for Space Structures.
- Amirjanov, A. (2004). A Changing Range Genetic Algorithm. International Journal For Numerical Methods in Engineering, 61, 2660-2674.
- Arora, J.S. (Editor) (1997). Guide to Structural Optimization. ASCE.
- Arora, J.S. (1989). Introduction to Optimum Design. Mc-Graw Hill Book Company.
- Arya, C. (2003). Design of Structural Elements, Spon Press.
- ASCE 7-98. Minimum Design Loads for Buildings and Other Structures. ASCE. Revision of ANSI/ASCE 7-95.
- Azid, I.A., Kwan, A.S.K., Seetharamu, K.N. (2002). An Evolutionary Approach for Layout Optimization of a Three-Dimensional Truss. Structural Multidisciplinary Optimization, 24, 333-337.
- Azid, I.A., Kwan, A.S.K., Seetharamu, K.N. (2002). A Genetic Algorithm-Based Technique for Layout Optimization of Truss with Stress and Displacement

Constraints. International Journal of Numerical Methods in Engineering, 53, 1641-1674.

Bäck, T. (1996). Evolutionary Algorithms in Theory and Practice. Oxford University Press.

Bäck, T., and Hoffmeister, F. (1991). Adaptive Search by Evolutionary Algorithms. In: MOSES: Models of Selforganization in Complex Systems (Ebeling, W., Peschel, M., and Weidlich, W., eds.), Mathematical Research, 64, Akademie, Berlin, 156-163.

Bäck, T., Rudolph, G., and Schwefel, H.-P. (1993). Evolutionary Programming and Evolution Strategies: Similarities and Differences. In: Proc. 2nd Annual Conference on Evolutionary Programming (Fogel, D.B., and Atmar, W., eds.), Evolutionary Programming Society, San Diego, CA, 11-22.

Baker, J.E. (1985). Adaptive Selection Methods for Genetic Algorithms. In: Proc. 5th International Conference on Genetic Algorithms (Grefenstette, J.J., ed.), Lawrence Erlbaum Associates, 101-111.

Balling, R.J. (1991). Optimal Steel Frame Design by Simulated Annealing. Journal of Structural Engineering, ASCE, 117 (6) 1780-1795.

Bauer, J., Zawidzka, J., Sumec, J. (1995). Minimum Weight Design of Schwedler Shell. International Conference on Lightweight Structures in Civil Engineering.

Beasley, D., Bull, D.R., and Martin, R.R. (1993). An Overview of Genetic Algorithms: Part 1, Fundamentals. University Computing, 15 (2), 58-69.

- Belegundu, A.D., and Chandrupatla, T.R. (1999). Optimization Concepts and Applications in Engineering. Prentice Hall.
- Bendsøe, M.P., Ben-Tal, A., Zowe, J. (1994). Optimization Methods for Truss Geometry and Topology Design. *Structural Optimization*, 7, 141-159.
- Benjamin, B.S. (1963). The Analysis of Braced Domes. Asia Publishing House.
- Bennage, W.A., and Dhingra, A.K. (1995). Single and Multiobjective Structural Optimization in Discrete-Continuous Variables Using Simulated Annealing. *International Journal for Numerical Methods in Engineering*, 38, 2753-2773.
- Bojczuk, D., and Mróz, Z. (1999). Optimal Topology and Configuration Design of Trusses With Stress and Buckling Constraints. *Structural Optimization*, 17, 24-35.
- Botello, S., Marroquin, J.L., Onate, E., Van Horebeek, J. (1999). Solving Structural Optimization Problems with Genetic Algorithms and Simulated Annealing. *International Journal for Numerical Methods in Engineering*, 45, 1069-1084.
- Camp, C., Pezeshk, S., Cao, G. (1998). Optimized Design of Two-Dimensional Structures Using A Genetic Algorithm. *Journal of Structural Optimization*, 551-559.
- Castro, G., and Jan, C.T. (1995). Shape Optimization in Lateral Load Resistant Systems. *Structural Systems and Industrial Applications*, 505-515.
- Cerny, V. (1985). Thermodynamical Approach to the Traveling Salesman Problem: An Efficient Simulation Algorithm. *Journal of Optimization Theory and Applications*, 45, 41-51.

- Chen, S.Y., and Rajan, S.D. Using Genetic Algorithm as an Automatic Structural Design Tool. Fulton School of Engineering, <http://www.ceaspub.eas.asu.edu/structures/rajan/buffalo.pdf>. Last visited on October 28th,2005
- Chen, T.Y., and Chan,C.J.(1997). Improvements of Simple Genetic Algorithms in Structural Design. International Journal for Numerical Methods in Engineering, 40, 1323-1334.
- Cheng, F.Y., and Li, D. (1997). Multiobjective Optimization Design with Pareto Genetic Algorithm. Journal of Structural Engineering, 1252-1261.
- Choi, S.H., and Kim.,S.E. (2002). Optimal Design of Steel Frame Using Practical Non-linear Inelastic Analysis. Engineering Structures, 24, 1189-1201.
- Coello, C.A., and Christiansen, A.D. (2000). Multiobjective Optimization of Trusses Using Genetic Algorithms. Computers and Structures, 75, 647-660.
- Cohn, M.Z. (1994). Theory and Practice of Structural Optimization. Structural Optimization, 7, 20-31.
- Davis,L. (1989). Adapting Operator Probabilities in Genetic Algorithms. In Proc. 1st International Conference on Genetic Algorithms (Schaffer,J.D.,ed.), Morgan Kaufman, 61-69.
- Deb, K.,and Gulati, S.(2001). Design of Truss-Structures for Minimum Weight Using Genetic Algorithms. Finite Elements in Analysis and Design, 37, 447-465.
- De Jong, K.A. (1975). An Analysis of the Behaviour of a Class of Genetic Adaptive Systems. PhD Thesis, University of Michigan.

- Dowland, K.A. (1995). Simulated Annealing. In C.R Reeves, ed., Modern Heuristic Techniques for Combinatorial Optimization Problems. McGraw-Hill Book Co., Europe.
- Dragone, G. (1979). Wind Effect on Hemispherical Domes. MSc Thesis , University of Surrey.
- Erbatur, F. Hasançebi, O, Tütüncü, İ., Kılıç, H. (2000). Optimal Design of Planar and Space Structures with Genetic Algorithms. Computers and Structures, 75, 209-224.
- Escrig, F., and Sanchez, J. Great Space Curved Structures with Rigid Joints. International Database and Gallery of Structures, <http://www.en.structurae.de/refs/items/index.cfm>. Last visited on October 28th, 2005.
- Fogel, D.B. (1991). System Identification Through Simulated Evolution: A Machine Learning Approach to Modeling. Ginn Press, Needham Heights.
- Fogel,L.J., Owens,A.J., and Walsh,M.J.(1966). Artificial Intelligence Through Simulated Evolution. Wiley, New York.
- Fraser, A.S.(1962). Simulation of Genetic Systems. Journal of Theoretical Biology, 2, 329-346.
- Galambos, T.V. (Editor) (1988). Guide to Stability Design Criteria for Metal Structures. John Wiley&Sons.
- Gen, M., and Cheng, R. (1997). Genetic Algorithms and Engineering Design. John Wiley&Sons Inc.

- Goldberg, D.E. (1989). Genetic Algorithms in Search, Optimization, and Machine Learning. Addison-Wesley Publishing Company Inc.
- Groenwold, A.A., and Stander, N. (1997). Optimal Discrete Sizing of Truss Structures Subject to Buckling Constraints. *Structural Optimization*, 14, 71-80.
- Groenwold, A.A., Stander, N., Snyman, J.A. (1999). A Regional Genetic Algorithm For the Discrete Optimal Design of Truss Structures. *International Journal of Numerical Methods in Engineering*. 44, 749-766.
- Hajela, P., and Lee, E. (1995). Genetic Algorithms in Truss Topological Optimization. *International Journal of Solids and Structures*, 32 (22), 3341-3357.
- Hasançebi, O. (2001). Optimum Structural Design Using Analogies to Natural Processes. Ph.D.Thesis.
- Hasançebi, O., and Erbatur, F. (2000). Evolution of Crossover Techniques in Genetic Algorithm Based Optimum Structural Design. *Computers and Structures*, 78, 435-448.
- Hasançebi, O., and Erbatur, F. (2002). Layout Optimization of Trusses Using Simulated Annealing. *Advances in Engineering Software*, 33, 681-696.
- Hayalioğlu, M.S. (2001). Optimum Load and Resistance Factor Design of Steel Space Frames Using Genetic Algorithm. *Structural Multidisciplinary Optimization*, 21, 292-299.
- Holland, J.H. (1992). Adaptation in Natural and Artificial Systems. MIT Press.

- Huang, M.W., and Arora J.S. (1997). Optimal Design with Discrete Variables: Some Numerical Experiments. International Journal for Numerical Methods in Engineering, 40, 165-188.
- Huybers, P. (1995). Super-Elliptic Geometry as a Design Tool for the Optimization of Dome Structures. Structural Systems and Industrial Applications, 387-399.
- Johnston, B.G., Lin, F.J., Galambos, T.V. (1986). Basic Steel Design. Prentice-Hall Inc.
- Kang, W., Chen, Z., Lam, H.F., Zuo, C. (2003). Analysis and Design of the General and Outmost-Ring Stiffened Suspen-Dome Structures. Engineering Structures, 25, 1685-1695.
- Katayama, K., Hirabayashi, H., Narihisa, H., (1999). Performance Analysis for Crossover Operators of Genetic Algorithms. Systems and Computers in Japan, 30, 20-30.
- Kaveh, A., and Abdi-tehrani, A. (2004). Design of Frames Using Genetic Algorithm; Force Method and Graph Theory. International Journal of Numerical Methods in Engineering, 61, 2555-2565.
- Kaveh, A., and Kalatjari, V. (2003). Topology Optimization of Trusses Using Genetic Algorithm, Force Method and Graph Theory. International Journal of Numerical Methods in Engineering, 58, 771-791.
- Kaveh, A., and Kalatjari, V. (2004). Size/Geometry Optimization of Trusses by the Force Method and Genetic Algorithm. Mathematical Mechanics, 5, 347-357.
- Kawaguchi, M., Tatemichi, I., Chen, P.S. (1999). Optimum Shapes of a Cable Dome Structure. Engineering Structures, 21, 719-725.

- Kawamura, H., Ohmori, H., Kito, N. (2002). Truss Topology Optimization by a Modified Genetic Algorithm. Structural Multidisciplinary Optimization, 23, 467-472.
- Kim, J.H., and Myung,H. (1996). A Two Phase Evolutionary Programming for General Constrained Optimization Problem. In: Proc.of the 5th Annual Conference on Evolutionary Programming, San Diego.
- Kirkpatrick, S., Gelatt, C.D., and Vecchi, M.P.(1983). Optimization by Simulated Annealing. Science, 220 (4598), 671-680.
- Koçvara, M. (2002). On the Modelling and Solving of the Truss Design Problem with Global Stability Constraints. Structural Multidisciplinary Optimization, 23, 189-203.
- Krishnamoorthy, C.S., Venkatesh, P.P., Sudarshan, R. (2002). Object-Oriented Framework for Genetic Algorithms with Application to Space Truss Optimization. Journal of Computing in Civil Engineering, 66-75.
- Lamberti, L., and Pappalettere, C. (2003). Move Limits Definition in Structural Optimization with Sequential Linear Programming. Computers and Structures, 81, 215-238.
- Langdon, W.B., and Qureshi, A. Genetic Programming-Computers Using “Natural Selection” to Generate Programs. <http://www.leitl.org>. Last visited on November 12th, 2005.
- Lemonge,A.C.C., and Barbosa, H.J.C. (2004). An Adaptive Penalty Scheme for Genetic Algorithms in Structural Optimization. International Journal For Numerical Methods in Engineering, 59, 703-736.

- Letchford, C.W., and Sarkar, P.P. (2000). Mean and Fluctuating Wind Loads on Rough and Smooth Parabolic Domes. Journal of Wind Engineering, 88, 101-117.
- Liew, J.Y.R., and Tang, L.K., (2000). Advanced Plastic Hinge Analysis for the Design of Tubular Space Frames. Engineering Structures, 22, 769-783.
- Lin, C.Y., and Wu, W.H. (2004). Self-Organizing Adaptive Penalty Strategy in Constrained Genetic Search. Structural Multidisciplinary Optimization, 26, 417-428.
- Liu, G.R., and Han, X. (2003). Computational Inverse Techniques in Nondestructive Evaluation. CRC Press.
- Liu, X., Begg, D.W., Matravers, D.R. (1997). Optimal Topology/Actuator Placement Design of Structures Using Simulated Annealing. Journal of Aerospace Engineering, 119-125
- Loorits, K., and Talvik, I. (1999). A Comparative Study of the Design Basic of the Russian Steel Structures Code and Eurocode 3. Journal of Constructional Steel Research, 49, 157-166.
- Lopez, A., Puente, I., Serna, M.A. (2004). Buckling Loads of Semi-Rigidly Jointed Single Layer Latticed Domes. Computer Aided Engineering Group, Graduate Institute of Civil Engineering, National Taiwan University, <http://www.tecnun.es/estructuras/paper04.pdf>. Last visited on November 12th, 2005.
- Lopez, A., Puente, I., Serna, M.A. (2003). Analysis of Single Layer Latticed Domes; A New Beam Element. Campus Tecnológico De la Universidad de

Navarro, <http://eee.caece.net/iass2003/Finalprogram.htm>. Last visited on November 12th, 2005.

Luke, B. Simulated Annealing. <http://www.members.aol.com/btluke/featur05.htm> . Last visited on November 12th, 2005..

Lundy, M., and Mees, A. (1986). Convergence of an Annealing Algorithm. Mathematical Programming, 34, 111-124.

Makowski, Z.S. (Editor) (1984). Analysis, Design and Construction of Braced Domes. Granada.

Metropolis, N., Rosenbluth, A.W., Rosenbluth, M., Teller, A., and Teller, H. (1953). Equations of State Calculations by Fast Computing Machines. Journal of Chemical Physics, 21 (6), 1087-1091.

Michalewicz, Z. (1995). Heuristic Methods for Evolutionary Computation Techniques. Journal of Heuristic, 1 (2), 177-206.

Missoum, S., Gürdal, Z., Gu, W. (2002). Optimization of Nonlinear Trusses Using A Displacement- Based Approach. Structural Multidisciplinary Optimization, 23, 214-221.

Mitchell, M. (1996). An Introduction to Genetic Algorithms. The MIT Press.

Montes, P., and Fernandez, A. (2001). Behaviour of a Hemispherical Dome Subjected to Wind Loading. Journal of Wind Engineering, 89, 911-924.

Myung, H., and Kim, J.H. (1996). Hybrid Evolutionary Programming for Heavily Constrained Problems. Bio-Systems, 38, 29-43.

- Nash,S.G., and Sofer,A. (1996). Linear and Nonlinear Programming. McGraw-Hill, New York.
- Nelson, J.K.Jr, and Mc Cormac, J.C. (2003). Structural Analysis, Using Classical and Matrix Methods. John Wiley&Sons Inc.
- Newberry, C.W., and Eaton, K.J. (1974). Wind Loading Handbook. Building Research Establishment Report, HM Stationery Office.
- Niemi, E., and Mäkeläinen, P.(Editors)(1990). Tubular Structures, The Third International Symposium. Elsevier Applied Science.
- Nooshin, H., and Disney, P. (1991). Elements of Formian. Computers&Structures, 41, 1183-1215.
- Obrebski, J.B. (1995). Philosophy of Lightweight Structures. International Conference on Lightweight Structures in Civil Engineering.
- Ohsaki, M., and Nakamura, T. (1994). Optimum Design With Imperfection Sensitivity Coefficients for Limit Point Loads. Structural Optimization, 8, 131-137.
- Onwubiko, C. (2000). Introduction to Engineering Design Optimization. Prentice Hall.
- Orvosh, D., and Davis, L. (1995). Using a Genetic Algorithm to Optimize Problems with Feasibility Constraints. In: Proc. Of the 6th International Conference on Genetic Algorithms. Echelman,L.J. ed. , 548-552.
- Osyczka, A. (2002). Evolutionary Algorithms for Single and Multicriteria Design Optimization. Physica-Verlag (A Springer-Verlag Company).

- Quinn, M.P., and Izzuddin, B.A.(1998). Global Structural Cost Optimization by Simulated Annealing. In: Proc. Advances in Engineering Computational Technology (Topping, B.H.V., ed.), Edinburg, 143-147.
- Parsons, R., and Canfield, S.L. (2002). Developing Genetic Programming Techniques for the Design of Compliant Mechanisms. Structural Multidisciplinary Optimization, 24, 78-86.
- Pezeshk, S., Camp,C.V., Chen, D. (2000). Design of Nonlinear Framed structures Using Genetic Optimization. Journal of Structural Engineering, 382-388.
- Pham, D.T. and Karaboga, D. (2000). Intelligent Optimization Techniques, Springer.
- Pyrz, M. (2004). Evolutionary Algorithm Integrating Stress Heuristics for Truss Optimization. Optimization and Engineering, 5, 45-57.
- Rafiq, M.Y, Mathews, J.D., Bullock, G.N. (2003). Conceptual Building Design- Evolutionary Approach. Journal of Computing in Civil Engineering, 150-158.
- Rajan, S.D. (1995). Sizing, Shape and Topology Design Optimization of Trusses Using Genetic Algorithm. Journal of Structural Engineering, 1480-1487.
- Rajasekaran, S., Shalu Mohan, V., Khamis, O. (2004). The Optimization of Space Structures Using Evolution Strategies with Functional Networks. Engineering with Computers, 75-87.
- Rajeev, S., and Krishnamoorthy, C.S. (1992). Discrete Optimization of Structures Using Genetic Algorithms. Journal of Structural Engineering, Vol.118, No.5, 1233-1250.

- Rao, S.S. (1996). Engineering Optimization. A Wiley-Interscience Publication.
- Rechenberg, I. (1965). Cybernetic Solution Path of an Experimental Problem. Royal Aircraft Establishment, Library Translation No.1122, Farnborough, Hants, UK.
- Rechenberg, I. (1973). Evolutionstrategie: Optimierung Technischer Systeme Nach Prinzipien der Biologischen Evolution. Frommann-Holzboog, Stuttgart.
- Ryoo, J., and Hajela, P. (2004). Handling Variable String Lengths in Genetic Algorithm-based Structural Topology optimization. Structural and Multidisciplinary Optimization, 26, 318-325.
- Sack, R.L. (1989). Matrix Structural Analysis. PWS-KENT Publishing Company.
- Sait, S.M., and Youssef, H. (1999). Iterative Computer Algorithms with Applications in Engineering. IEEE Computer Society.
- Saka, M.P. (1990). Optimum Design of Pin-Jointed Steel Structures with Practical Applications. Journal of Structural Engineering, Vol. 116, No.10, 2599-2620.
- Saka, M.P., and Kameshki, E.S. (1998). Optimum Design of Nonlinear Elastic Framed Domes. Advances in Engineering Software, 29, 519-528.
- Salajegheh, E. (1995). Optimum Design of Structures with Reference to Space Structures. International Conference on Lightweight Structures in Civil Engineering.
- Salajegheh, E., and Vanderplaats, G.N. (1993). Optimum Design of Trusses With Discrete Sizing and Shape Variables. Structural Optimization, 6, 79-85.

- Sandıkçı, B. (2005). Genetic Algorithms. Bilkent University, <http://www.benli.bcc.bilkent.edu.tr/~lors/ie572/burhaneddin.pdf>. Last visited on November 12th, 2005.
- Sarma, K.C., and Adeli, H. (2000). Fuzzy Genetic Algorithm for Optimization of Steel Structures. Journal of Structural Engineering, 596-604.
- Sergeyev, O., and Pedersen, P. (1996). On Design of Joint Positions for Minimum Mass 3-D Frames. Structural Optimization, 11, 95-101.
- Shrestha, S.M., and Ghaboussi, J. (1998). Evolution of Optimum Structural Shapes Using Genetic Algorithm. Journal of Structural Engineering, 1331-1338.
- Soh, C.K., and Yang, J. (1996). Fuzzy Controlled Genetic Algorithm Search For Shape Optimization. Journal of Computing in Civil Engineering, 143-150.
- Tang, W., Tong, L., Gu, Y. (2005). Improved Genetic Algorithm for Design Optimization of Truss Structures with Sizing, Shape and Topology Variables. International Journal For Numerical Methods in Engineering, 62, 1737-1762.
- Taylor, J.E. (1997). On the Prediction of Topology and Local Properties for Optimal Trussed Structures. Structural Optimization, 14, 53-62.
- Trosset, M.W. (2001). What is Simulated Annealing? Optimization and Engineering, 2, 201-213.
- Tzan, S.R., and Pantelides, C.P. (1996). Annealing Strategy for Optimal Structural Design. Journal of Structural Engineering, 815-827.

- Uematsu, Y., Yamada, M., Inoue, A., Hongo, T. (1997). Wind Loads and Wind-Induced Dynamic Behaviour of a Single Layer Latticed Dome. Journal of Wind Engineering, 66, 227-248.
- Ulusoy, A.F. (2002). Use of Evolution Strategies in Optimum Structural Design, M.S.Thesis.
- Uskon, Technical Specification for Space Structures.
- Voss, M.S., and Foley, C.M. Evolutionary Algorithm For Structural Optimization. The Site of Mark Voss, Ph.D., <http://www.evolutionarystructures.com/papers/genetic.pdf>. Last visited on November 12th, 2005.
- Xie, Y.M., and Steven, G.P. (1997). Evolutionary Structural Optimization. Springer.
- Wiese, K., and Goodwin, S.D. (2001). A New Selection Strategy for Genetic Algorithms That Yields Better Results. University of Glasgow, <http://www.dcs.gla.ac.uk/~drg/cp97-workshop/06:wiese-final.ps>. Last visited on November 12th, 2005. .
- Williams, M.S., and Todd, J.D. (2000). Structures: Theory and Analysis. Mac Millan Press.
- Yang, J., and Soh., C.K. (1997). Structural Optimization by GAs with Tournament Selection. Journal of Computing in Civil Engineering, 195-200.
- Yıldız, H. (2000). Simulated Annealing & Applications to Scheduling Problems. Bilkent University, <http://www.benli.bcc.bilkent.edu.tr/~lors/ie572/hakan.pdf>. Last visited on November 12th, 2005.